Vol. XXVI, B, No. 1 April, 1956

JOURNAL

OF

THE MADRAS UNIVERSITY

CONTRIBUTIONS IN MATHEMATICS, PHYSICAL AND BIOLOGICAL SCIENCES

PUBLISHED BY THE UNIVERSITY
MADRAS

INSTRUCTIONS TO AUTHORS

Three numbers of the Journal are published every year, in April, August and December respectively and contributions for publication should be sent to the Editor not later than February 1, June 1, and October 1 respectively.

Contributors are requested to be clear and concise. Manuscripts should not exceed 8,000 words and should be in a final form for the press. Each paper should start with a short summary which should be an abstract of the whole paper, complete and clear in itself, and not over 3 per cent. of the length of the paper. The introduction and reviews of literature should be restricted to closely pertinent papers.

The manuscript should be typewritten on one side of the paper only, with wide margins and be double spaced throughout including titles, footnotes, literature citations and legends. Symbols, formulae and equations must be written clearly and with great care. Scientific names of genera and species are printed in italics and should be underlined in the typescript. Too many tables, graphs, etc. should be avoided. Each table should be typed on a separate sheet with its proper position marked in the text in pencil.

Literature citations: All references to literature cited in the text should be presented together at the end of the paper in alphabetical order of authors' names. Each reference should be given in a standard form as follows: (1) name(s), followed by initial(s), of author(s); (2) year of publication in brackets; (3) full title of paper; (4) title of journal, abbreviated according to *World List of Scientific Periodicals*, 1952, and underlined; (5) volume number in Arabic numerals, underlined with two lines to indicate bold type; (6) page numbers without the prefix, p. When books are mentioned in the references, the order should be: name of author(s), initial(s), year in brackets, title of the book, which should be underlined, volume number, edition, page, followed by place of publication and name of publisher. Where a reference has not been seen in original, it should be indicated by an asterisk and the name of the abstracting journal or other source should be mentioned in brackets. If the title is in a language other than English, the diacretic signs, etc., should be precisely given as in the original.

Examples:

Text: (Patel, 1948); but, e.g., 'Patel (1948) showed that . . . .'. For two authors, write as, e.g., Khanna & Sharma (1947), using the ampersand (&). If there are more than two authors, all names should be given when cited for the first time and thereafter the first name only, adding *et al.*

References:

Raman, C. V. (1949) The theory of the Christiansen experiment. *Proc. Indian Acad. Sci.*, A, 29: 381-90.

Sahni, B. (1936a) Wegener's theory of continental drift in the light of Palaeobotanical evidence. *J. Indian bot. Soc.*, 15: 31-32.

Sahni, B. (1936b) The Karewas of Kashmir. *Curr. Sci.*, 5: 10-16.

Drawings should be on white board in India ink. As many of the illustrations as possible should be grouped together so that they may be reproduced as a single cut. Photographs should be glossy prints with strong contrasts. They are best submitted in the exact size in which it is desired to have them reproduced. Full page drawings and photographs should be made so as to allow reduction to a maximum size of 8" × 5". The name of the author, figure number and the title of the article should be written in pencil on the back of each figure. Each figure should have a legend. Legends should be typed on separate sheets.

Contributors will receive only a galley proof and *no alterations should be made at the proof stage.* 25 reprints without covers are supplied free to authors. Extra reprints may be had at cost price, but this should be ordered when returning the corrected proof.

Communications should be addressed to Professor T. S. Sadasivan, Editor, Journal of the Madras University (Section B), University Botany Laboratory, Madras-5, India.

Vol. XXVI, B, No. 1 April, 1956

JOURNAL

OF

THE MADRAS UNIVERSITY

"Mode of Citation : *J. Madras Univ. B*"

Issued on 16-6-56

PUBLISHED BY THE UNIVERSITY
MADRAS

CONTENTS

J. Madras Univ., B, XXVI, No. 1, pages 1-9, 1956

Dyke Rocks from Davangere (Mysore State)

BY

C. NAGANNA,
Department of Geology and Geophysics,
University of Madras, Madras—25.

(Received for publication on January 31, 1956)

ABSTRACT

Dyke rocks of the composition of Noritic olivine dolerites and Olivine dolerites occur around Davangere, Mysore State. The plagioclase of these rocks are all twinned and the anorthite content in them ranges from 58 to 72 per cent. All types of twin laws, normal, parallel, complex and interpenetration are noticed. Of the mafic minerals olivine and both ortho-and clino-pyroxenes are found. Two specimens of these rocks, texturally different are chemically analysed and their petro-chemistry discussed. The magma which has given rise to these two types is found to fit into the "gabbroide magmen" of Niggli's magma types and lies in between "eukritisch" and the next "c-gabbroid" types; the difference in colour and texture in these rocks is found to be due to the different cooling history of these rocks. These rocks bear a close resemblance to the dyke rocks of Dodkanya (Mysore State) which have an ultrabasic and charnockitic geological setting.

Dyke rocks occurring as boulders are found strewn about in the gneissic soil around the University campus, Davangere. The exact trend of these dykes are not clearly seen but the boulders have a trend NW-SE.

The anorthite content and twin laws of felspars were determined on the Federov Stage after the method of Reinhard (1931). The results were checked on Reinhard's Table V, by plotting poles of twinning planes got by Berek's and Nikitin's constructions. The optic axial angle was measured directly on the Universal Stage; and Troger's correction applied using β values. Since there were no twinned pyroxenes the extinction angle was determined by drawing a stereogram of the morphological and optical elements after the method of Burri (1950). Mineral grains separated in heavy liquids were used to determine the refractive index β. α and γ were calculated by determining the birefringence on the Universal Stage after the method recommended by Hess (1949). The volume percentage of the minerals in these rocks was determined on a Leitz six spindle integrating Stage. Chemical analyses were carried out by the methods outlined by Groves (1951).

Petrography

The study of textures, the nature of the plagioclase and the predominance of plagioclase or the mafic minerals leads us to recognise two types of dyke rocks. The more dark coloured variety is noritic in composition and the other has euhedral felspars and subophitic texture, (gabbroid). The Noritic dolerite is a hard compact rock dark in colour with granular texture. In thin section it shows abundant euhedral pyroxenes which range in size from 2mm × 1·3 mm to 0·05 mm × ·05mm. The plagioclases are found as irregular laths and needles. Sometimes these needles are flow oriented, and many of them are interpenetrated. The anorthite content of these felspars varies from 58 to 68 per cent.

Olivine grains are all euhedral and some are poikilitic in plates of pyroxenes, thus indicating their earlier crystallization. The olivine crystals are all bordered by iron ore. Some irregular grains of iron ores are also seen. A hand specimen of gabbroid dyke is greyish in colour and has a granular texture. The felspars here are euhedral, tabular, and in their interspaces are moulded pyroxenes. The felspar grains range in size from 1·88 mm × 1·0 mm to 0·08 mm × 0·05mm. The anorthite content of the plagioclase felspars varies from 68 to 72 per cent. In some places intergrowth between the pyroxene and the felspar is seen indicating the simultaneous crystallization of both the minerals in the later stages of crystallization. Both ortho- and clino-pyroxenes occur and in some cases one grades on to the other. Even here olivine grains are found as euhedral grains surrounded by altered iron ore. Some of the felspar grains are clouded with iron dust. Small irregular grains of iron ores are found here and there.

Table I

Rock Types	An percentage	No. of grains worked	Albite	Manebach	Baveno	Carlsbad Akline = Manebach Ala	Pericline	Ala	Albite ala	Albite-Carlsbad
Olivine — dolerite (gabbroid)	68 to 72	25	13	—	—	7	—	—	—	5
Olivine dolerite (noritic)	58 to 68	20	9	—	—	5	3	—	—	3
Total :		45	22			12	3			8

Mineralogy

Felspars: All the felspars are twinned, the twin laws determined are given in Table I, along with the range of anorthite percentage. The twinning plane is dominantly 010. In a few cases it is 001. Well developed interpenetration twins are also found. They cross each other either at 90° or at 60° and at 120°. The two individuals crossing at 90° are found to have twinned after Carlsbad and Albite-Carlsbad Law while the pole of the association plane of the arms falls on 021 curve of Plate 2 of Reinhard, thus indicating the parallelism of the association plane with the 021 face. The pole of the association plane in the other case does not fall on any one of the curves of Reinhard's Plate 2 and hence it is concluded that the association plane is parallel to an irrational pyramid. These interpenetration twins are found to be quite similar to those reported by Suryanarayana (1955), from the dyke rocks of Closepet. The twin laws recorded are Albite, Carlsbad and Albite-Carlsbad (Table I). Gorai (1951) groups these laws under c-twin groups and says that they are characteristic of volcanic and plutonic igneous rocks. The study of twin laws in these felspars confirms this view.

Pyroxenes: The gabbroid rock has the ortho- and clino-pyroxenes in almost equal proportion. The ortho-pyroxene has the following optical characters. $-2V=72°$ to $76°$. $\alpha=1{\cdot}674$, $\beta=1{\cdot}682$, $\gamma=1{\cdot}687$.

From the above optical data the ortho-pyroxene is identified as Bronzite.

The other Ortho-pyroxene found is pleochroic and is in abundance in the noritic type. The optical characters are

$-2V=49°$ to $51°$. $\alpha=1{\cdot}711$, $\beta=1{\cdot}721$, $\gamma=1{\cdot}726$

Pleochroic Scheme

X Brick red.
Y nearly colourless.
Z light green.

From the optical characters it is clear that it is hypersthene. The clino-pyroxene is found in both the types but it is seen reduced to a very low percentage in the noritic type. The clino-pyroxene shows the typical system of cleavages cutting each other approximately at 90°. The optical characters are

$+2V=42°$ to $48°$, $\alpha=1{\cdot}683$, $\beta=1{\cdot}689$, $\gamma=1{\cdot}711$.

$Z\Lambda C = 38°$ to $43°$ (Measured with reference to the prismatic cleavages).

West (1952) calls the pyroxene of the Deccan Traps having 2V between 30° to 48° as sub-calcic augite, as suggested by Benson (1944) and modified by Walker. The clino-pyroxene described above can also be called sub-calcic augite.

Olivine: These are found more in the noritic type than in the other. The optical characters are

$-2V=79°$ to $81°$ (By projection). $\beta=1{\cdot}710$ to $1{\cdot}689$, $\gamma-\alpha=0{\cdot}042$, $\gamma-\beta=0{\cdot}018$ to $0{\cdot}020$.

Petrochemistry

The analyses of the two types are given below. The C. I. P. W. Norm, Niggli values and Niggli basis are calculated and given in Table II. Two analyses of rocks which have resemblance to these analyses are also given for comparison.

Table II

	A	B	C	D
SiO_2 ..	48·59	48·30	49·29	47·92
TiO_2 ..	0·41	0·44	0·24	1·40
Al_2O_3 ..	19·03	14·06	12·98	18·87
Fe_2O_3 ..	0·74	1·78	0·12	1·18
FeO ..	6·63	7·72	8·40	8·65
MnO ..	Tr	0·05	0·15	0·11
MgO ..	11·93	13·96	9·82	7·82
CaO ..	10·29	9·89	15·73	10·46
Na_2O ..	1·68	1·43	1·52	2·44
K_2O ..	0·28	0·10	0·32	0·19
P_2O_5 ..	0·18	ND	—	0·07
H_2O+ ..	0·55	1·23	0·76	0·51
H_2O- ..	0·20	0·07	0·07	
Total ..	100·51	99·03	99·40	99·62

C.I.P.W. Norm

	A	B	C	D
Q ..	—	—	—	—
Or ..	1·67	0·56	1·67	1·11
Ab ..	14·15	12·06	12·58	20·44
An ..	43·37	31·69	27·80	40·03
Di ..	5·56	14·03	40·96	9·06
Hy ..	19·05	25·27	3·95	13·65
Ol ..	13·68	10·76	11·55	9·82
Il ..	0·76	0·76	0·46	2·74
Mt ..	0·93	2·55	0·23	1·86
Ap ..	0·34	—	—	0·34
H_2O ..	0·75	1·35	0·76	0·51
Total ..	100·26	99·03	99·96	99·56
	Niggli Values			
Si ..	101·4	98·54	102·7	107·5
al ..	23·31	16·90	15·86	24·90
fm ..	49·88	58·50	45·69	44·41
c ..	23·05	21·67	35·08	25·17
alk ..	3·76	2·93	3·37	5·52
ti ..	0·627	0·61	0·374	0·305
P ..	0·125	—	—	0·135
K ..	0 100	—	0·111	0·049
mg ..	0·749	0·73	0·672	0·591
	Niggli Basis			
cp ..	0·28	—	—	0·28
Kp ..	0·98	0·30	1·01	0·67
Ne ..	8·85	7·72	8·10	13·08
Cal ..	25·57	19·12	16·86	24·16
Cs ..	2·05	5·29	15·24	3·36
Fs ..	0·66	1·85	0·22	1·34

	A	B	C	D
Fa ..	7·54	8·98	9·89	9·99
Fo ..	24·42	29·26	20·74	16·36
Ru ..	0·28	0·28	0·17	1·01
Q ..	29·37	27·20	27·77	29·75
Q ..	29·37	27·20	27·77	29·75
L ..	35·40	27·14	25·97	37·91
M ..	35·23	45·66	46·26	32·34

A—Olivine dolerite (gabbroid), Davangere. Analyst: C. Naganna

B—Noritic olivine dolerite, Davangere. Analyst: C. Naganna.

C—Olivine gabbro dyke, Hebye (Dodkanya). Analyst: S. Ramanathan (1955), *J. Madras Univ. B*, XXV, No. I, p. 48 analysis C.

D—Chilled marginal Olivine gabbro; Wager, L. R. and Deer, W. A. Quoted from "Igneous and Metamorphic Petrology", by Turner and Verhoogen, (1951) p. 230. Analysis No. 1.

From Table II it is clear that these dyke rocks show a close similarity in chemical composition to the dyke rocks from Dodkanya. In Dodkanya we see these dykes amidst the ultrabasic dunites and charnockites while the geological surrounding here is gneissic and schistose.

The normative plagioclase calculated to a total of hundred shows Ab : An as 25 : 75 in gabbroid type and 28 : 72 in the second case, which closely matches with the composition of the plagioclase determined optically.

The modal composition of the rock is given in Table III.

Table III

	A	B
Plagioclase ..	49·10	34·77
Pyroxene ..	43·06	50·31
Olivine ..	6·66	13·33
Iron Ore ..	1·18	1·59
Total ..	100·00	100·00

The metasilicates Ca SiO_3, Mg SiO_3 and Fe SiO_3 of the ortho- and clino-pyroxenes of these rocks together with that of other rocks taken for comparison are recalculated from norm and are shown in Table IV. It can be seen that the composition of these pyroxenes are almost uniform. The Wo molecules in the clinopyroxene are found to be more than 50% in all cases, while the En molecules come next. In the ortho pyroxenes the En molecules are more.

Table IV

	A	B	C	D
Cli. Pyr. ..	$Wo_{52}En_{36}Fs_{12}$	$Wo_{52}En_{36}Fs_{12}$	$Wo_{52}En_{32}Fs_{16}$	$Wo_{51}En_{30}Fs_{19}$
Orth. Pyr. ..	$En_{73}Fs_{27}$	$En_{74}Fs_{26}$	$En_{66}Fs_{34}$	$En_{63}Fs_{37}$

The (f) norm of these rocks are calculated as suggested by Barth (1936) in order to determine the order of crystallization of pyroxene and plagioclase in the magma.

This is given in Table V.

Table V

Rock Types.	ab'	an'	di'	hy'	(f) Norm
A	17·22	52·82	6·77	23·19	84·87
B	14·53	38·15	16·89	30·43	133·84
C	14·75	32·59	48·01	4·65	121·46
D	24·57	48·13	10·89	16·41	85·64

From the above table it can be seen that rock type "A" having (f) norm 84·87 which is a value far below 123, suggests that the

felspar started crystallizing very early and the pyroxenes later. This fact is clearly evidenced by the texture of the rock "A" where we notice euhedral plagioclases and sub-hedral pyroxenes. Moreover the pyroxenes are moulded in the interspaces of the felspar grains.

In contrast to this in the rock type "B" we get (f) norm value 133·84 whereby one infers that pyroxenes started crystallizing earlier than the felspars. This fact is also supported by the texture of the rock "B", where we notice the big plates of pyroxenes euhedral with felspars moulded into the interspaces.

The Niggli values for these rocks of Davangere closely match with 'gabbroid magmen' and they lie in between the 'eukritisch' and the next 'c-gabbroid' type of Niggli's magma types.

By comparing the analyses of the two rocks we can note the similarity of all the constituents except Al_2O_3, MgO and FeO. In "A", Al_2O_3 is higher and MgO and FeO are lower. In type "B" Al_2O_3 is lower and MgO and FeO are higher.

It is clear from the optical and analytical data that much of Al_2O_3 has been used for the development of euhedral felspars in rock "A", which has a felspar volume percentage of about 49, thus bringing down alumina content and an enrichment of FeO and MgO in the residual magma, which has rightly given rise to rock "B", which has pyroxene volume percentage of about 50. The relative poverty of Al_2O_3 in the residual magma has probably given rise to the abundance of the hypersthene in the rock "B".

Noritic dykes and olivine dolerites have been reported from various parts of Mysore. Wetherell has classified the dyke rocks of Mysore under eleven different groups. The dyke rocks now under study find their place under the subclass (F), which he names as dolerites with rhombic pyroxene and olivine.

The norite dolerites have been considered by Rama Rao (1940) as related to Charnockites. In this area there is no such evidence of relationship to charnockites. It is held that the two types of dykes are the differentiates from the same gabbroid magma. Since the crystallization of hypersthene requires high temperature it is inferred that the noritic types have been drawn from the deeper portions of the magma and the gabbroid types from shallower depths.

ACKNOWLEDGMENT

The author places on record his deep sense of gratitude to Dr. P. R. J. Naidu for his help and guidance throughout the work.

REFERENCES

Barth, T. F. W. (1936) The crystallization process of basalt. *Amer. J. Sci.* 31: 321-351.

Berek, M. (1924) *Mikroskopische. Mineral bestimmung mit Hilferder Universal drehtisch methoden, Gebrüder* Börntraeger, Berlin.

Burri, C. & Niggli, P. (1945) *Die jungen eruptivegestone des mediterranein orogens,* kommissions Verlag von *güggenbühl* und Hüber, Schweizer Spiegel Verlag, Zurich, p. 52.

Burri, C. (1950) *Das polarisations mikroskop, verlag Bürkhauser, Basel.*

Gorai, M. (1951) Petrological studies on plagioclase twins. *Amer. Min,* 36: pp. 884-901.

Groves, A. W. (1951) *Silicate Analysis,* Second Edition, George Allen and Unwin Ltd., pp. 336.

Hess, H. H. (1949) Chemical composition and optical properties of common clino-pyroxenes. *Amer. Min,* 39: 621-666.

Nikitin, W. (1936) *Die Federov Methode,* Verlag von Gerbrüder Börntraegar, Berlin.

Rama Rao, B. (1940) Archaen complex of Mysore. *Bull. Geol. Dep. Mysore,* 17:

Ramanathan, S. (1955) Vogesites and Noritic olivine dolerites from Salem and Dodkanya. *J. Madras Univ. B,* 25: 29-54.

Reinhard, M. (1931) *Universal drehtischmethoden,* B. Wepf & Co., Vergal, Basel.

Suryanarayan, K. V. (1955) Interpenetration Twin in plagioclase feldspar. *Curr. Sci.,* 24: 120-121.

Turner, F. J. & Verhoogen, J. (1951) *Igneous and metamorphic petrology,* McGraw Hill Book Co., Inc. New York, p. 230.

Wetherell, Dyke rocks of Mysore, *Mem. geol. Dep. Mysore,* 2.

West, W. D. (1952) Note on pyroxenes of Deccan Traps. *Quart. J. geol. min. met. Soc. India,* 24, 153-157.

J. Madras Univ., B, XXVI, No. 1, pages 11-17, 1956

An Amperometric Method for the Estimation of Germanium

BY

S. Hamsath Ibrahim and A. P. Madhavan Nair,
Chemical Technology Laboratories,
Alagappa Chettiar College of Technology, University of Madras.

(Received for publication on January 31, 1956)

ABSTRACT

An accurate method of estimation of Germanium by the amperometric technique, has been developed. The method is based on the precipitation of divalent germanium as a complex with tannin in an acid medium containing ammonium sulphate. The titration is performed at—0·6 Volts (VS. SCE) in presence of a little cresol red added as maximum suppressor. Temperature is without effect on the precipitation and on the titre values.

Many gravimetric methods for the estimation of minute quantities of germanium have been developed based upon the principle that germanium forms complexes with organic substances like tannin, cinchonine, 5, 6, Benzoquinoline, etc. (H. H. Krause et. al. 1953). All these methods being gravimetric are necessarily time consuming. The present investigation was therefore undertaken to work out the possibility of using one of these reagents, tannin, as the precipitant in an amperometric estimation of germanium. It is known that the amperometric technique combines accuracy with rapidity of estimation.

It has been shown that tetravalent germanium can be precipitated quantitatively by tannin from solutions containing oxalate or sulphate (H. Holnes, 1948). Previously G. R. Davies and Sir G. Morgan (1938) suggested a method for the precipitation of germanium from ammonium sulphate solution at an acidity not exceeding N. sulphuric acid. A chloride medium was indicated by W. R. Scholler (1944). H. Holnes (1948) however stated that in chloride medium (0·5 N Hydrochloric acid) the precipitation is only 90·2% at ordinary temperature. All this work has been done with tetravalent germanium. The behaviour of divalent germanium towards tannin has not so far been studied. We have found that divalent germanium also forms a complex with tannic acid and that the precipitation is quantitative. As shown below,

we had also a special reason for preferring divalent germanium to tetravalent germanium for our work.

The Polarographic characteristics of tetra and divalent germanium, described by various investigators (Das Gupta, A. K., et. al. 1953; D. A. Everest, 1953; Valenta, P., et. al 1954; B. N. Evonov. Amin., et. al. 1944) indicate that maxima obtained in acid and alkaline medium (for tetravalent germanium) could be suppressed by gelatin, an observation that has been verified by us. But as gelatin gives a precipitate with tannin (C. Ainsworth Mitchell, 1936) this suppressor was unsuitable for our work. The maxima of divalent germanium could however be suppressed by Cresol red which has no such influence on the maxima of tetravalent germanium and which in no way interferes with tannin. Besides, divalent germanium gives better polarograms than tetravalent germanium. These practical considerations led us to the view that the divalent germanium lends itself to amperometric titration better than tetravalent germanium and so the reduction of tetravalent germanium to divalent germanium (using sodium hypophosphite and hydrochloric acid) was necessary before the amperometric titration.

As a preliminary to the amperometric titration and for fixing up the correct constant potential for the titration, the polarograms of divalent germanium were studied following the method of Evonov. Amin. et. al. and D. A. Everest (1953) with suitable modification. As an acid solution of a strength higher than 0·5 N. dissolves the germanium-tannin complex partially, the acidity was maintained well below this limit.

Hydrochloric acid seems to be essential for the polarographic reduction of divalent germanium (I. M. Kolthoff and Lingane, J.J. 1952) although the chloride ion polarogram interferes in certain cases (D. A. Everest, 1953). Further as the Germanium-tannin complex can be precipitated out only in the presence of an ammonium salt, ammonium sulphate had also to be added to the solution taken for the polarographic study. Owing to the influence of chloride ion mentioned above it is obvious that ammonium chloride could not be used for this purpose. Polarograms were obtained using solutions containing divalent germanium in the range 4 to 50 milli moles/litre with an acidity in the range of 0·25 to 0·35 N and an ammonium sulphate content 0·8 to 1·0 M; using Cresol red as the maxima suppressor. The polarograms obtained were smooth, with a definite step and no maxima appearing below a germanium concentration of 30 m. moles/litre. Half wave potentials and the

diffusion currents are recorded in Table I. Two of the polarograms are reproduced in fig. 1.

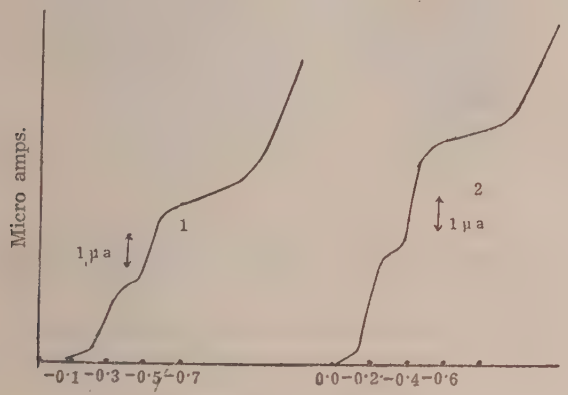

FIG. 1

Polarograms of + 2. Ge in 0·5N HCl and 1M. Ammonium Sulphate.

1. 8×10^{-4}M Ge. 2. $1{\cdot}2 \times 10^{-3}$M Ge.

Table I

Polarograms of + 2 Ge

	Ge. Concentration	Half wave potential (cathodic) $-E_{1/2}$	Diffusion current (id)
	(m. moles/litre)	Volts. (Vs. SCE)	μa
1.	4	— 0·49	1
2.	8	— 0·49	2
3.	13	— 0·48	2·9
4.	16	— 0·48	3·9
5.	20	— 0·475	5·1
6.	30	— 0·470	7·6
7.	40	— 0·47	10·5

As the diffusion current plateau is above — 0·5 V. (VS. SCE) the constant potential for the amperometric titration could be safely fixed at — 0·6 V. (VS. SCE). This potential (— 0·6 V) is also well in advance of the hydrogen discharge wave. It is found that tannin in this range and medium is non-reducible under dropping mercury electrode.

Experimental:

0·2 gms of spectroscopically pure germanium dioxide was weighed and dissolved with minimum amount of sodium hydroxide and neutralised with hydrochloric acid, adding dropwise. 2·0 gms. of pure sodium hypophosphite followed by 8 ml. of pure Hydrochloric acid were added, and after dilution to about 40 ml, the solution was heated over a water bath for an hour. When the reduction was complete the solution was made up to 100 ml. The final acidity of this solution was 0·5N. 3·0 gms. of BDH. tannic acid was dissolved in hot water and made up to 50 ml. A mixture of equal volumes 0·5 N. hydrochloric acid and 2 M. ammonium sulphate was taken as the supporting electrolyte.

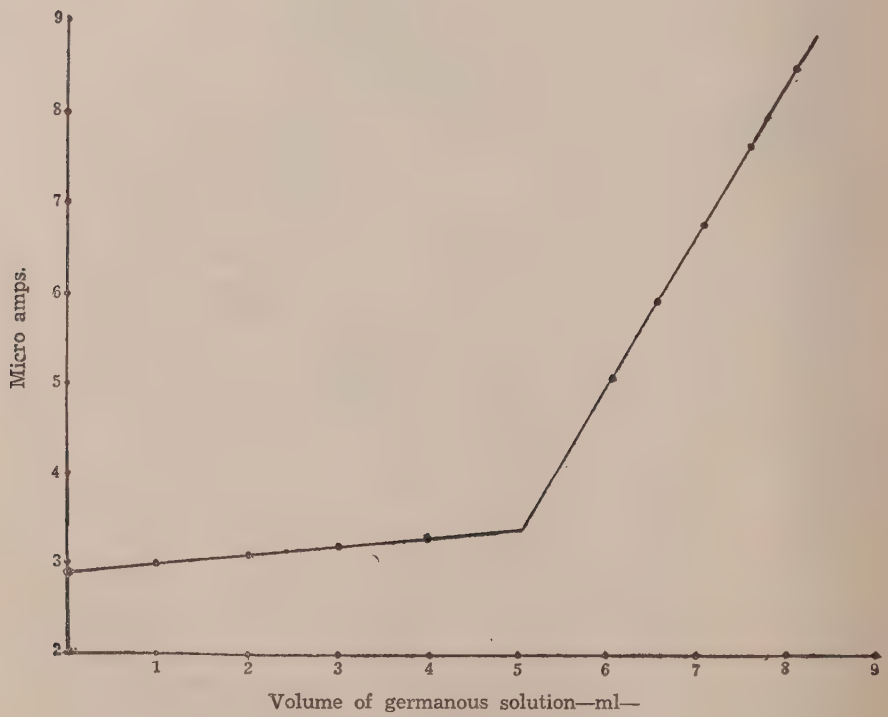

FIG. 2

Amperometric Titration Curve.

To a known volume (1-5 ml) of tannic acid solution, were added 0·2 ml cresol red and a sufficient quantity of the above solution of supporting electrolyte to give a total volume of 25 ml.

The standard germanous solution was then added in 0·5 ml. increments. It was not necessary to bubble inert gas to expel dissolved oxygen (D. A. Everest, 1953). The current was read two minutes after each addition at a constant potential —0·60 V. (VS. SCE) on a Tinsley Model recording polarograph. The volumes of germanous solution plotted against the current yielded two straight lines intersecting at the end point (Fig. 2). The values are given in Table II. The experiments were repeated also at a higher tem-

Table II

Amperometric Titration of Tannic Acid against Germanons Solution at Room Temperature

Tannic acid 0·1676 moles/litre	Germanous solutions 0·0192 moles/litre	Deviation
ml	ml	ml
1·00	1·67	0·005
2·00	3·35	0·00
3·00	5·02	0·005
3·50	5·85	0·012
4·00	6·70	0·000
5·00	8·40	0·025

perature (75° C) when no appreciable difference in titre value was observed (Table III). The calibration curve is given in fig. 3.

Table III. At 75° C

Tannic acid 0·1676 moles/litre.	Germanous solution 0·0192 moles/litre	Deviation from Room temperature.
.ml	ml	ml
1·00	1·68	0·005
2·00	3·35	0·000
3·00	5·025	0·005

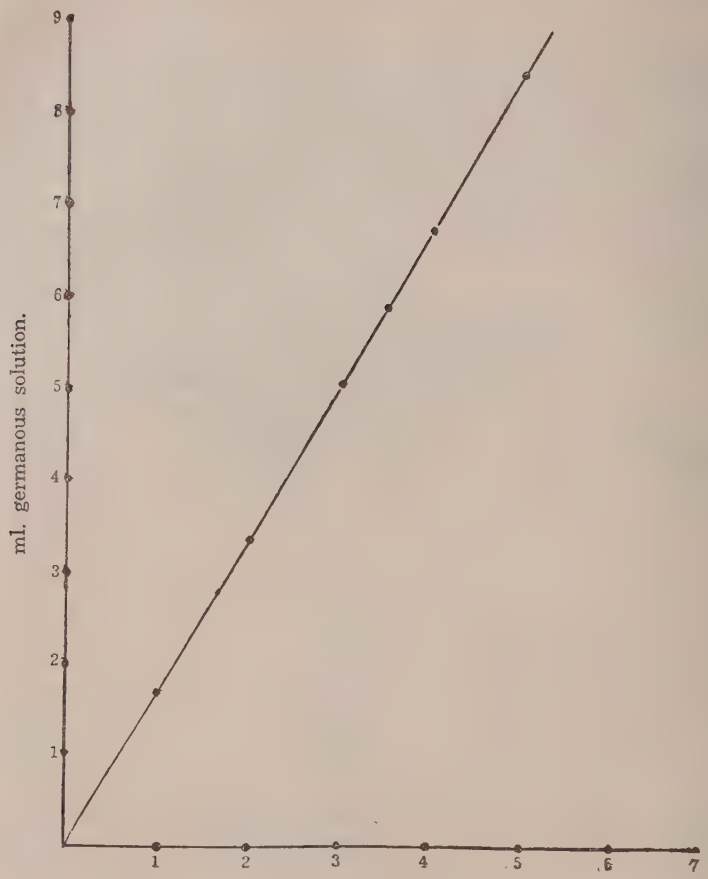

FIG. 3
Calibration Curve.

Discussion :

Fig. 2 illustrates that the variation of the diffusion current with the volume of the germanous solution added is strictly linear. The high accuracy possible in the method is evident from the fact that the maximum error is only of the order of 0·3%. Therefore the amperometric titration of divalent germanium with tannic acid in chloride solution in presence of ammonium sulphate, should be considered as a standard method of estimation. Apart from the simplicity of operation and economy of the time, this method has

got the added advantage that arsenic which is a usual impurity in germanium compounds, does not interfere in this, because it forms no complex with tannin (H. Holnes, et. al. 1946). It must however be mentioned that the addition of tannic acid solution to the germanous solution does not give reproducible results. This may be due to the sluggish precipitation of the germanium complex, when the tannin present is less than in equivalent quantities; so it is essential that the germanous solution is added to the tannin solution and not vice versa.

The object in performing a set of titrations at an elevated temperature (75°C) was to investigate whether the precipitation is in any way affected by temperature. Table III illustrates that almost identical titre values are obtained at the higher temperature, as at the room temperature. So no temperature control during titration is necessary.

REFERENCES

1. Ainsworth, M. C. (1936) A survey of the methods of analysing tannins. *Analyst* **61**: 295.
2. Davies, G. R. & G. Morgan, (1938) The gravimetric determination of Germanium. *Analyst* **63**: 388.
3. Das Gupta, A. K. & Nair, C. K. N. (1953) Polarographic reduction of Germanium. *Analyt. chim. acta.* **9**: 287.
4. Everest, D. A. (1953) The polarographic behaviour of bivalent germanium. *J. chem. Soc.* Part I: 660.
5. Holnes, H. (1948) The precipitation of germanium by tannin. *Analyt. chim. acta,* **2**: 254.
6. Holnes, H. & Scholler, W. R. (1946) Precipitation of tin by tannin. *Analyst,* **71**: 70.
7. Krause, H. H. & Johnson, C. H. (1953) Analytical methods for germanium. *Analyt. chem,* **25**: 135.
8. Scholler, W. R. (1944) Tannin as a selective reagent for Zirconium *Analyst,* **69**: 261.
9. Kolthoff, I. M. & Lingane, J. J. (1952) *Polarography,* Interscience Publishers, New York.
10. Valenta, P. & Zuman, P. (1954) Note on the article "Polarographic reduction of Germanium by A. K. Das Gupta and C. K. N. Nair." *Analyt. chim. acta.* **10**: 591.

J. Madras Univ., B, XXVI, No. 1, pages 19-30, 1956

Humic Acid from South Arcot Lignite

BY

B. Jagannadhaswamy and A. P. Madhavan Nair,
Chemical Technology Laboratories,
Alagappa Chettiar College of Technology, Guindy,
University of Madras

(Received for publication on January 23, 1956)

ABSTRACT

South Arcot lignite when suitably oxidised has been shown to be a rich source of humic acid. Aerial oxidation of fixed beds and fluidised beds has been effected and the optimum conditions for obtaining the best yield of humic acid, have been worked out. The ultimate analysis and the electrometric determination of the equivalent weight of humic acid have been performed. Ammonium humate has been prepared by two different methods and its nitrogen and ammonia contents estimated. The role of humic acid as a soil conditioner has been studied in an extensive series of pot culture experiments.

Humic acids form a class of substances obtained from peat, lignite or coals by alkali extraction. (Brusset, 1943). The extent of humic acid derivable from coal depends on two factors, i.e., (1) the geological age of the coal, low ranking coals being richer in their humic acid contents and (2) the oxidising treatment that the coal has received. Lignites in general being lower in rank than bituminous coals have a higher humic acid content (Lowry, 1945) and South Arcot lignite is no exception to this generalisation (Lahiri, 1954).

The alkaline extract on acidification yields humic acids as a dark brown precipitate which on drying becomes a dark, shining substance. These humic acids are generally a mixture of different carboxylic acids of unknown constitution and separable into groups by fractional extraction with solvents (Bangham, 1950). A review of existing knowledge on this subject has been published by Brusset (1943). With a view to increasing the humic acid content many methods of oxidation have been suggested such as the use of chemical reagents like nitric acid, with or without a catalyst (Bangham, 1950) or aerial oxidation preferably at an ele-

vated temperature or a combination of the two modes of oxidation.

In the scheme of work which forms the subject matter of this paper, prolonged aerial oxidation of a stationary bed and of a fluidised bed at different temperatures has been performed.

A great many possible technical applications of humic acids have been suggested. Those include their use in colloidal fuel, water purification wood staining, etc. (Bangham, 1950) besides their indirect applications as in the manufacture of active carbon, carbon black, plastics and resins, lead storage batteries (Waksman, 1938) and in ceramics.

Two important aspects of their utilisation which have been studied by the authors are (1) the function of humic acids as a soil conditioner in improving the uptake of fertilisers by plants, (2) the use of humic acid for preparation of ammonium humate which can be used as a nitrogeneous fertiliser in place of ammonium sulphate (Crowther and Brencheley, 1936).

A. *Preparation of humic acid*:

Experimental: Humic acid was prepared from lignite as such and also from oxidised lignite. A weighed quantity of sample (about 4 gms.) was heated with 100 ml. of a 2% solution of sodium hydroxide for 20 minutes on a water bath. This was filtered and the residue left was again extracted with fresh sodium hydroxide solution and filtered. The combined filtrate was acidified with 60 ml. of N. hydrochloric acid when the humic acid precipitates out. An excess of hydrochloric acid tends to peptise the humic acids into collodial state. The humic acid was filtered and well washed, dried to constant weight at 110°C and the yield calculated (Chowdhury and Biswas, 1942).

Two methods of oxidation of the lignite were employed.

Method I: Two lots of lignite were spread out in thin layers in two dishes and were exposed to air, one at a constant temperature of 100°C and the other 150°C in a thermostatically controlled electric oven for 40 days. The layers were stirred every day and samples taken out every five days. They were then subjected to alkali extraction as described above and the humic acid contents were estimated. In Table I are given the results of the above method.

Method II: In this method, the lignite was subjected to aerial oxidation in the fluidised state. For this a special column was designed and constructed. (Fig. I).

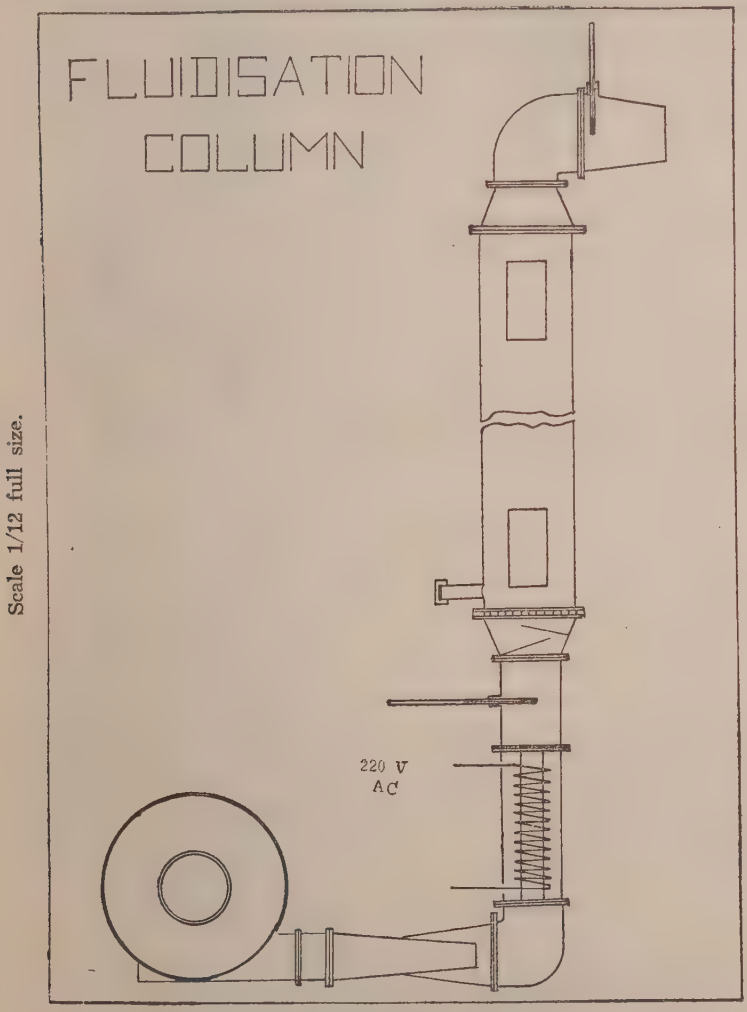

Fig. 1

Apparatus for oxidising lignite in a fluidised state (Method II)

The column is made of 22 gauge G. I. sheet, 2½″ square section and 2 ft. long. The air is supplied by a ¼HP., 2000 r.p.m. blower whose r.p.m. can be controlled. The air is made to pass

through a heater unit of nichrome wire wound on an insulating base and enclosed in a 2″ square section of G.I. tube and attached to the column by another 2″ section of G.I. tube of 6″ in length, where the air attains a uniform temperature by mixing. The output of the heater unit can be controlled by a rheostat. Two thermometers are placed, one in the mixing chamber and the other at the top of the column. Two baffles are put just above the mixing chamber so as to trap any lignite falling into the heater unit. The lignite is supported on a 200 mesh sieve cloth which in turn is supported by a ⅛″ copper plate having ⅛″ holes to allow the air to pass through. The column is provided with sight glasses, one at the top and the other at the bottom and a sampling outlet is provided at about 1″ above the sieve to take samples and when not required is closed with a cap. The column is designed to fluidise about 2 lbs. of lignite and the heater to give air at temperatures ranging from 80° C to 180° C. The column is lagged with absestos-magnesia.

About 350 gms. of lignite—30 to 50 mesh was placed in the column. The blower was so adjusted as to give an amount of air which would raise the bed height by about 1½″. The input of heat is then regulated to give the desired temperature (100°C in one experiment, 125°C in the second and 150°C in the third). The bed density was calculated and the volume of air flowing was measured by a wet gas meter. The oxidation was continued for 60 hours, samples being taken at 6 hour intervals. Table II gives the yields obtained at different temperatures and for different durations of oxidation.

Results and Discussion:

Table I

Oxidation of Lignite by Method I

Time in days.	% Humic acid content of Lignite.	
	110°C	150°C
0	60·2	60·2
5	61·6	62·8
10	63·1	65·0
15	64·6	68·6
20	66·0	72·8
25	67·3	76·0
30	68·5	77·8
35	69·8	79·6
40	71·0	80·6

The above results are plotted in Fig. 2.

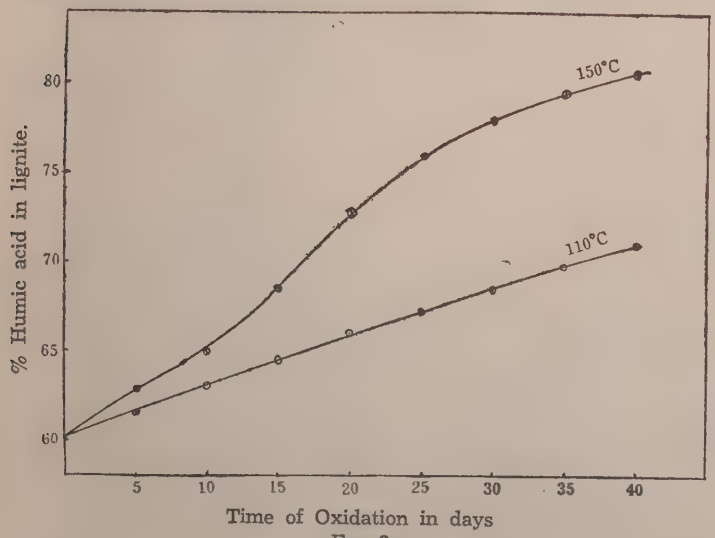

Fig. 2

Oxidation of Lignite in a Stationary Bed (Method 1).

These show that at 110°C, even though the oxidation is slow, the humic acid content increases uniformly with time. At 150°C, the oxidation is comparatively slight till the 10th day after which

there is a more rapid increase in the humic acid content upto about 35 days, but afterwards the process again slows down. Oxidation at 150°C gives consistently better yields over oxidation at 110°C. But in view of the long duration required for oxidation even at 150°, this type of oxidation cannot be recommended for industrial adoption.

Table II

Oxidation of Lignite by Method II

Bed density = 0·36 gm/ml
Air rate = 30 c.ft/hr. at 80°F

Time in hours.	% Humic acids content of lignite		
	100°C	125°C	150°C
0	60·4	60·4	60·4
6	62·8	65·6	67·2
12	66·2	70·0	72·6
18	68·4	72·2	76·0
24	69·5	73·4	78·3
30	70·3	74·5	79·6
36	71·1	75·4	80·3
42	72·0	76·3	80·8
48	72·6	77·2	81·2
54	73·2	78·0	81·5
60	73·8	78·8	81·8

The results of Table II are plotted in Fig. 3. In the fluidised oxidation by method II, it can be seen that at 100°C, the oxidation is slow compared to the higher temperatures, and after an initial steep increase in the rate of oxidation lasting for 18 hours, the process becomes slow at longer durations. At 125°C the oxidation pattern follows that at 100°C except that even after 60 hours, the oxidation seems to continue at a comparatively high rate. At 150°C, the humic acid content reaches about 80% in about 40 hours and remains fairly constant afterwards. The main difference between the oxidation at various temperatures, apart from the general increase in humic acid content, is the steep increase in humic acid content within the first 36 hours of oxidation at the higher temperatures. Generalising from the above data, it can be re-

commended that oxidation in a fluidised bed will be the best mode of oxidation when conducted under the following conditions: — (1) a temperature of 150°C (2) a duration of 40 hours at a bed density of 0·36 gm/ml and (3) air rate of 30 c. ft. per hour.

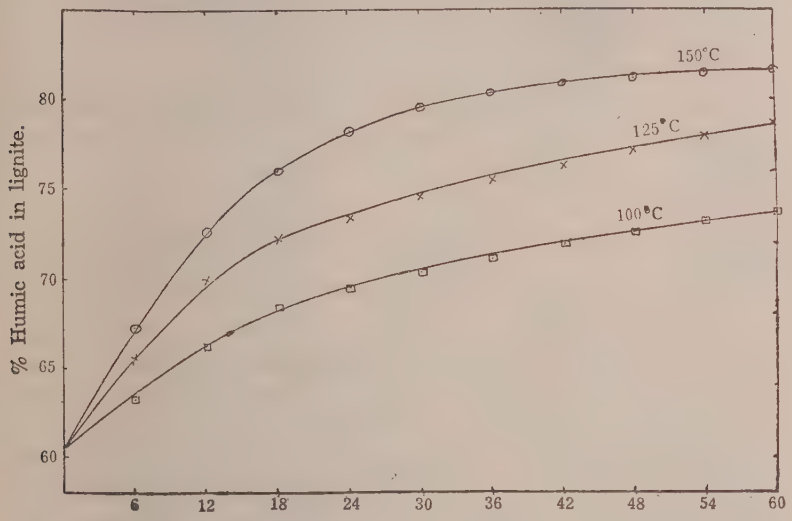

Fig. 3

Oxidation of Lignite in a fluidised bed (Method II)

B. *Ultimate analysis and equivalent weight of humic acid:* —

The ultimate analysis of humic acid obtained from unoxidised lignite was carried out by the micro methods in the chemistry laboratories of the Presidency College, Madras through the kind co-operation of the Professor of Chemistry. For purposes of comparisons the values for the ultimate analysis of humic acid from other lignites reported by other authors are also given alongside in Table III. The nitrogen content of the humic acids obtained by different methods was also estimated by us by the micro Kjeldahl technique and the result obtained, irrespective of the mode of preparation of the humic acid, was 0·98%.

The equivalent weight of humic acid was determined electrometrically using a Beckmann pH meter with a saturated calomel electrode and glass electrode assembly. The values obtained ranged between 210 to 214, the higher value being characteristic of humic acids obtained from oxidised lignite (Russel, 1932).

Table III

Ultimate analysis of humic acids obtained from various sources.

	Humic acid from		
	South Arcot Lignite	German * Lignite	Indian † oxidised coals
Carbon ..	60·0 %	60%	69·15
Hydrogen ..	4·0 %	4%	3·13
Nitrogen ..	0·96%	1%	27·72
Oxygen ..	35·04%	35%	

* (Brusset, 1943).

† (Chowdhury and Biswas, 1942).

C. *Preparation of ammonium humate:*—

Experimental:—The ammonium salt of the humic acid can be prepared by two methods. Method—I, Humic acid (10 gms) previously prepared by alkali extraction of lignite or oxidised lignite, was neutralised with a slight excess of ammonium hydroxide and after filtration, the filtrate was evaporated to dryness and kept at 100°C until all ammonia was expelled. Method—II, The humic acid was extracted with ammonium hydroxide as ammonium humate directly from lignite instead of extracting as sodium humate. For this 15 gms lots of oxidised lignite (containing about 80% humic acid) were mixed with 40 ml of ammonium hydroxide of different strengths. Extraction was done both in the cold and in a nearly boiling solution. The products of method I and II obtained were analysed both with regard to their ammonia content and their total nitrogen content by the micro-Kjeldahl technique.

Results and Discussion: The results are tabulated in Tables IV and V.

From Table IV, it is seen that in the method I of ammonium humate preparation, the nitrogen present as ammonia, agrees within 2% of the value calculated on the basis of the equivalent weights of humic acid (6·08%). This value is also nearly equal to that reported by Waksman (1938). The total nitrogen experimentally obtained (7·2 to 7·3%) is however difinitely higher than the calculated value obtained by adding together the nitrogen present in

Table IV

Preparation of ammonium humate from humic acid

Strength of ammonia soln. (30 ml.)	Mode of preparation	Yield %	Nitrogen content	
			as Total	as NH_3
5 N	Without heating	92·8	7·08	5·88
10 N	„ „	93·6	7·08	5·9
5 N	With heating	98·0	7·18	5·86
10 N	„ „	98·6	7·2	5·92
15 N	„ „	99·6	7·3	5·92

humic acid and the nitrogen present as ammonia. This difference though small has to be explained. It may be attributed to the possibility of some nitrogen entering into the constitution of the humic acid molecule during the ammonia treatment. This view is supported by the fact that for the more concentrated ammonia solution and at the higher temperature of treatment where the conditions are more drastic, the increase in the total nitrogen is still more appreciable.

Table V

Extraction of ammonium humate from lignite

(Method — II)

Strength of ammonia soln. (40 ml.)	Mode of Preparation	Yield %	Nitrogen present	
			as Total	as NH_3
5 N	Without heating	11·6	8·2	5·86
10 N	„ „	12·2	8·2	5·88
5 N	With heating	23·2	8·86	5·9
10 N	„ „	36·6	9·1	5·96
15 N	„ „	48·2	9·3	6·00

In the preparation of ammonium humate by method II it can be seen from Table V, that the extraction in the cold is not efficient since the yield is only 7-9% of the total humic acid present. Hot extraction with a recovery upto 65% of the total humic acid is obviously more efficient. It is to be expected that pressure extraction of lignite with ammonia is likely to give a much better yield in which case this method is bound to prove more economical than method I which involves two steps and loss of caustic soda. In method II, the same type of disparity exists, even to a higher degree, as in the method I, between the total nitrogen experimentally obtained and that calculated on the basis of the values for the nitrogen content of humic acid and the ammonia content of ammonium humate. This can be explained on the basis that in method II, since it is lignite that comes into contact with ammonium hydroxide, there is a possibility of greater amount of nitrogen reacting with the constituents of lignite leading to a higher absorption of nitrogen.

D. *Study of the effect of humic acid on plant growth:—*

The usefulness of humic acid as a fertiliser was investigated on an exploratory basis in a series of pot culture tests.* The following layout of pot culture tests was arranged. (a) 4 pots of soil only, (b) 4 pots of soil with a fertilising solution, (c) 4 pots of soil with 5 gms of humic acid, (d) 4 pots of soil with 5 gms of humic acid and the fertilising solution, (e) 4 pots of soil with 20 gms of humic acid and (f) 4 pots of soil with 20 gms of humic acid and fertilising solution.

All the pots contained 500 gms of garden soil of uniform quality and the fertiliser solution used contained potassium, nitrogen and phosphorus essential for plant growth. 100 seeds of mustard of uniformly good quality were sown in each pot and after 22 days the weights of each group of plants in each pot were determined. The dry weight was also obtained by drying at 80°C for 24 hours. In Table VI are given the results obtained.

* This section of the work was conducted with the kind and enthusiastic co-operation of Dr. T. S. Sadasivan, Professor of Botany, University of Madras and with the help of his staff, particularly Dr. C. S. Venkatram. The gratitude of the authors to them is hereby acknowledged.

Table VI

Effect of humic acid and fertilising solution on plant growth

	Conditions of growth		Fresh weight (gm)	Dry weight (gm)
1.	Soil only (Control)	1	6·505	0·4062
		2	6·200	0·4264
		3	6·010	0·4158
		4	6·530	0·4228
2.	Soil + fertilising solution.	1	7·98	0·4818
		2	7·550	0·4928
		3	7·792	0·4788
		4	7·323	0·5022
3.	Soil + 5 gms. humic acid.	1	7·9510	0·4274
		2	6·823	0·3988
		3	7·526	0·4428
		4	7·583	0·4346
4.	Soil + 5 gms humic acid + fertilising solution.	1	9·623	0·5978
		2	9·610	0·5898
		3	9·262	0·6138
		4	9·430	0·6106
5.	Soil + 20 gms humic acid.	1	6·606	0·3568
		2	6·021	0·3349
		3	6·038	0·3048
		4	6·28	0·3076
6.	Soil + 20 gms humic acid + fertilising solution.	1	10·231	0·5898
		2	9·270	0·4926
		3	10·336	0·6004
		4	9·136	0·4836

From Table VI, it can be seen that there is no appreciable increase in growth with humic acid alone. On the other hand there is a noticeable improvement in the uptake of fertiliser and hence in the quality of the plants, when humic acid and fertilising solution

were used in combination. Further it is seen that the humic acid required for the purpose is only about 1% of the soil.

These observations establish the significant fact that although humic acid by itself contributes little to plant growth, it plays a vital role in increasing the uptake of fertilisers by plants and can therefore find extensive application as a soil conditioner.

REFERENCES

1. Bangham, D. H., (1950) *Progress in Coal Science*, Interscience Publishers Inc. New York, 290 pp.

2. Brusset, M. H. (1943) Chemical Constituents of Lignites, *Bull. Soc. Chim. Fr.* **10**: 109.

3. Chowdhury, J. K. & Biswas, A. B. (1942) Studies on aerial oxidation of coal with special reference to the distribution of oxygen and carbon in coal and its oxidation products. *J. Indian chem. Soc.* **19**: 289.

4. Crowther, E. M. & Brencheley, W. E. (1936) The fertilising value and nitrifiability of humic materials prepared from coal, *J. agric. Sci.* **24**: 156.

5. Lahiri, A. (1954) *Utilisation of South Arcot Lignite.* Fuel Research Institute (India) Bulletin. C.S.I.R., Publications, Delhi.

6. Lowry, H. H. (1945) *Chemistry of coal utilisation* Vol. 1. John Wiley & Sons, New York, p. 70.

7. Russel, E. J. (1932) *Soil conditions and plant growth* Longman's Green & Co., London, p. 222.

8. Waksman, S. A. (1938) *Humus*. The Williams & Wilkins Co. Baltimore, p. 375.

J. Madras Univ., B, XXVI, No. 1, pages 31-50, 1956

Tectonic and Structural Study of Chamundi Granites and Gneissic Environs, Mysore

BY

S. K. Babu,

Department of Geology and Geophysics,
University of Madras, Madras-25.

(Received for publication on January 27, 1956)

ABSTRACT

The tectonic and structural study of the Chamundi granites and their gneissic environs are dealt with briefly in this paper. A map embodying structural features such as mineral orientation, foliation planes and joints is prepared along lines enunciated by Hans Cloos (described by Balk 1937). The field relations of the different rock types found in the area are summarised. Megafabric as well as petrofabric diagrams have been prepared. Since it is seen from the fabric study, that there is preferred orientation in all the diagrams of granites, gneisses and migmatites, the rocks are regarded as tectonites.

Introduction

The paper deals with the tectonic and structural study of Chamundi granite and the surrounding gneisses called the Nanjangudu gneiss. The Chamundi granite is regarded by the Mysore Geological Department as of the same age as Closepet granites. Closepet granite is the name given in Mysore to a band of coarse grained granites which form a chain of rounded bosses and domes, running N-S right through the middle of the state for a length of over 200 miles with an average width of 20 miles. Jayaram (1911) has described the Closepet granite as a complex of pink and grey granites with porphyritic, uniform, medium and coarse grained members traversed by fine pink and grey pegmatites and aplites all derived from a granite magma but belonging to different periods of intrusion and consolidation. It is considered to intrude all the earlier formations including Charnockites (Jayaram, 1907). The Closepet granites contain inclusions of many of the older rock formations e.g., hornblende granulites, hypersthene granulites, banded magnetite quartzite, garnetiferous quartzites and several types of crystalline schists. From a detailed study of some exposures of this granite and its inclusions near Closepet, it is inferred that the

magma which gave rise to these granites was initially potassic and that by contamination with older basic rocks it turned highly sodic and later diffirentiated (Rama Rao, 1940).

Outside this well defined zone of Closepet granites, there are other exposures of similar pink and grey porphyritic granites some of which have been regarded as belonging to this series, and of these, the Chamundi granite is one such, belonging to the Closepet granite series. Earlier literature on Chamundi granite is scanty. Bruce Foote's (1900) is the earliest report. He considered it as an older granite on which the schists were deposited. Wetherell and Sampath Iyengar described it as a mottled syenite boss intrusive into the gneisses. Smeeth (1916) considered it to be a granite belonging to Closepet age and in its isolated occurrence resembled the Arasikere and Banavar granites. The economic importance of these granites as ornamental stones has been touched upon by Laxmana Rao (1935).

The Chamundi granite has not so far been mapped. The area has been mapped for the first time by the author on a scale of 4″=1 mile. A structural map based on methods originated by Hans Cloos (described by Balk, 1937) has been prepared on a scale of 1″=1 furlong. Its structural features such as mineral orientation, foliation and joints were recorded in keeping with the technique suggested by Hans Cloos (See Map).

General Geology

The Chamundi hill is situated between Long. 76° 40′ and 76° 42′ and Lat. 12° 15′ and 12° 17′. The general level of the country around Chamundi hills is 2400 feet, above sea level, and is almost a plain, fairly cultivated land. The Chamundi hill rises abruptly from the plain to a height of 3405 feet above sea level and forms a high hill. The difference in heights between the top of this hill (3405) and the general level of the country (2400) is 1000 feet and the sudden rise of 1000 feet from the general level of the country renders it a prominent topographic feature in the scenery of the land. A temple and a palace built on the hill, with electric flood lighting makes it a landmark for miles around by day and by night.

The hill has an irregular outline somewhat elongated in an E-W direction. The western half of the hill is irregularly circular, at the top of which are situated the Chamundi shrine and the Royal palace. The hill gets elongated in the east tapering off ultimately

PART OF TOPO SHEET No 57 D/11

SCALE.

FURLONGS 3 2 1 0 1 MILE.

MANDYA AND MYSORE Dts

76 40'

Rifle Range

Palace

Chamundi

3405

Lalitadri Park

2840

Lalitadripura

Naronhalli

Yandahalli

2440

2476

Bandipalya

Ullanahalli

12° 15'

76° 40'

INDEX TO SYMBOLS

- Joint (inclined).
- Joint (Vertical).
- Planar Structure.
- 32° Lineation - strike of linear element and value of plunge.
- Horizontal Lineation.
- 65° Basic Schlieren (Dipping).
- Basic Schlieren (Vertical).
- 50° Foliation.

Nature Of Linear Element

- P Felspar Phenocryst.
- B Biotite.
- H Hornblende.

at Lalitadri park. This elongated portion runs like a ridge in an east-west direction.

The rain water falling on this hill flows as a number of small water courses down the slope of the hill in all directions from its top. These water courses constitute a radiating set of streams. These streams form tributaries to bigger streams which flow all round the hills at the bottom, and empty themselves into a number of tanks.

The rock exposures of Chamundi hills (Refer Map, Babu 1955) may conveniently be grouped as hereunder:

1. Porphyritic granite (Both pink and grey). 2. Coarse grained grey granite. 3. Coarse grained pink granite. 4. Fine grained grey granite. 5. Fine grained pink granite. 6. Medium grained pinkish grey granite. 7. Banded gneiss. 8. Amphibolites. 9. Hornblende schists. 10. Pegmatites and Aplites.

Field Relations

Porphyritic granites are found mostly at the foot of the hills, extending only to some distances up into the flanks. There are pink and grey types present here. The colour mainly depends upon the colour of the phenocrysts present in the rock. It becomes exceedingly difficult often to trace gradual passage of one variety into the other. There are various mixtures of grey and pink varieties in different proportions. The pink members of the porphyritic granites are intensely crushed. The felspar phenocrysts (Microcline) are embedded in a coarse grained matrix composed of felspar, quartz and biotite. The length of the phenocryst varies from $2\frac{1}{2}''$ to $\frac{3}{4}''$ length and breadth varies from $2''$ to $\frac{3}{4}''$. There are also phenocrysts of $\frac{1}{2}''$ square. The felspar phenocrysts show lineation. At places the phenocrysts and mica show platy parallelism or planar structure due to their alignment with their largest faces in parallel planes. The strike of planar structure is almost N-S being vertical or dipping at high angles to the west. There are caught up patches of dark basic material occurring in it as streaks, patches and lenticles. These basic patches and the porphyritic granites are cut across by veins of aplites and pegmatites.

The porphyritic granites pass into coarse grained granites, with the decrease in the grain size of the phenocrysts of felspar. Here also we find coarse-grained pink and grey granites. The pink members show intense crushing. The pink and grey coarse grained

granites also grade into each other, and it is difficult to demarcate the boundary between the two. They also occur as caught up patches in porphyritic granites. One such patch of coarse grained grey granite in grey porphyritic granite is found to the north of Uttanahalli.

There are fine grained and medium grained pinkish grey granites. The fine grained pink granites are found at the southern extension of the hills. There are well developed, pronounced sets of joints in them. The contact of these granites with the adjoining coarse grained granites is sharp and there are no gradational contacts. The sharp contact probably points to their intrusive nature, and the fine grained texture to their formation from the consolidation of highly acidic residual liquors devoid of any volatile constituents. These fine grained pink granites occur mostly amidst gneisses and in contact with amphibolites often exhibiting intrusive relationship with the latter.

The medium grained pinkish grey granite is fairly extensive and occurs as an elongated patch roughly in a NE-SW direction. It is found in contact with grey porphyritic granite in the NE half, and with coarse grained pink and grey granites in the western half of the map. There is also a small exposure of this pinkish grey granite to the north of the map amidst porphyritic granite in contact with the gneiss. Caught up patches of coarse grained pink granite are found in pinkish grey granite in the exposures to the NE of the map at Lalitadri Park. Pinkish grey granite shows crude banding. At a few places they also show lineation and planar structure. There are veins of pegmatites and aplites, both grey and pink, cutting across the pinkish grey granites.

The banded gneisses are found in contact with the porphyritic granite. The gneisses are found at the foot of the hill or 2-3 furlongs away from the foot of the hill. At places, as for example to the north of the map, the bands are so sharp and mineral grains so fine that the rock looks like a flaser gneiss. In a well to the NW foot of the hill granites passing downwards into well banded gneisses could be easily traced. The banding is due to injection of silica rich liquids along the planes of schistosity of the original hornblende schist of the area. Caught up patches of Hornblende schist and amphibolite in the gneisses substantiate this statement.

Pegmatites and aplites cut across all rock formations in this area. There are two types of these rocks namely, grey and pink. The grey variety is confined only to the grey members of the granite series, and the pink ones to the pink series. Aplites are

younger than pegmatites, as they cut across pegmatites. The same can also be proved from another evidence, i.e., there are veins of aplites bounded on either side by pegmatites. The pegmatite margin is highly coarse grained. The aplite portion at the centre is fine grained and is devoid of mafic minerals. Aplite veins have small dioritic patches as inclusions. Pegmatites and aplites strike in different directions. In general they strike EW, S 70° W, N 70° W. They are mostly vertical, some dip at angles of 40°-50°.

There is a small belt of hornblende schist 3 miles to the east of Chamundi hills near the village Varuna. It is a small belt running for over 7 miles northwards from Varuna with a width of 2-4 furlongs. The band forms a small ridge whose trend is also N S. The rock is composed of big, long prismatic crystals of hornblende and garnet. The band is bordered on either side by hornblende gneiss.

Granite

The rocks are essentially composed of platy minerals like mica and felspars. They show platy parallelism or planar structure, with the largest face (010) lying parallel to the layers. Here and there, at the exposed surfaces felspars show a slight linear trend in a N-S direction. These cannot be taken as lineation, as they are only one of the crystal faces of the felspars exposed on the surface and lying in the plane of platy structure. The manner in which the felspar phenocrysts are arranged in the porphyritic granites of Chamundi is shown in block diagram Fig. 1.

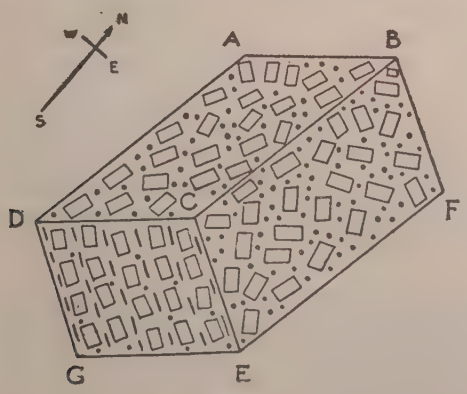

Fig. 1

In Fig. 1 ABCD is the top of the exposed surface. Here the felspar phenocrysts are apparently linear. On the vertical sur-

face DCEG the phenocrysts trend vertically. In this vertical surface the platy structure formed by the phenocrysts is dipping eastwards. This manner of arrangement of phenocrysts is seen in some of the quarries. But on the surfaces ABCD and DCEG only one of the faces of the felspar phenocrysts is exposed. If the lineation is to be formed it must be searched for in the plane of the planar structure, which in Fig. 1 is the inclined surface CBFE. In this plane it is seen that the felspar phenocrysts lie in all directions and do not show any linear trend in any particular direction.

At only one portion, i.e., at the south western extremity of the hill and N 15° E of Bandipalya do the felspar phenocrysts show some sort of lineation, and this is shown in block diagram Fig. 2.

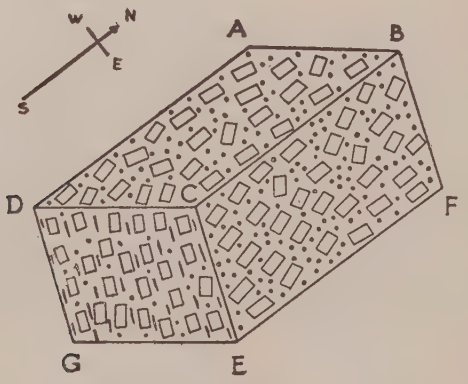

Fig. 2

The arrangement of the felspar phenocrysts on the surfaces ABCD and DCEG is the same as in Fig. 1. But in the plane BCEF, which is the plane parallel to the planar structure the felspar phenocrysts show lineation pitching south at 32°. This is so at the place N 15° E of Bandipalya.

In the greater part of the hill, where the exposed surface of rocks are perpendicular or diagonal to the cleavage planes of biotite mica, mica appears as thin streaks and lines. At a first glance they are likely to be mistaken for lineation. But in the quarries where granitic rocks are cleaved parallel to the cleavage flakes of mica, no such elongation of mica flakes is found. In fact

they are irregularly rounded or almost even in outline. Such a case is shown in block diagram Fig. 3.

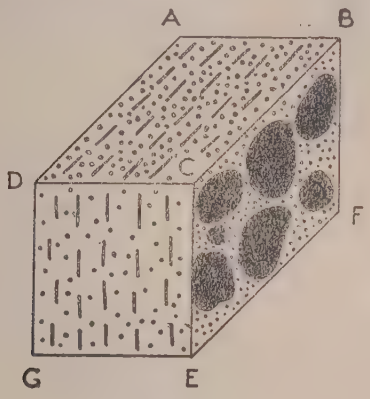

Fig. 3

Surfaces ABCD and DCEG are perpendicular to the cleavage flakes of mica shown as black areas in the plane CBFE. Hence on the surfaces ABCD, DCEG micas appear as thin streaks and lines. On the surface BCEF which is parallel to the cleavage flake, mica flakes are irregularly rounded or even.

There are caught up patches of dark basic schlieren in the granitic rocks. They range in size from a few inches to several feet. They are rounded, lenticular and some are oval. They all trend in a N-S direction, and dip vertically or at high angles to the west. These basic patches are also drawn out in N-S direction in thin streaks in the form of flow layers parallel to planar structure. There are two types of xenoliths.

1. The original foliation is parallel to the length of xenolith and thus to the planar structure of the granite.

2. The original foliation is destroyed and the only macroscopic minerals are porphyroblasts of felspars, which show little tendency to parallel orientation.

3. There are autoliths, which consist of segregations of biotite in a ground mass of quartz and felspar. There are also autoliths of salic segregations of felspars.

Country Rocks

The country rocks are the hornblende granitic gneisses found at the flanks in the low lying regions immediately in contact with

porphyritic granite. Lineation is well exhibited by the prismatic crystals of hornblende to the N and NE of the map. Lineation pitches to the north at angles from 26°-37°. The strike and dip of the gneisses and the trend of lineation are shown in block diagram in Fig. 4.

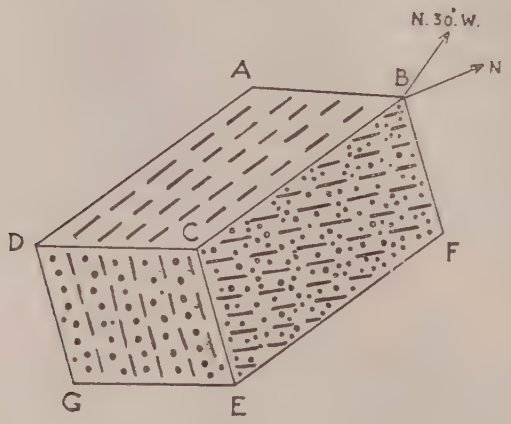

Fig. 4

On the horizontal surface ABCD, is shown the strike of gneisses which is N 30° W. The face of the foliation plane which dips eastwards is shown in the vertical plane DCEG. CBEF is the plane of foliation itself, where in lie the prismatic crystals of hornblende (shown in black dashes). The longest axes of this prismatic mineral are oriented parallel to one another, whereas the strike of the foliation is N 30° W, the horizontal projection of the lineation is north, and lineation pitches north at an angle of 26°. Surface DCEG is perpendicular to lineation, and hence linear elements (hornblende needles) appear as dots. Dots on CBFE represent salic elements.

Gneissic foliations are found in the low lying regions all around the hill. To the west of the hill, foliation strikes north and dips west at low angles. To the SW of the hill, they strike NW and dip SW at angles ranging from 30°-35°. The northern portion of the area is interesting from the structural and genetic point of view, on account of rapid variations in the direction and amount of strike and dip of the foliation planes. At the very foot of the hill near the rifle range the foliation strikes almost E-W and dips at higher angles varying from 50°-80°. The dip is generally outward away from the hill, but at portions it is inwards into the

hill. This rapid variation in the direction of dip of foliation planes indicates the contortions undergone by these gneissic bands in this portion of the area. Away from the foot of the hill and to the north and east of rifle range, the foliation strikes north or a few degrees to the east or west of north, and dips at angles of more than 60°. To the east and south east of Lalitadri-Park, the foliation strikes in a general N-S direction dipping east again. Only at a few places here the direction of dip changes to the west. This points to local small foldings here and there in the gneisses in an otherwise N-S regional structure. The margin of the south eastern foot of the hill is in a general N-S direction, and the foliation here trends N 20° W parallel to the margin of the hill, dipping east again.

It is seen from the above description that the planes of foliation of the gneisses sweep around the hill and in the low lying regions and that their strike is parallel to the margin of the hill at the foot, and away from the foot of the hills, they strike generally N-S dipping east at the N, NE, E and SE of the region, and to the west and south west at the western and south western parts of the region forming almost a quaquaversal pattern.

Joints

A study of the structural map of Chamundi granites indicates, that of the several types of structures characteristic of granitic bodies, joints are more dominant and well developed in the granitic rocks of Chamundi. Though lineation is not well developed and seen in these rocks, the planar structure which is found at several places trends in a N-S direction. The joints of the area are resolved by considering their relation to the planar structure.

1. Longitudinal Joints which are parallel to planar structure.
2. Cross joints which cut the planar structure at 90°.
3. Diagonal joints which cut the planar structure at angles of about 45° or less.

Longitudinal and diagonal joints are very well developed in the granitic rocks of Chamundi. These joints account for more than 75% of the joints of the area. There are other minor joints dipping at low angles. At the south eastern portion of the hill near Jwalamuki road there are flat lying joints, dipping at low angles of less than 10° and some of them are almost horizontal.

The jointing in the gneisses is not so regular as in granites. The joints developed in gneisses are mostly bedding or strike joints trending in the direction of foliation. At a few places we find these joints being folded due to buckling of gneisses.

The field observations were checked by analysing the joints on a Schmidt equal area projection.

The planar structure was made to coincide with the vertical plane through N-S axes. The poles of the joints were then plotted so that the original geometric relation of the joints to the planar structure was maintained. Although 1200 readings of joints were recorded in the field, it was possible to plot only 750 poles of joints. The poles were plotted on the southern hemisphere, and the subsequent point diagram contoured with 1% counter. (Ref. Fig. 5 and 6.)

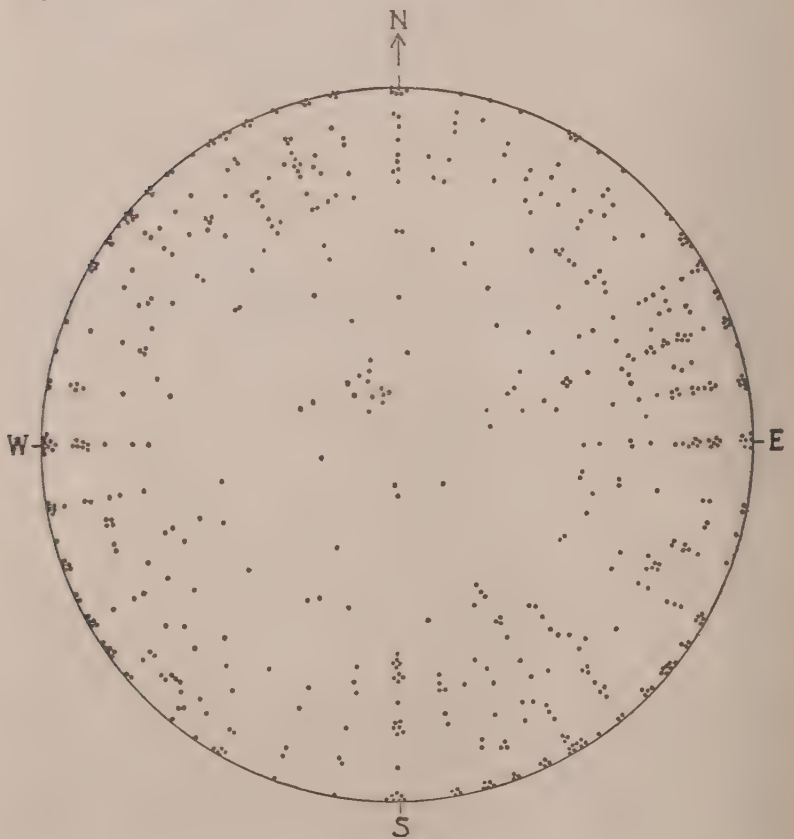

Fig. 5

The joints do not show any preferred orientation in any particular direction. They trend in all directions with a high angle of dip. The scatter diagram of these joints explains this. The points which are the poles of the joint planes lie on and very near the circumference of the projection indicating a high angle of dip for the majority of these joints.

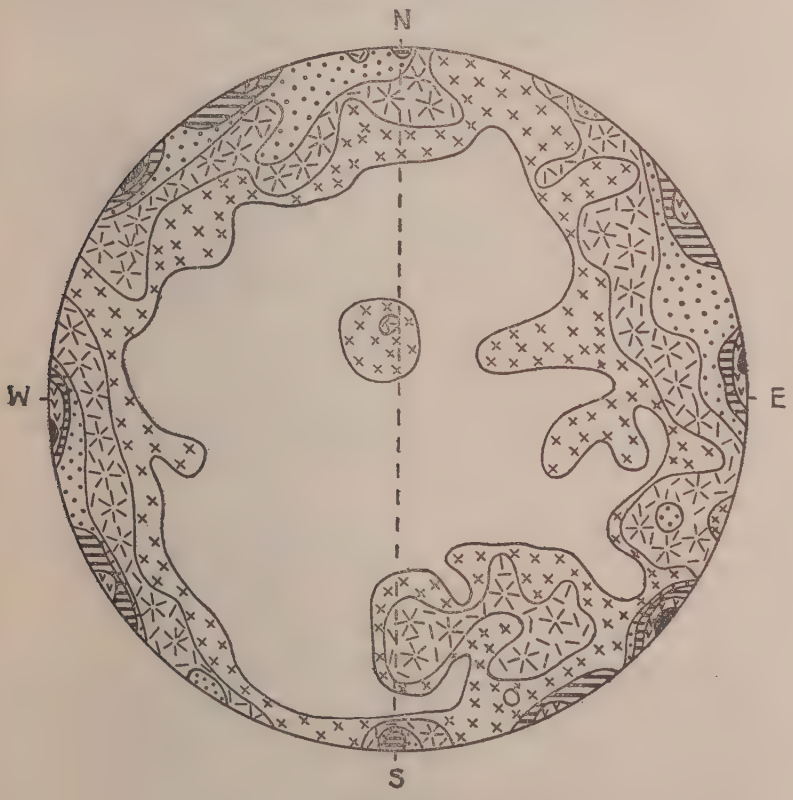

FIG. 6

Plot of 740 Joint pole readings.

In the contour diagram however, four maxima are found two to the NW and SE of the diagram, and also to the east and west of the diagram. This means that there are two sets of prominent joints, one set striking NE because the maxima are at NW-SE of the diagram. They are the diagonal joints, because they are

roughly 45° to the planar structure. The other set strikes north because the maxima is at EW. They are longitudinal joints, because they are parallel to the planar structure. There is also a minor maxima at N-S, corresponding to cross joints striking east, and cutting the planar structure at 90°. In the centre of the diagram we find a small minor maxima corresponding to flat lying joints with low angles of dip. There are also other maxima on either side of planar structure corresponding to minor joints.

Nature of the Joint Surface

The joints developed in the granites of the Chamundi are generally smooth and even. At a few places they are rough and uneven. Generally they are free from mineral deposition. But often the joint surfaces are coated with a thin brown film of limonite. Striations are absent. Only one case was noticed near Lalitadri Park, where the joint surfaces are striated.

Movement on the Joints

Longitudinal joints show movement by the displacement of veins in granites. The displacement is not of a high magnitude. These joints are filled in by pegmatites and aplites.

The other set of joints show no movement or displacement. They show only offsetting of one against the other. But the diagonal joints show crushing on either side of the joint plane.

Contact

The contact is not visible in the field, and very few sections across the contact were available. But at the northern portion of the hill in a nalla we find gneisses passing right into the hill and granite intruding into the gneisses. This indicates intrusive contact of the granite with the gneisses. Also in a well at the north-western foot of the hill near Gavimut, granites passing downwards into well banded gneisses could be easily traced. At the northern portion of the area the foliation shows rapid variations in strike and dip. The variation is due to frictional movement at the contact caused by the intrusion of the granitic body into the original rock which was a hornblende rock. The presence of a number of hornblende schist patches in the gneisses confirms this. This intrusion obviously causes the formation of foliation planes in the wall rocks, and especially these foliation planes are more pronounced in the wall rocks which are more

basic in composition. The wall rock constituents which were originally hornblende schists have now been converted into biotite and this platy mineral biotite has facilitated the formation of foliation planes all along their contact. The foliation plane found all round the hill may therefore be taken as the contact of the granite with the gneisses represented by the foliation planes.

Veins

The veins are represented mostly by pegmatites and aplites. They vary in size from a few inches to several feet in width. Usually they cut across all the rock formations of the area. There are both pink and grey veins. Pink ones confine only to pink members of the granite, and grey ones to the grey members of the granite. Evidences of the association of the former with the latter are wanting.

Aplites :—These occur mainly in porphyritic granites. They vary in width from a few inches to 2-3 feet. They usually follow up the joints, and fill up the joint planes. They sometimes enclose small oriented dioritic patches (Fig. 7). These veins usually cut across the planar structure.

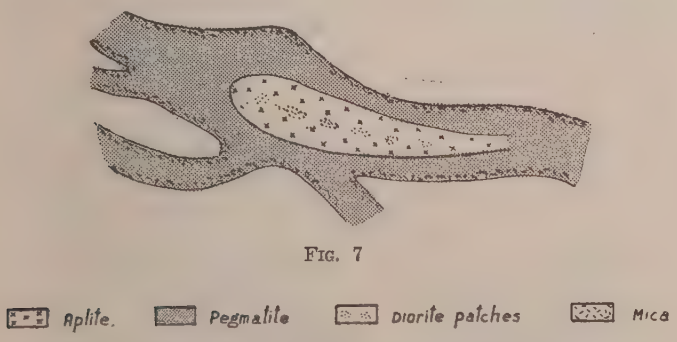

Fig. 7

Pegmatites :—They are coarsely crystalline aggregates of quartz and felspar intergrown with each other. There are two types of pegmatites namely grey and pink. They are found sometimes bounding aplites. They are coarse at their margins, and we find development of flakes of mica. They cut across aplites and also displace them (Fig. 8). They vary from small veins to big dykes. There are also dilational pegmatites.

Felspathic Veins:—The felspar phenocrysts in porphyritic granites are segregated, tending to form felspathic veins. These veins vary in width from 2″-3″. Grey felspathic veins are also

FIG. 8

Aplite Pegmatite P.G Granite Basic patch.

found along the planes of schistosity in the hornblende schists. They seem to be injection veins. These veins are transected by another set of veins (Fig. 9 and 10).

FIG. 9

G.P. Granite. Felspathic Vein. Basic Patch.

Petrofabric Study

To determine preferred orientation in these rocks, sections were cut perpendicular to the planar structure in both granites and gneisses. The gneiss shows a well banded structure of mafic

and salic streaks. The granites, however, show only an irregular arrangement of the constituents in a plane.

FIG. 10

FIG. 11
Petrofabric diagram of 200 quartz grains.
Contour interval 1% maximum 5%.

The poles were plotted in the lower hemisphere of a schmidt net. The a-c diagram of the gneiss is given in diagram (Fig. 11). This shows four maxima and several minor maxima at the periphery with an incomplete "a-c" girdle. The maxima have an interval of 45° between each other and one on either side of the a axis. This corresponds to the quartz pattern maximum II of Sander, but the interval between the maxima there is 90° (Fairbairn, 1954, p. 10). Such diagrams however with angular intervals less than 90° have been recorded by Sander in schists and granites (Sander, 1950, Fig. 14, 16 and 17, p. 358). These seem to correspond to the position of the lamellae of quartz. It was seen in the slide of the gneiss studied that most of the quartzes showed an undulose extinction and were segmented into broad lamellae. The C-axis in each of the lamellae was plotted.

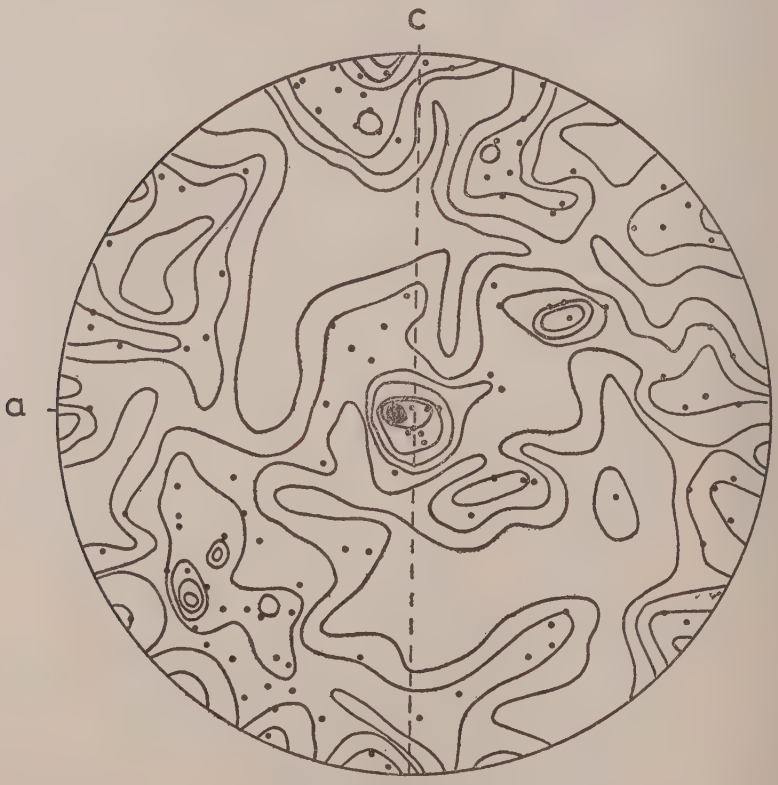

Fig. 12

Petrofabric diagram of 200 quartz grains.
Contour interval 1% maximum 6%

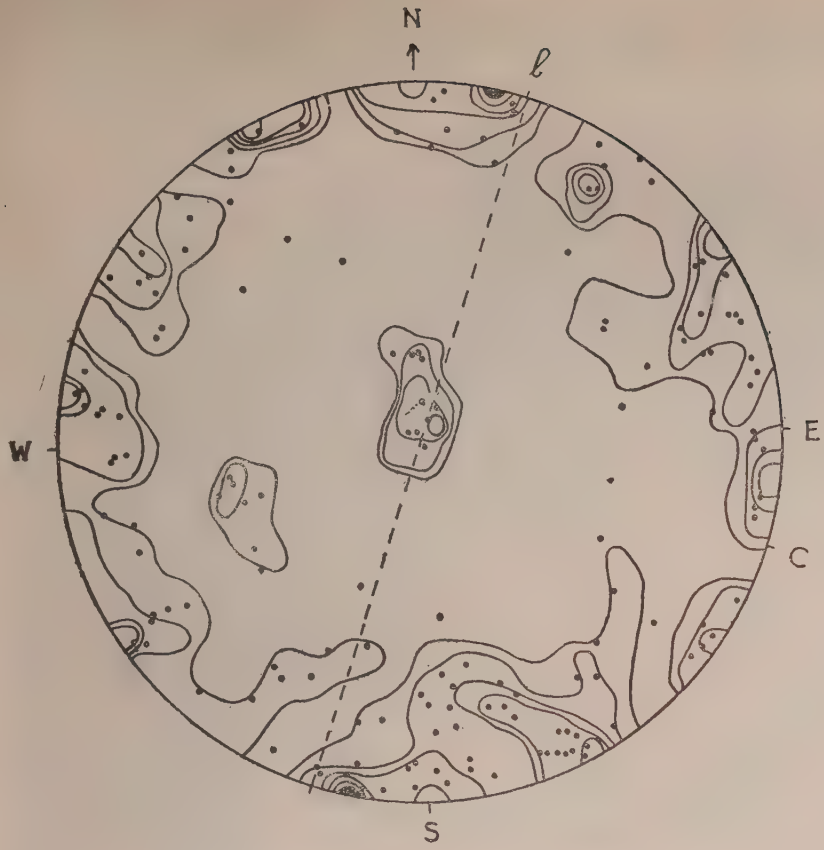

FIG. 13
Petrofabric diagram of 200 quartz grains
Contour interval 1% maximum 6%

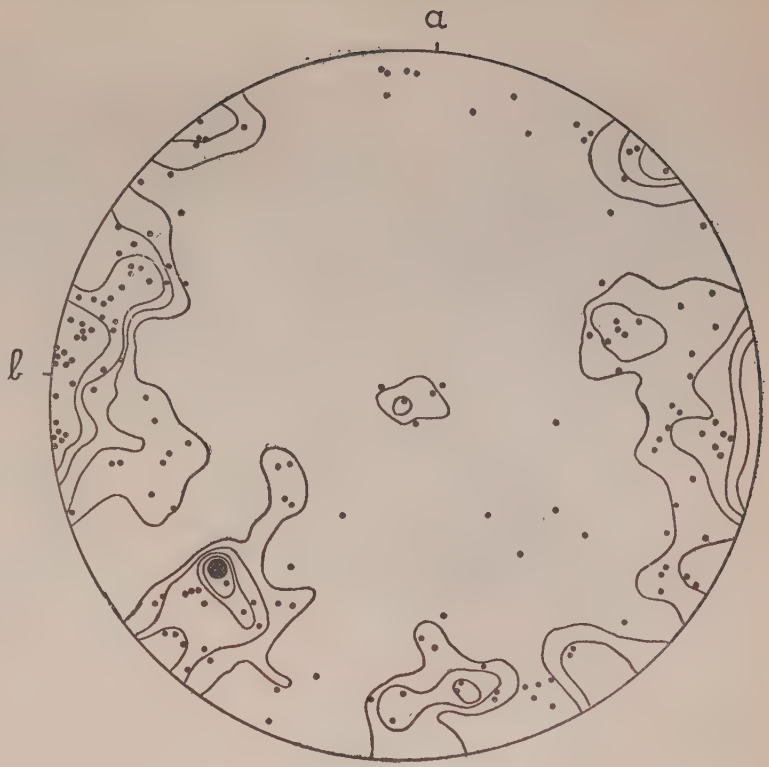

FIG. 14
Petrofabric diagram of 200 quartz grains.
Contour interval 1% maximum 4%.

FIG. 15

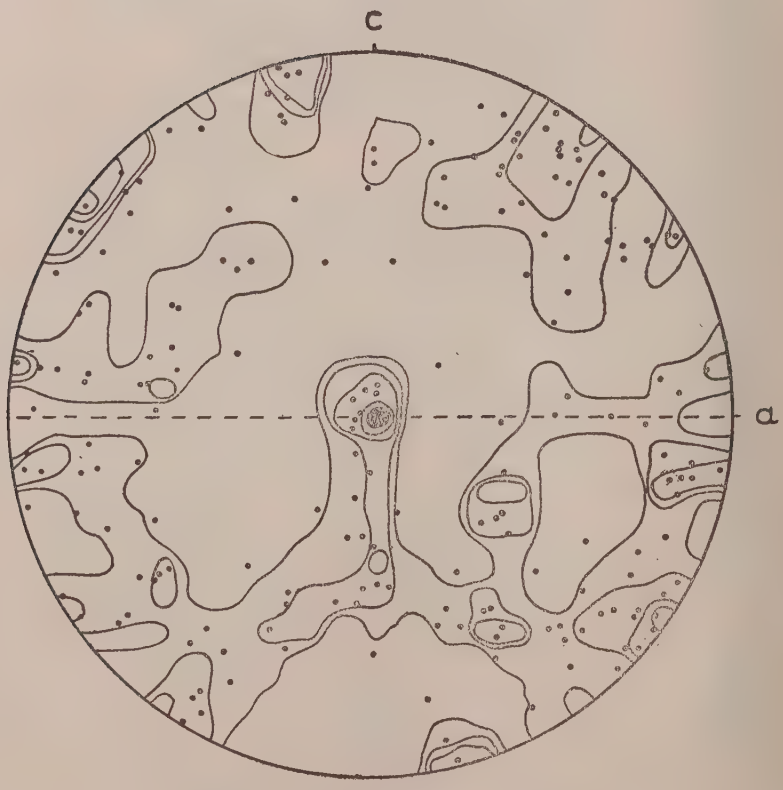

FIG. 16

Petrofabric diagram of 200 quartz grains.
Contour interval 1% maximum 5%.

Diagrams (Figs. 12 to 14) are of a grey porphyritic granite. Petrofabric diagrams were prepared for all the planes a-c, b-c, and a-b. The granite in hand specimen is porphyritic with phenocrysts of felspar, which are flow oriented, and the mafic minerals sweep round these phenocrysts, sometimes assuming linear trends and shows a rough planar structure. The relation of these diagrams to the several aspects of granite is shown in sketch in Fig. 15.

Here the central maximum has a cross girdle (a-b) and also an incomplete a-c girdle developed. It therefore represents maximum VII of Sander (Fairbairn, 1954, p. 10).

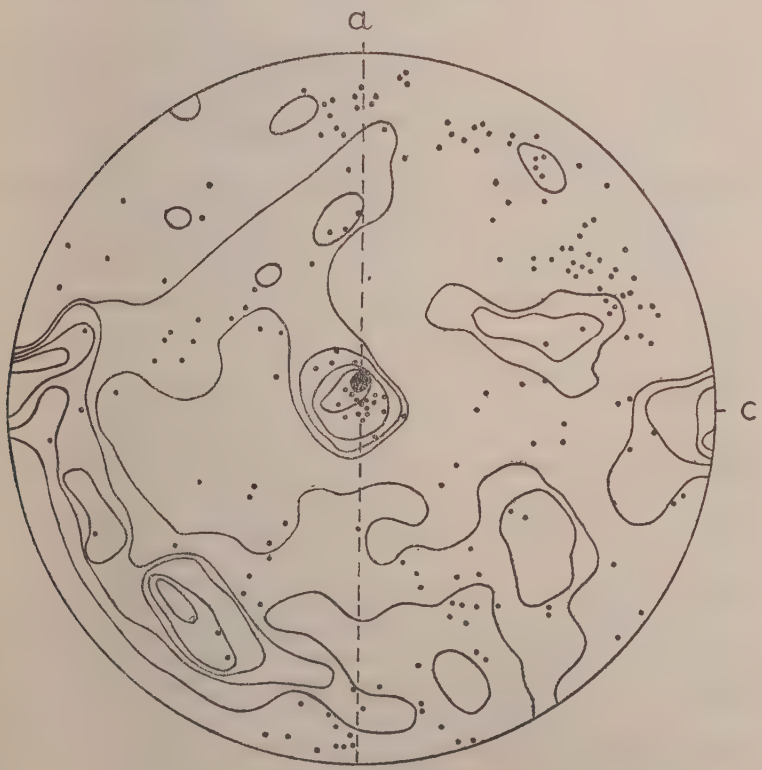

Fig. 17
Petrofabric diagram of 200 quartz grains.
Contour interval 1% maximum 11%.

Diagrams (Figs. 16 and 17) are again a-c diagrams of another porphyritic granite and a migmatite. These also show a single maximum in the centre but the a-b girdles are ill developed.

Since there is preferred orientation in all the diagrams studied, of gneiss, granites and migmatite, the rocks can be classified as tectonites.

Acknowledgments

The author avails this opportunity to place on record his gratitude and indebtedness to Dr. P. R. J. Naidu for his valuable guidance and encouragement throughout the work, and to Sri K. V. Suryanarayana for his guidance and helpful suggestions during the field work.

REFERENCES

Babu, S. K. (1955) Heavy accessories of Chamundi granites and surrounding gneisses. *J. Madras Univ.*, B, 25: 291-300.

Balk, R. (1948) Structural behaviour of igneous rocks, Edward Ann. Arbor.

Bruce Foote. (1900) Traverses through the Mysore state *Mem. Mysore geol. Dep.*, 1: 88.

Fairbairn, H. W. (1954) *Structural Petrology of Deformed Rocks*, Addison Wesley Press, Inc. Cambridge, Mass, p. 10.

Jayaram, B. (1911) Report on a portion of the closepet granite and associated rocks, *Rec. Mysore, geol. Dep.*, 22: 75 and 99-101.

Laxmana Rao, S. (1935) The occurrence of ornamental building stones in parts of Mysore state, *Rec. Mysore, geol. Dep.*, 33: p. 47.

Rama Rao, B. (1940) The Archaean complex of Mysore, *Bull. Mysore geol. Dep.* 17: 79.

Sander, B. (1948) *Einfuhrung in die Gefugekunde der geologischen Korper*, 2 Vols. J. Springer, p. 358.

Sampath Iyengar, P. Report on the felsite porphyry dykes of Srirangapattam taluk and parts of the adjoining taluks of Mysore, Frenchrocks, and Mandya, *Rec. Mysore geol. Dep.*, 7: 22.

Smeeth, W. F. (1916) The Dharwar system, *Bull. Mysore. geol. Dep.*, 6: 9.

Wetherell, E. W. *Rec. Mysore. geol. Dep.*, 3: 98.

J. Madras Univ., B, XXVI, No. 1, pages 51-61, 1956

Methyl Ethyl Ketone Peroxide as an Initiator in the Polymerization of Methyl Methacrylate

BY

M. R. Gopalan and M. Santappa
Physical Chemistry Laboratory,
University of Madras

(Received for publication on February 7, 1956)

ABSTRACT

Methyl Ethyl Ketone Peroxide was employed to catalyse the polymerization of methyl methacrylate in the range 65-80°C in bulk as well as in solution. From two simple measurements of overall rates and degrees of polymerization under various conditions it was possible to evaluate (i) the ratio of the propagation constant to the termination constant raised to half power (ii) transfer coefficient for the monomer (iii) transfer coefficient for the catalyst (iv) transfer coefficient for the solvent (v) Rates of initiation etc. The specific rate transfer constants for the monomer and the catalyst in solution appeared to differ slightly from those in bulk.

Methyl ethyl ketone peroxide (MEKP) has not been extensively employed as an initiator of vinyl polymerizations. Vaidhyanathan and Santappa (1955) and Mahadevan and Santappa (1955) have briefly reported polymerization of styrene and methyl acrylate with this catalyst. A systematic investigation of kinetics of vinyl polymerization with MEKP as initiator was undertaken. A few results in the polymerization of methylmethacrylate at 65°-80°C are briefly reported here.

Theoretical: Various rate equations and equations relating to degrees of polymerizations under a variety of conditions have been explained in great detail in the previous publications by Santappa et al (1955). The following relationships which are relevant to our present work are being reproduced.

Catalysed overall rate R, is given by

$$R = \frac{k_p\, k_d^{1/2}\, f^{1/2}[\mathrm{Cat}]^{1/2}[\mathrm{M}]}{[k_{to} + k_{td}]^{1/2}} = K[\mathrm{Cat}]^{1/2} \qquad .. \quad (1)$$

where k_p, k_{to} and k_{td} are the rate constants for propagation, termination by combination and disproportionation respectively in the

polymerization of monomer (M), k_d, f are the rate constant for the spontaneous decomposition of the catalyst (Cat) and catalyst efficiency respectively. The latter, according to definition by Matheson (1945) is

$$f = \frac{k_a[M]}{\{k_a[M] + k_b\}} \quad .. \quad (2)$$

k_a and k_b are the rate constants for the initiation and irreversible association respectively of the primary radicals.

Further, the reciprocal of the degree of polymerization P_n is given by

$$1/P_n = AR + C_M + C_{cat}\frac{R^2}{K^2[M]^3} + C_s\frac{[S]}{[M]} \quad .. \quad (3)$$

C_M C_{cat}, C_s are transfer coefficients for monomer, catalyst and solvent respectively; A is $[k_{tc} + 2k_{td}]/k_p^2[M]^2$. The third term in the R.H.S. of equation (3) may be replaced by $C_{cat}\frac{(Cat)}{(M)}$.

Experimental: Methyl methacrylate, a Rohm and Haas product, was purified by repeated distillation in oxygen free nitrogen under reduced pressure and was always stored in a refrigerator. Methyl ethyl Ketone peroxide was supplied as 60% solution by Laporte Chemicals. Details of estimation and purity of the monomer and catalyst as well as deaeration of the system are reported in previous publications. (Santappa et al)

Polymerization of methyl methacrylate was carried out in a glass ampoule (8 cms. long and 1 cm. diameter) well cleansed and flamed before use. After deaeration of the monomer catalyst system with nitrogen for about half hour, the ampoule was sealed and heated in a thermostat bath at the desired temperature till the monomer was converted to ca. ten percent, found by few trial experiments. The time for polymerization was usually one to two hours. Afterwards the ampoule was taken out of the thermostat and chilled in a beaker containing ice. The fused capillary of the ampoule was then broken open and the contents were dissolved in small quantities of acetone and quantitatively transferred to a beaker. Addition of methanol precipitated the polymer which was transferred to a weighed sintered glass crucible, washed with methanol and dried to a constant weight at 70°C. From the weight

of the polymer, rate of monomer disappearance was evaluated. The degrees of polymerization of the polymers were determined by measuring the viscosities of 0·1 percent polymer solutions in benzene in B.S. No. 1 Ostwald Viscometer and using the well known Staudinger's relationship $n = k[\eta]^{\alpha}$, the values of $k = 2{\cdot}8 \times 10^3$ and $\alpha = 1{\cdot}32$ having been determined by Baxendale, Bywater and Evans for polymethyl methacrylate, (1946).

Results and Discussion:

Percentage conversion against time (Fig. 1) was studied in the polymerization of methyl methacrylate catalysed by MEKP

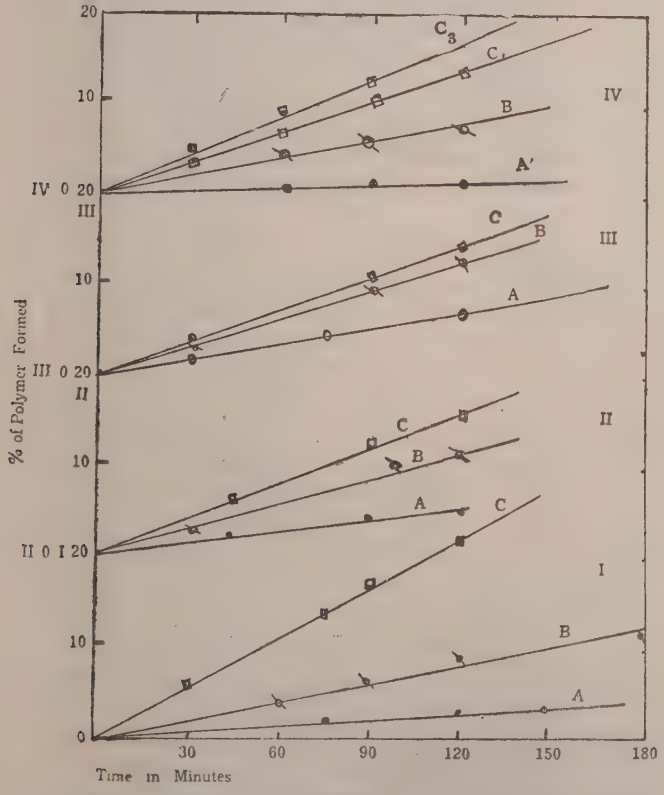

FIG. 1. Percentage Polymer formed vs. Time in bulk and in solutions. Catalyst concentration were: $A' = 10^{-3}$; $A = 10^{-2}$; $B = 5 \times 10^{-2}$ $C = 10^{-1}$.

Set I Bulk; II Ethyle Acetate; III Benzene; IV A' and C_1 Toluene; IV B and C_3 Methyl Ethyl Ketone.

both in bulk (monomer M 9·2 molar) and in solution (M = 4·6 molar). It was found that all the lines in the Fig. 1 passed through origin. This indicated the absence of period of induction and suitability of the catalyst in the further studies of polymerization.

Employing a hundred fold variation of concentration of MEKP the order of reaction with respect to catalyst was studied. As with radical initiated vinyl polymerizations and in conformity with equation (1) above, plots of Rate vs (Cat)$^{1/2}$ were all linear (Fig 2)

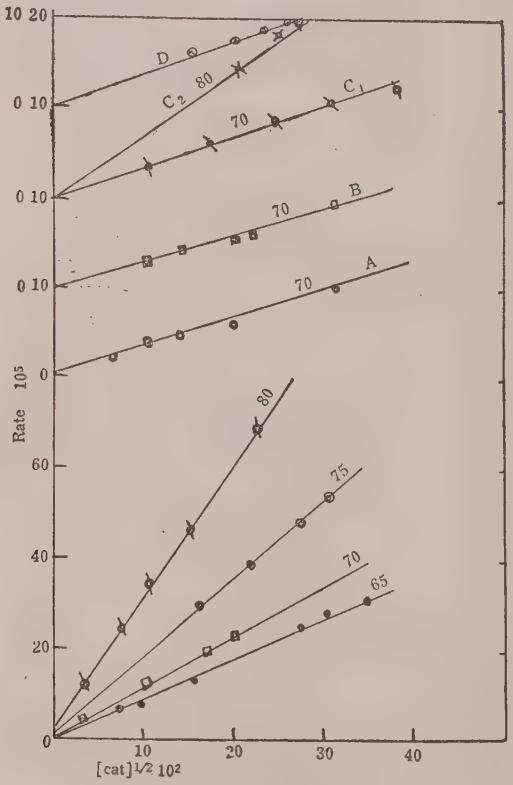

Fig. 2. Rate vs. (Cat)$^{1/2}$ in Bulk at temperatures 65°, 70°, 75 and 80°C from below and in solution (4·6 molar).

A Benzene, B Ethyl Acetate, C_1 Toluene D Methyl Ethyl Ketone at 70°C and C_2 Toluene at 80°C.

both in bulk and in solution. The absence of any intercept on the ordinates of the plots indicated that the thermal rate did not make any contribution. The slopes of the plots in bulk gave the values of $K \times 10^3$ as 0·83, 1·0, 1·7, 2·89 and the values for the constant

$K' = \frac{k_p (k_d f)^{1/2}}{k_t^{1/2}}$ as $0{\cdot}9053 \times 10^{-4}$, $1{\cdot}086 \times 10^{-4}$, $1{\cdot}848 \times 10^{-4}$, $3{\cdot}142 \times 10^{-4}$ at 65°, 70° and 80°C respectively and $K' = 1{\cdot}936 \times 10^{3}$, exp (−9065/RT for temperatures 65° to 70°C and $K' = 4{\cdot}43 \times 10^{6}$, exp (−16760/RT) for 65-75°C. Values of $K \times 10^3$ in benzene, toluene, ethyl acetate and methyl ethyl ketone solvents ($M = 4{\cdot}6$ molar) at 70° C were 0·3, 0·318, 0·3 and 0·4 respectively and for toluene $K = 2{\cdot}79 \times 10^{9}$ ex (−20440/RT) was found. The values of activation energy for overall rate thus varied within wide limits. A value of ca 10 ± 3 K Cals was reported for the overall activation energy in bulk by Flory (1937). This value was supported recently by Umasankar Nandi and S. R. Palit (1955) in the homogeneous polymerization of methyl methacrylate catalysed by hydrogen peroxide. The latter authors have given divergent values for overall activation energy in solution polymerization. A calculation of the activation energies from values of K by various authors given in the paper by Tobalsky (1953) indicated the divergent nature of the values and therefore in our opinion a great uncertainty appeared to be attached for the accuracy of those values.

The relationship between the degree of polymerization and rate has been studied both in bulk and in solution in the four solvents mentioned above. It may be pointed out at the outset that equation (3) given under theoretical above, generally obeyed for bulk and solution polymerizations though it must be admitted that methyl ethyl ketone peroxide conformed to the same behaviour as Tertiery Butyl Hydroperoxide and Cumene hydroperoxide, which exhibit certain curvature in the plots of $1/P_n$ vs Rates. From studies of $1/P_n$ vs Rates both in bulk and solution it was possible to evaluate $A (= k_t/k_p^2[M]^2)$, transfer constants for monomer, catalysts and solvent. In bulk and at very low concentration MEKP ($\sim 10^{-3}$) it was presumed that the transfer of growing polymethyl methacrylate chain with the catalyst was negligible and from plots of $1/P_n$ vs Rates (Fig. 3) the slopes gave A and the intercepts gave C_M The A values at 65, 70, 75 and 80°C were 1·5, 1·22, 0·895 and 0·3 respectively. Values of $k_p/k_t^{1/2}$ obtained from A at 65, 70, 75 and 80°C were $8{\cdot}87 \times 10^2$ $9{\cdot}84 \times 10^{-2}$ $11{\cdot}62 \times 10^{-2}$ and $19{\cdot}85 \times 10^{-2}$ respectively and $k_p/k_t^{1/2} = 1{\cdot}69 \times 10^4$ exp (—5112/RT). The C_M values from the intercepts at 65, 70, 75 and 80°C were 2×10^{-5}, 3×10^{-5}, $3{\cdot}3 \times 10^{-5}$ and 4×10^{-5} respectively. With C_M values so obtained two methods of evaluating C_{sol} values in bulk were conceived. The first method was to plot $\{(1/P_n) - C_M\}/R$ against R at high catalyst concen-

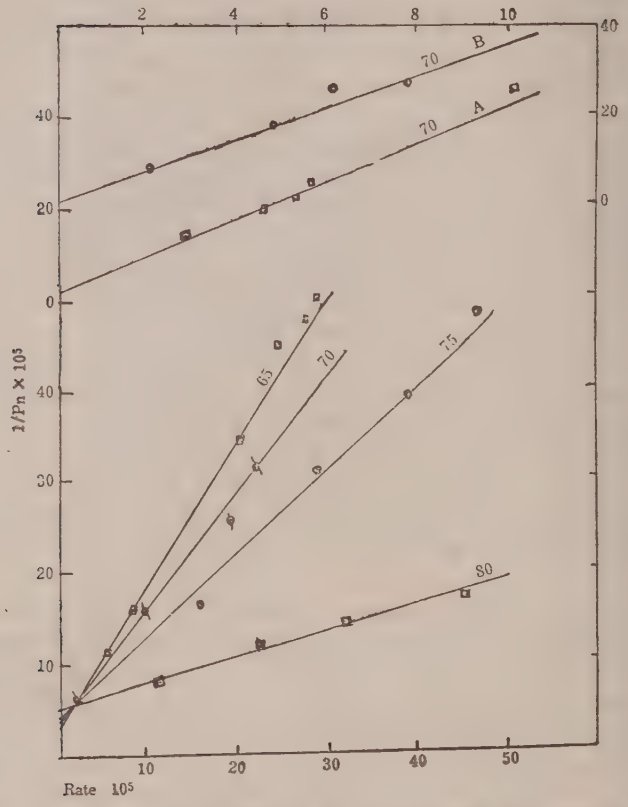

FIG. 3. Rate vs. 1/Pn in Bulk at 80°, 75°, 70 and 65°C from below and in solution. A Ethyl Acetate, B Benzene at 70°C.

trations ($\sim 10^{-1}$ to 10^{-2}) and evaluating C_{cat} from the slope, $C_{cat}/K^2[M]^3$. The second method was to plot $\left\{ \frac{1}{P_n} - AR \right\}$ against (Cat)/(M) and evaluating C_{cat} from the slope. Both the methods gave more or less identical values for C_{cat}. Since small variations in the slope produced large divergences in the C_{cat} values by the first method it was discarded and therefore the second method was resorted to for the accurate evaluation of the constant. The values for the C_{cat} at 65, 70, 75 and 80°C were all in the neighbourhood of $\sim 5 \times 10^{-3}$ showing surprisingly very little variation with temperature. From the values of K and A it was possible to evaluate by methods described previously (Santappa et al 1955) the rate of initiation R_i in the bulk polymerization of methyl methacrylate catalysed by MEKP. The values for Ri/cat at 65, 70, 75 and 80°C

were $2{\cdot}08 \times 10^{-6}$, $2{\cdot}44 \times 10^{-6}$, $5{\cdot}17 \times 10^{-6}$, 5×10^{-6}, respectively and an activation energy of $\sim$ 30 Kcals for initiation was obtained;

$$R_i'/\text{cat} = 5{\cdot}608 \times 10^{13} \times \exp\ (-30700/RT)$$

Polymerization experiments at 70°C in the four solvents indicated above were also conducted and all the constants K, A, C_{cat}, C_M C_S and R_i'/Cat were evaluated. Values of K′ in the four solvents ranged from 6 to 8×10^{-5} indicating approximately 40 to 20 per cent decrease of the constant from the bulk value. The decrease in the value of K′ in solution may be attributed either to increase in k_t or decrease in k_p or $k_d f$. Probably increase of k_t and f were responsible.

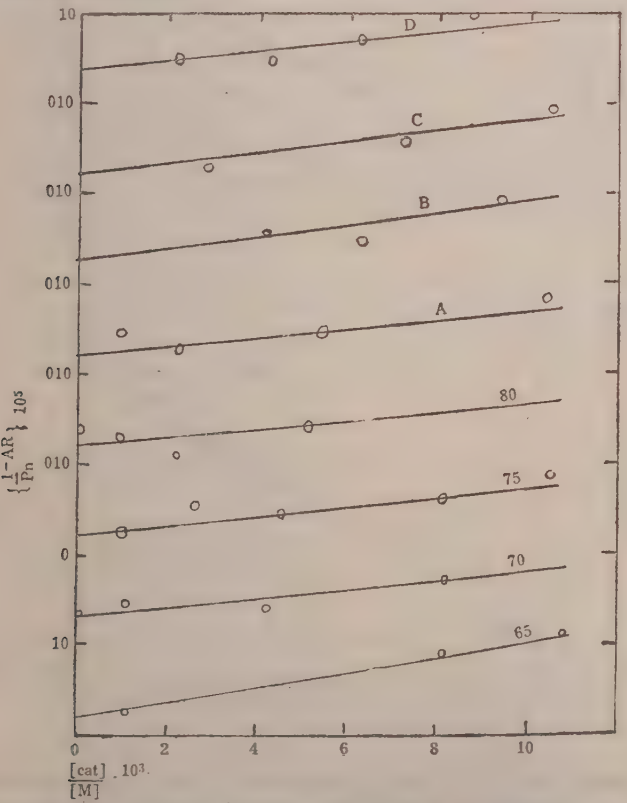

FIG. 4. $\{(1/P_n) - AR\}$ vs. [Cat]/[M] in Bulk at temperatures 65°, 70°, 75° and 80°C and in solution A (Ethylacetate), B (Benzene), C (Toluene), D Methyl Ethyl Ketone at 70°C.

Evaluation of A, C_{cat}, C_M values in solution was also possible. From the slopes of the plots I/P_n vs R (Fig. 3) in the four solvents

at 70°C the A value was ~ 4 and $k_p/k_t^{1/2}$ value was ~ $11{\cdot}9\times10^{-2}$. The values of $k_p/k_t^{\frac{1}{2}}$ in solution appeared to be in better agreement than these in bulk with the value calculated from Matheson's et al (1949) values for k_p and k_t. The A′ values got by plotting $1/P_n$ vs $R/[M]^2$ in solution at different monomer concentrations was used to plot $\left\{\frac{1}{P_n}-\frac{A'R}{[M]^2}\right\}$ against [S]/[M] at constant [Cat]/[M]. {Method (i) in the Table 1} (Fig. 5) From the

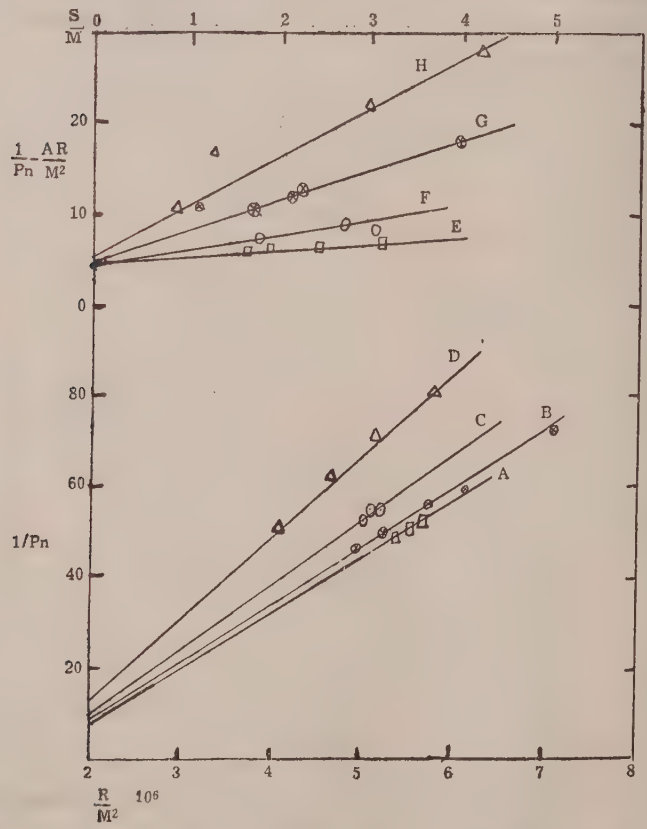

Fig. 5. $1/P_n$ vs. $R/[M]^2$ in solution at 70°C A Benzene; B Ethyl Acetate; C Methyl Ethyl Ketone; and D Toluene.
(Above) $\{(1/P_n) - A'R/[M]^2\}$ vs. [S]/[M] at 70°C in E Benzene F Methyl Ethyl Ketone; G Ethyl Acetate and H Toluene.

slopes of the linear plots values for C_s at 70° were evaluated. From the intercept given by $(C_M + C_{cat}\ Cat/M)$ it was also possible

to evaluate C_M and C_{cat}. Alternatively $\left\{\frac{1}{P_n} - AR\right\}$ vs [Cat]/[M] at constant [S]/[M] were plotted (Method (ii) Table 1) C_{cat} was given by the slope and $\left\{C_M + C_s\frac{[S]}{[M]}\right\}$ was furnished by the intercept. The values for C_s and C_M by the two methods did not differ much, the respective values are for ethylacetate $3{\cdot}3\times10^{-5}$, and 2×10^{-5}; for benzene $1{\cdot}43\times10^{-5}$, 2×10^{-5}, for toluene $5{\cdot}5\times10^{-5}$ and 0, and for methyle ethyle ketone $1{\cdot}43\times10^{-5}$ and 2×10^{-5}. The values of the transfer constants in the solvents were in the expected order (Sadan Basu, Jyotirindra Nath Sen and Santi R Palit, 1952). It was seen that C_M values for all the solvents studied were of the same order. The values for C_{cat} by method (i) and (ii) differed, though were of the same order in their powers of ten. These differences we felt were within errors accompanying the graphical evaluations. We further found that method (i) represented a more accurate and suitable evaluation because constant catalyst concentration was used and (M) was widely varied and the plots were more linear.

Values for C_{cat} in the solution were found to be generally slightly lower than in bulk for the same concentration of the catalyst. Probably specific rate transfer constant for catalyst might have decreased in the presence of solvent molecules.

Table I

C_{cat} Method	Benzene	Toluene	Ethyl Acetate	Methylethyl Ketone
(i)	$3{\cdot}3\times10^{-3}$	$3{\cdot}68\times10^{-3}$	$2{\cdot}3\times10^{-3}$	$1{\cdot}96\times10^{-3}$
(ii)	5×10^{-3}	$3{\cdot}3\times10^{-3}$	$3{\cdot}3\times10^{-3}$	4×10^{-3}

With the known values for C_{cat} and C_s it was possible to plot $\left\{\frac{1}{P_n} - C_{cat}\frac{[cat]}{[M]} - C_s\frac{[S]}{[M]}\right\}$ against R/M^2 and get more accurate values of the slope A′ referred to above. The value of the slope thus determined in ethyl acetate solution was 62·5.

With the known K′ value from Rate vs $Cat^{1/2}$, the rate of initiation was calculated, $2K'^2\ A' = R_i'/[Cat] = 5{\cdot}311\times10^{-7}$. The value for other solvents were also about the same. The low values got

in solution may be due to the lowering of the rate constant for the spontaneous decomposition of the catalyst in a mixture of solvent and monomer or dependence of catalyst efficiency "f" on monomer concentration or both.

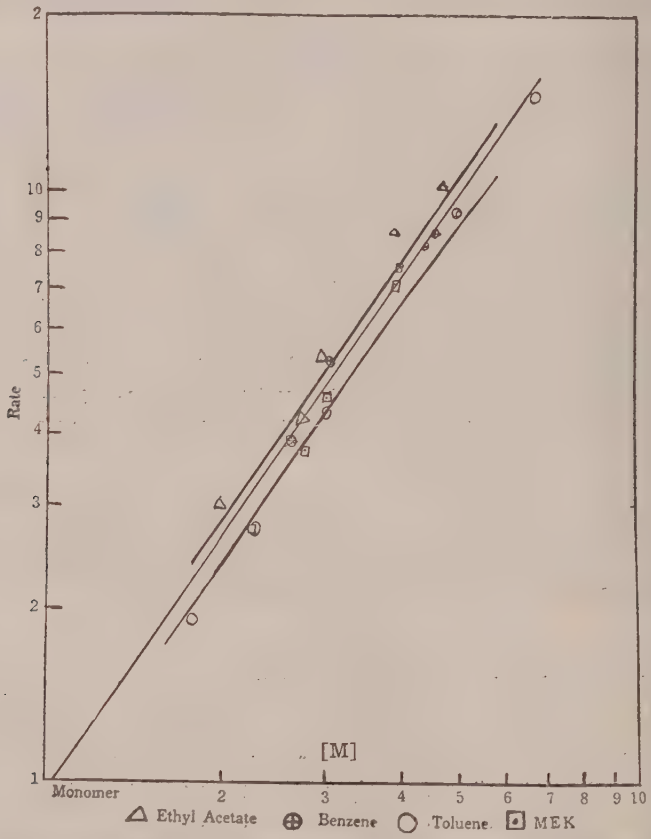

Fig. 6. Rate vs. Monomer Concentration on Logarithmic graph-slope of lines is 3/2 indicating first order reaction with respect to Monomer.

The order of the reaction with respect to monomer concentration was evaluated by carrying out polymerization at 70°C with constant catalyst concentration in the four solvents mentioned above. Log R vs Log M (Fig. 6) were plotted and the slope in all the solvents was 1·5. It could therefore be described that the reaction was of the first order with respect to monomer concentration and the other one half power of monomer concentration might be explained by the catalyst efficiency, f, being dependent on it.

REFERENCES

Baxandale, J. H., Bywaters, & Evans, M. G.	(1946)	*J. Polym. Sci.* **1**: 237.
P. J. Flory	(1937)	Mechanism of Vinyl Polymerizations *J. Amer. chem. Soc.* **59**: 241.
Mahadevan & Santappa	(1955)	Rates of Initiation and Chain transfer constants in the polymerization of methylacrylate *Makromol. Chem.* **16**: 119.
Matheson et al	(1949)	*J. Amer. chem. Soc.* **71**: 497.
Sadan Basu, Jyotirindranath Sen, & S. R. Palit,	(1952)	Studies in Chain Transfer, *Proc. roy. Soc.* A **214**: 247
Tobalsky, A. V. & B. Baysal	(1953)	A Review of Rates of Initiation in Vinyl Polymerization: Styrene and Methyl Methacrylate, *J. Polym. Sci.* **11**: 471-486.
Umasankar Nandi & Santi R. Palit	(1955)	Hydrogen Peroxide in Vinyl Polymerisation, *J. Polym. Sci.* **12**: 65.
Vaidhyanathan & Santappa	(1955)	Chain transfer reactions and nature of initiation in the polymerization of styrene. *Makromol.* **16**: 140.

J. Madras Univ., B, XXVI, No. 1, pages 63-78, 1956

A Spectrophotometric Investigation of the Complexes of Ferric Iron with Oxalic and Citric Acids

BY

R. V. Subramanian & M. Santappa

University Physical Chemistry Laboratory, Madras-25

(Received for publication on February 7, 1956)

ABSTRACT

The complexes of ferric iron with oxalic acid and citric acid which are active photoinitiators of vinyl polymerization have been studied spectrophotometrically. Two oxalate complexes have been detected at a pH $\sim$ 2·5; and it has also been found that one was destroyed by increasing the acidity of the solution. These observations were confirmed and the formula and stability of the complex existing even at low pH ($\sim$ 0·7) were determined. The values of the equilibrium constant for its formation were evaluated at ionic strengths 0·5 and 0·2. The equilibrium constant for the formation of the citrate also was likewise determined at $\mu = 0{\cdot}2$. The extinction curves for the citrate and oxalate complexes in the ultraviolet were also drawn.

It has been indicated by Evans and Uri (1949) that the complexes of ferric iron with oxalic as well as citric acids are active photosensitizers for vinyl polymerizations. A detailed study of the kinetics of vinyl polymerizations initiated by these complexes requires a correct estimation of the light absorption fraction and concentrations of these complexes in solution. Such an estimation is possible by a determination of the formula and stability of the complexes.

Bobtelsky, Chasson and Klein (1953) were able to detect two complexes Fe^{3+}/Ox and $1Fe^{3+}/3\,Ox$ by the photometric titration of solutions of ferric chloride with sodium oxalate. Since the formation of more than one complex has thus been detected, we have used, in our study of these complexes spectrophotometrically, Job's method of variations (1928) modified and extended by Vosburg and Cooper (1941). Accordingly the optical densities of solutions of ferric nitrate and oxalic acid (pH $\sim$ 2·5) mixed in the ratios 1 : 1, 1 : 2 and 1 : 3 were measured in the range 250 mμ—400mμ.

(Fig. 1). It was seen that the 1 : 1 mixture had a well defined maximum at $\lambda = 290 m\mu$. The difference between the observed extinction at this wavelength and that calculated on the basis of no reaction between the components was greatest for this mixture, thus indicating clearly the formation of a complex in equimolar proportions of ferric iron and oxalic acid, having a characteristic maximum absorption at ~ 290 mμ. At other wavelengths, the largest difference in optical density for the 1 : 1 mixture was not observed due to interference probably of other complexes formed.

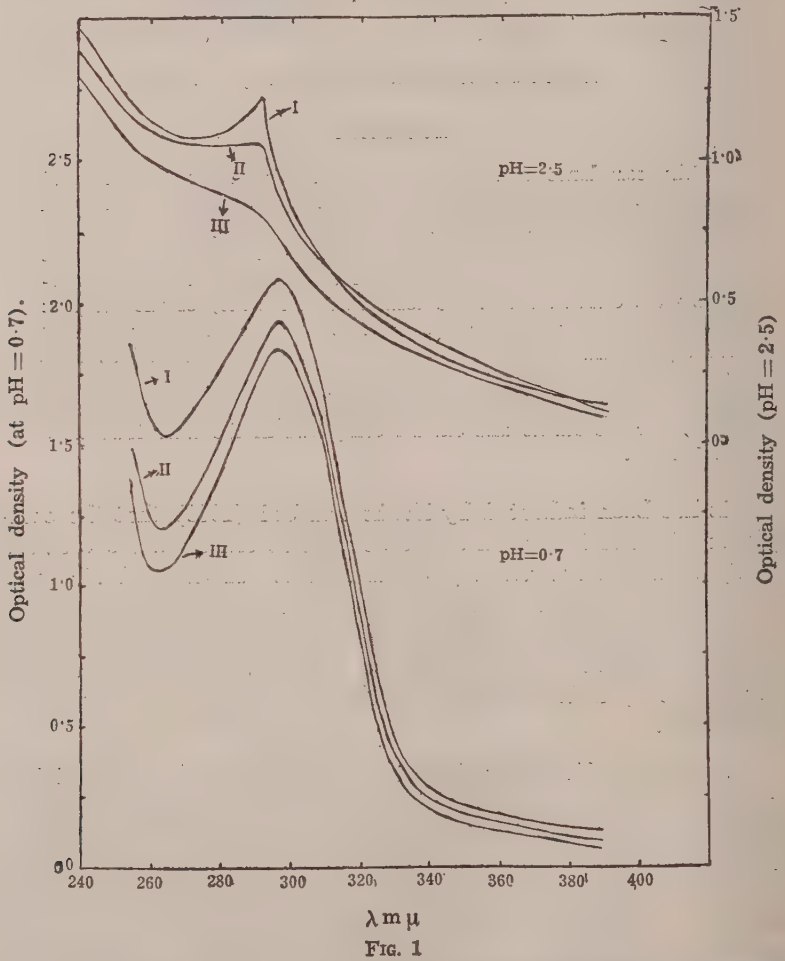

Fig. 1

Optical densities of mixtures of Ferric nitrate and Oxalic acid in the ratios 1:1 (curve I), 1:2 (curve II) and 1:3 (curve III), at pH = 2·5 and pH = 0·7 plotted against wavelengths.

From measurements of optical densities of the mixtures at pH = 1, and 0·7, it was found that the peaks at 290mμ became sharp with a lowering of pH. All these curves (Fig. 1) were characteristic of the equimolar ferric oxalate complex which indicated that the other complexes were gradually destroyed by increasing acidity, in agreement with Bobtelsky's observation. The existence of a single complex was further confirmed by measuring the optical densities of ferric nitrate and oxalic acid solutions in which their

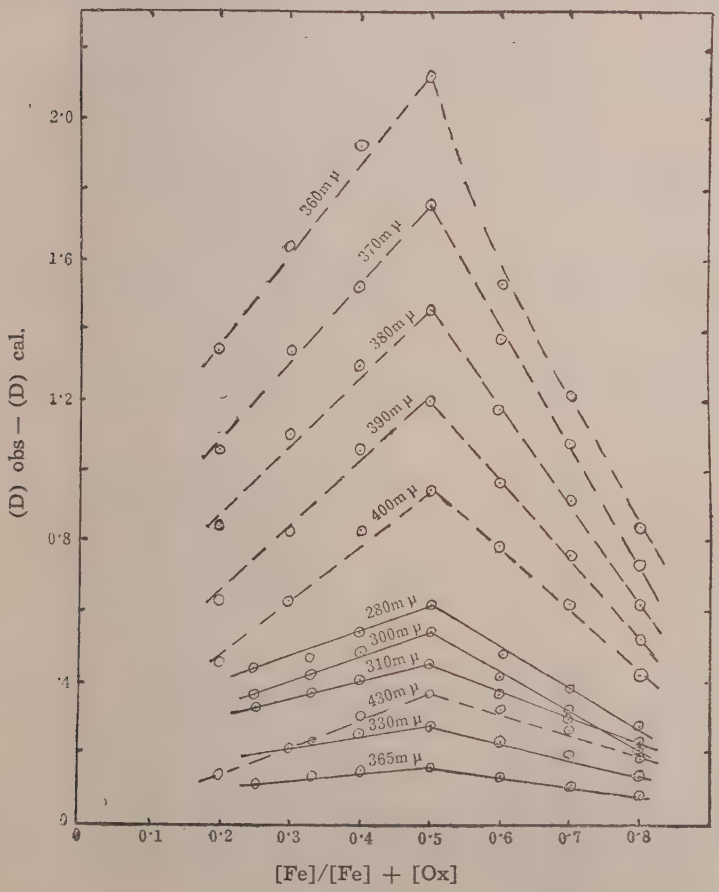

FIG. 2

Difference between the observed and calculated optical density (D)obs—(D)cal, for the ferric oxalate solution plotted against the molar fraction of iron in the solution, at the wavelengths indicated above the line. — — — Data from Table 1-b; ——— Data from Table 1-a.

Table I (a)

$[HNO_3]$	$M \times 10^3$		$D\lambda$ (λ in mμ)									
	$[Fe(NO_3)_3]$	$[H_2C_2O_4]$	270	280	300	310	330	350	365	380	390	400
0·2M	0·25	0·75	1·1	1·37	1·8	1·53	0·388	0·157	0·120	0·092	0·075	0·055
„	0·33	0·66	1·24	1·48	1·87	1·58	0·425	0·178	0·142	0·107	0·088	0·063
„	0·40	0·60	1·37	1·6	1·95	1·62	0·454	0·20	0·157	0·122	0·102	0·08
„	0·50	0·50	1·55	1·72	2·03	1·68	0·475	0·215	0·170	0·130	0·110	0·090
„	0·60	0·40	1·59	1·70	1·92	1·6	0·433	0·182	0·143	0·105	0·095	0·08
„	0·70	0·30	1·74	1·68	1·84	1·55	0·382	0·148	0·117	0·079	0·076	0·060
„	0·80	0·20	1·80	1·66	1·75	1·48	0·335	0·11	0·088	0·059	0·060	0·051
„	1·0	—	2·0	1·55	1·58	1·27	0·212	0·025	0·013	0·013	0·012	0·001
„	—	1·0	0·425	0·73	1·38	1·18	0·185	0·015	0·008	0·007	0·006	0·006

Table I (b)

$[HNO_3]$	$M \times 10^2$		$D\lambda$ (λ in mμ)									
	$[Fe(NO_3)_3]$	$[H_2C_2O_4]$	350	360	370	380	390	400	420	430	450	470
0·2M	0·2	0·8	1·65	1·36	1·078	0·84	0·635	0·46	0·215	0·142	0·062	0·025
,,	0·3	0·7	1·88	1·655	1·367	1·107	0·845	0·63	0·318	0·208	0·92	0·037
,,	0·4	0·6	2·20	1·95	1·54	1·315	1·07	0·83	0·435	0·305	0·143	0·062
,,	0·5	0·5	2·52	2·18	1·78	1·46	1·195	0·95	0·53	0·37	0·182	0·08
,,	0·6	0·4	1·76	1·585	1·405	1·197	0·985	0·785	0·455	0·328	0·154	0·07
,,	0·7	0·3	1·456	1·275	1·114	0·935	0·77	0·615	0·356	0·257	0·122	0·059
,,	0·8	0·2	1·05	0·90	0·775	0·648	0·532	0·42	0·242	0·175	0·087	0·04
,,	1·0	—	0·135	0·082	0·05	0·030	0·018	0·01	0·006	0·003	0·000	0·000
,,	—	1·0	0·008	0·005	0·003	0·003	0·002	0·001	0·000	0·000	0·000	0·000

mole fractions varied from 0·2 to 0·8. The total molar concentration was kept constant at 10^{-3} M at a pH = 0·7 (Table 1a). The difference between the observed extinction and that calculated on the basis of no reaction of the components was plotted against $[Fe^{3+}]/([Fe^{3+}] + [Ox])$ Fig. 2. The sharpmaxima at the ratio 0·5 over the whole wavelength range studied (280—400mμ) showed conclusively that the only complex formed under these conditions was that in which iron and oxalic acid combined in equimolar ratios. The experiments with ten times the total molar concentrations i.e., 10^{-2}M gave identical results (Fig. 2) (Table 1b) proving that 1Fe/1 Ox was the only complex formed at higher concentrations also.

The possible reaction in equimolar ratio is

$$Fe^{3+} + H_2C_2O_4 \rightleftharpoons (FeH_xC_2O_4)^{(1+x)+} + (2-x)H^+ \quad .. \quad (1)$$

Also,

$$\log K_1 - \log \frac{[Fe\ Hx\ C_2O_4]^{(1+x)+}}{[Fe^{3+}]\ [Ox]} = (2-x)\ \log\ (H^+)$$

where K_1 is the equilibrium constant for reaction (1) and $[Ox] = [H_2C_2O_4]$.

The value of x and hence the ionic state of the complex was found by studying the effect of change in hydrogen ion concentration on the reaction (1).

For a series of solutions of different $[H^+]$ the variable term log $[FeOx]/[Fe^{3+}]\ [Ox]$ was plotted against-log $[H^+]$. (Fig. 3). The value obtained for the slope (2—x) was 2 i.e., x = O and therefore the reaction that takes place is

$$Fe^{3+} + H_2C_2O_4 \rightleftharpoons (Fe^3C_2O_4{}^{2-})^+ + 2H^+$$

$[FeOx]/[Fe^{3+}]\ [Ox]$ was evaluated by using thiocyanate as indicator for ferric ions at equilibrium. Extinction measurements of the solutions containing $[Fe(NO_3)_3] = 9{\cdot}5 \times 10^{-4}$m, $[H_2C_2O_4] = 10^{-3}$m $[KSCN] = 10^{-3}$m and of varying concentrations of $[HNO_3]$ (0·18—0·26M) all adjusted to an ionic strength (μ) = 0·5 were made at λ = 520mμ at which the absorption due to all other

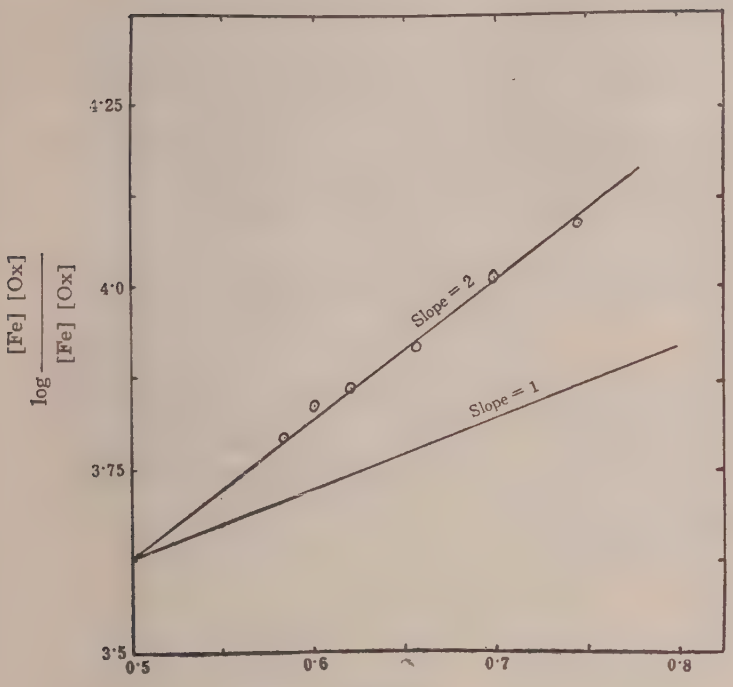

$\log \frac{[FeOx]}{[Fe]\,[Ox]}$ plotted against $-\log[H^+]$

FIG. 3

The theoretical curve for slope = 1 is also shown for comparison.

species except $FeSCN^{++}$ was utterly negligible. If D is the measured optical density and $\varepsilon_{520}^{FeSCN^{++}}$ is the molar extinction coefficient of $FeSCN^{++}$ at 520 mμ, then,

$$\frac{D_{520}}{\varepsilon_{520}^{FeSCN^{++}}} = [FeSCN^{++}]$$

and $[SCN^-] = [KSCN] - [FeSCN^{++}]$

also $[Fe^{3+}] = \frac{[FeSCN^{++}]}{K_2[SCN^-]}$ where K_2 is the equilibrium constant at $\mu = 0{\cdot}5$ for $Fe^{3+} + SCN^- \rightleftharpoons FeSCN^{++}$ .. (2)

correcting for hydrolysis of ferric ions,

$[Fe^{3+}OH^-] = \frac{[Fe^{3+}]\,K_H}{[H^+]}$ where K_H is the equilibrium constant at $\mu = 0{\cdot}5$ for $Fe^{3+} + OH^- \rightleftharpoons Fe^{3+}OH^-$. Then $[FeOx] = [Fe(NO_3)_3] - \{[Fe^{3+}] + [FeSCN^{++}] + [FeOH^{++}]\}$ and unreacted oxalic acid $[Ox] = [H_2C_2O_4] - [FeOx]$.

Thus $K_1 = \frac{[FeOx]\,[H^+]^2}{[Fe^{3+}]\,[Ox]}$ can be calculated easily.

The values of K_2 and $\varepsilon_{520}^{FeSCN^{++}}$ have been evaluated by Frank and Oswalt (1947). In reaction (2), if 'a' and 'b' are the concentrations of Fe^{3+} and SCN^-, and x is the actual concentration of $FeSCN^{++}$ formed, ignoring hydrolysis and as long as no other complexes are formed,

$$K_2 = \frac{x}{(a-x)(b-x)}$$

i.e. $$X_2 - (a + b + \frac{1}{K_2})\,x + ab = 0;$$

i.e. $$X = \frac{ab}{a + b + \frac{1}{K_2}} + \frac{(ab)^2}{(a + b + \frac{1}{K_2})^2} + \ldots\ldots\ldots \quad .. \quad (3)$$

For the experiments reported, the second and higher terms on the right side of (3) can be neglected. If $D\lambda$ is the optical density of the solution, and $\varepsilon\lambda$ the molar extinction coefficient of $FeSCN^{++}$, then,

$$D_\lambda = \varepsilon_\lambda\, x = \varepsilon_\lambda \frac{ab}{a + b + \frac{1}{K_2}}$$

i.e., $$\frac{ab}{D_\lambda} = \frac{1}{\varepsilon_\lambda}(a + b) + \frac{1}{\varepsilon_\lambda K_2} \quad .. \quad (4)$$

Table 2 (a)

$[HC10_4]$ m/l	$[Fe^{3+}]$ m/l (a)	[KSCN] m/l (b)	400 mμ		440 mμ		460 mμ		500 mμ		525 mμ	
			D	$\frac{ab}{D} \times 10^6$	D	$\frac{ab}{D} \times 10^6$	D	$\frac{ab}{D} \times 10^6$	D	$\frac{ab}{D} \times 10^6$	D	$\frac{ab}{D} \times 10^6$
0·5	0·001	0·003	0·073	4·11	0·147	2·041	0·15	2·00	0·112	2·69	0·078	3·846
„	0·002	„	0·128	4·688	0·257	2·335	0·278	2·157	0·206	2·905	0·139	4·31
„	0·003	„	0·179	5·027	0·360	2·50	0·367	2·456	0·275	3·278	0·196	4·591
„	0·004	„	0·210	5·715	0·417	2·878	0·442	2·715	0·332	3·61	0·227	5·286
„	0·005	„	0·258	5·815	0·498	3·011	0·527	2·846	0·390	3·85	0·275	5·455
„	0·008	„	0·321	7·476	0·625	3·84	0·658	3·648	0·505	4·75	3·344	6·976

Table 2 (b)

λ mμ	380	400	420	440	460	480	500	525	540
ε $FeSCN^{++}$	1200	2100	3250	4150	4400	4000	3200	2200	1650
K_2	138·9	132·2	136·8	137·7	133·8	138·9	137·4	137·7	134·7

Mean $K_2 = 136·4$

Hence for various values 'a' and 'b', ab/D plotted against (a+b) should give, if $FeSCN^{++}$ is the only complex formed, a straight line with the slope $\frac{1}{\varepsilon_\lambda}$ and the intercept $\frac{1}{\varepsilon_\lambda K_2}$

Frank and Oswalt have obtained by the above method $\varepsilon_{520}^{FeSCN^{++}} = 2100$ and $K_2 = 136{\cdot}2 \pm 1{\cdot}9$. Repeating their experiments we have been able to reproduce the value of K_2 but differ slightly in our value of $\varepsilon_{520}^{FeSCN^{++}}$ which is 2375. The data are given in Tables 2 a and b and typical plots of ab/D against (a + b) in Fig. 4; and our extinction coefficient curve for $FeSCN^{++}$ in Fig. 5.

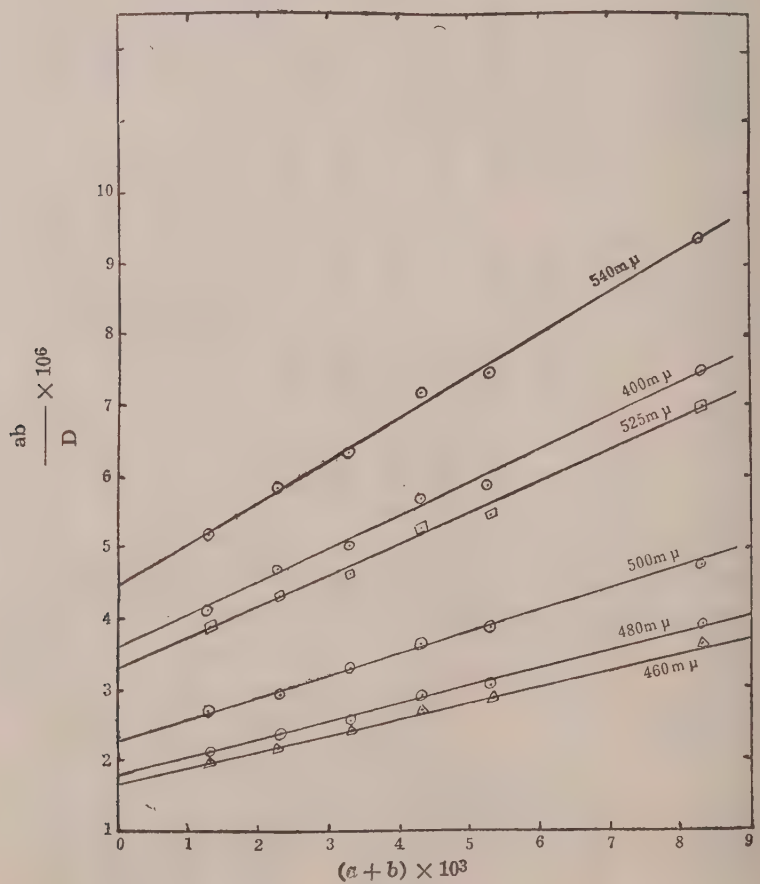

FIG. 4

ab/D × 10^6 plotted against $(a+b)10^3$ for $FeSCN^{++}$; the wavelengths are indicated above the lines.

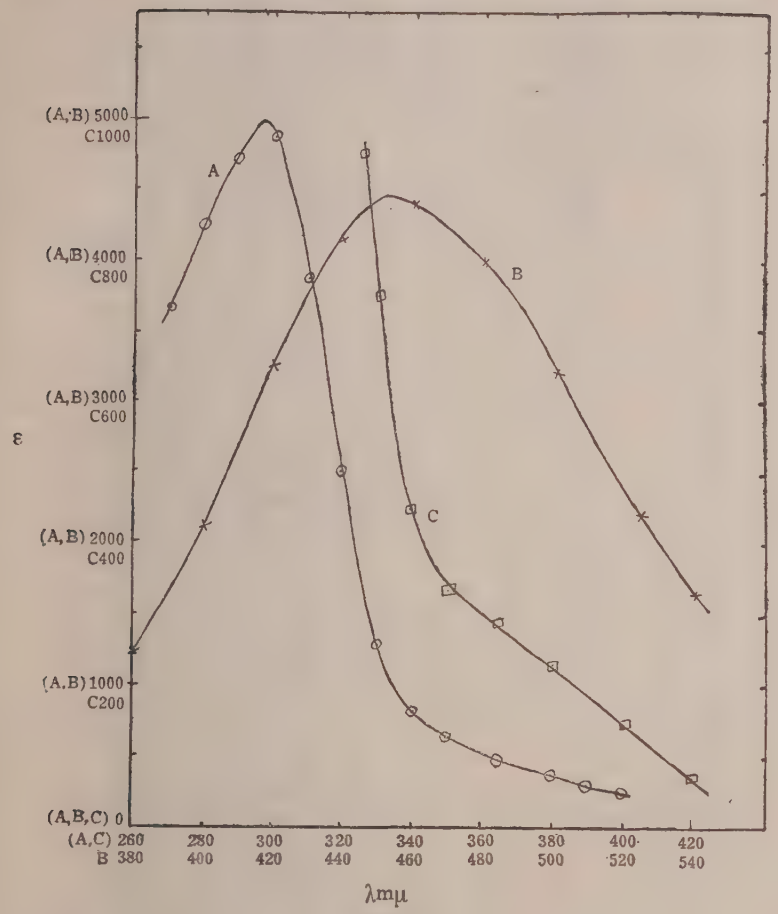

FIG. 5

The molar extinction co-efficients ε of the complexes $(FeC_2O_4)+$ (curve A) FeSCN++ (curve B) and FeHCitr)+ (curve C) plotted against wavelengths.

In our calculations of K_1 above, we have used, our own value 2375 for $\varepsilon_{520}^{FeSCN^{++}}$ and 136·2 for K_2 The values of K_H at ionic strengths 0·5, $(= 0{\cdot}5702 \times 10^{-3})$, and at 0·2, $(= 0{\cdot}76 \times 10^{-3})$ (used later) were calculated from Rabinowitch and Stockmayer's (1942) results. Mean value of K_1 obtained thus is $4{\cdot}13 \times 10^2$ (Table 3). Since we are using the complex at pH = 0·7 i.e., $[H^+] = 0{\cdot}2$ to photoinitiate polymerizations under irradiation with monochromatic light ($\lambda = 365$ mμ) it was necessary to determine the value of K_1 at $\mu = 0{\cdot}2$ and ε^{FeOx} at 365mμ. For this

Table 3

$[Fe^{3+}] = 0{\cdot}95 \times 10^{-3}$ M; [KSCN] $= 10^{-3}$ M; [OX] $= 10^{-3}$ M; $\mu = 0{\cdot}5$ adjusted with $NaNO_3$; $\varepsilon^{FeSCN^{++}}_{520-2375}$

H^+ m/l	D 520	$FeSCN^{++}$ m/l $\times 10^5$	SCN^- m/l $\times 10^4$	Fe^{3+} m/l $\times 10^4$	FeOx m/l $\times 10^4$	Ox m/l $\times 10^4$	$\log \frac{[FeOx]}{[Fe^{3+}][Ox]}$	$-\log H^+$	K_1
0·18	·065	2·737	9·7263	2·066	7·153	2·8462	3·9644	0·7447	$3{\cdot}942 \times 10^2$
0·20	·070	2·947	9·7053	2·230	6·9689	3·031	3·8899	0·6990	$4{\cdot}125 \times 10^2$
0·22	·077	3·243	9·6757	2·461	6·7083	3·292	3·7894	0·6576	$4{\cdot}007 \times 10^2$
0·24	·081	3·411	9·6589	2·593	6·5597	3·4403	3·7360	0·6200	$4{\cdot}236 \times 10^2$
0·25	·084	3·538	9·6462	2·688	6·472	3·528	3·7100	0·6021	$4{\cdot}296 \times 10^2$
0·26	·087	3·664	9·6336	2·793	6·3345	3·6655	3·6574	0·5850	$4{\cdot}183 \times 10^2$

mean $K_1 = 4{\cdot}13 \times 10^2$

Table 4

$[H^+] = 0{\cdot}2$ M $\mu = 0{\cdot}5$ $[FeOx] = 6{\cdot}969 \times 10^{-4}$M (a)			$\mu = 0{\cdot}2$; $[H^+] = 0{\cdot}2$ M (b)						
λmμ	D	ε^{FeOx}	λmμ	D	[FeOx] $\times 10^4$	[FeOx] $\times 10^4$ mean	$[Fe^{3+}]$ $\times 10^4$	[Ox] $\times 10^4$	K_1
365	·331	474·9	365	·349	7·348				
380	·256	367·3	380	·270	7·353	7·35	2·141	2·65	$5{\cdot}182 \times 10^2$
400	·166	238·2	400	·175	7·349				

purpose the optical density D at 365 mμ of the complex at $\mu = 0{\cdot}5$ was measured. The concentration of the complex being known in this solution, D/[FeOx] gave ε_{365}^{FeOx} since absorption by other species in the solution used was negligible. Hence the concentration of the complex in a solution of ionic strength 0·2 is easily calculated from its optical density at 365 mμ. Similar measurements at 380mμ and 400 mμ yielded values closely agreeing among themselves for [FeOx] at $\mu = 0{\cdot}2$. The concentrations of the other species in this solution are calculated as indicated before and K_1 at $\mu = 0{\cdot}2$ is then computed. (Table 4).

Optical densities were measured at lower wavelengths upto 270 mμ of (FeOx) solutions at $\mu = 0{\cdot}2$. These were corrected for absorption by the unreacted ferric ions and oxalic acid which had to be taken into account at these lower wavelengths. The corrections were calculated from measured extinction of 10^{-3}M ferric nitrate and 10^{-3}M oxalic acid in the presence of 0·2M HNO_3. (Table 1a). From the corrected values of optical density the molar extinction coefficients at different wavelengths were then calculated for (FeOx) and plotted in Fig. (5).

Similarly citric acid and ferric ions react in equimolar proportions to form the complex $(FeHCitr)^{++}$. This has been established by Lanford and Quinan (1948) who have determined the equilibrium constant for the formation of the complex (K_3) at $\mu = 1{\cdot}0$ as 0·274. They have made the optical density measurements at 525mμ and used the value of Frank and Oswalt for $\varepsilon_{525}^{FeSCN^{++}} = 1875$. Our corresponding value is 2200. Hence though the values of the optical density measured by Lanford and Quinan were almost exactly reproduced in our data, the value of K_3 at $\mu = 1{\cdot}0$ obtained by us (1955) was 1·2. The extinction coefficient of the ferric citrate complex (Fig. 5) and K_3 at $\mu = 0{\cdot}2$ were calculated as for the oxalate complex. (Tables 5 a & b).

A noteworthy feature of the results obtained was that since we calculated molar extinction coefficients of the oxalate and citrate complexes from measured optical densities which were unaffected by the value of $\varepsilon^{FeSCN^{++}}$ we used, any change in the calculated concentration of the complexes due to employing different values of $\varepsilon^{FeSCN++}$ was followed by a proportionate change in the molar extinction coefficient of the complexes i.e., $\varepsilon c = D$ was constant. Hence the value of the light absorbed by the complexes, which was used in the calculation of results of our polymerisation experiments, remained relatively unaffected.

Table 5 (a)

HNO_3 m/l	D_{525}		K_3	
	Exp.	Lit	Exp.	Lit
0·14	0·186	—	—	1·212
0·15	0·183	0·182	0·27	1·284

$[Fe^{3+}] = 10^{-3}$ m/l, $[KSCN] = 10^{-3}$ m/l

$\mu = 1{\cdot}0$ adjusted by $NaNO_3$; $[H_3citr] = 5 \times 10^{-3}$ m/l

Table 5 (b)

$[Fe(NO_3)_3] = 10^{-3}$ m/l; $[H_3citr] = 5 \times 10^{-3}$ m/l; $\varepsilon\, FeHcitr^+ = 283{\cdot}3$ $\mu = 0{\cdot}2$

HNO_3 m/l	D_{365}	$[FeHctr]^+$ m/l	$[Fe^{3+}]$ m/l	$[H_3Citr]$ m/l	K_3
·15	·09	$3{\cdot}180 \times 10^{-4}$	$6{\cdot}787 \times 10^{-4}$	$4{\cdot}682 \times 10^{-3}$	2·252
·18	·068	$2{\cdot}403 \times 10^{-4}$	$7{\cdot}567 \times 10^{-4}$	$4{\cdot}7597 \times 10^{-3}$	2·162
·200	·056	$1{\cdot}979 \times 10^{-4}$	$7{\cdot}991 \times 10^{-4}$	$4{\cdot}8021 \times 10^{-3}$	2·064

mean $k_3 = 2{\cdot}160$

Experimental:

Ferric Nitrate was a E. Merck product, standardised against potassium permanganate after reduction with $SnCl_2$.

KSCN was of B.D.H (A.R.) variety standardised against silver nitrate using fluorescein as indicator.

Oxalic and citric acids were also B. D. H. (A.R.) products; standard solutions were made by exact weighing and checked up by volumetric titrations.

$NaNO_3$, also B.D.H. (A.R.) product was used in adjusting the ionic strengths.

Optical density measurements were made in a Beckmann model D.U. Spectrophotometer using matched corex cells for the visible and silica cells for the ultraviolet region, at room temperature, 27°c.

ACKNOWLEDGEMENT

We acknowledge with thanks the facilities given to us in the Central Leather Research Institute for using their spectrophotometer.

REFERENCES

Bobtelsky, M., Chasson, D., & Klein, S. F. (1953) Photometric measurement of iron oxalates; *Anal. chim. acta.* 8: 460-470.

Evans, M. G., & Uri, N. (1949) Photochemical polymerisation in aqueous solution, *Nature, Lond.*, 164: 104.

Frank, H. S. & Oswalt, R. L. (1947) Stability and Light absorption of the complexion FeSCN++; *J. Amer. chem. Soc.* 69: 1321.

P. Job (1928) Formation and Stability of inorganic complexes in solution *Liebigs. Ann.* 10: 113-203.

Lanford, O. E. & Quinan, R. J. (1948) A spectrophotometric study of the reaction of ferric iron and citric acid; *J. Amer. chem. Soc.* 70: 2900-2903.

Rabinowitch, E. & Stockmayer, W. H. (1942) Association of ferric ions with chloride, bromide and hydroxyl ions; *J. Amer. chem. Soc.* 64: 335-47.

Subramanian, R. V. & Santappa, M. (1955) Citrate radical ion polymerisation of methyl methacrylate *Curr. Sci.*, 24: 229.

Vosburg, W. C. & Cooper, G. R. (1941) Identification of complex ions in solution by Spectrophometric measurements; *J. Amer. chem. Soc.* 63: 437-42.

J. Madras Univ., B, XXVI, No. 1, pages 79-92, 1956

Rates of Initiation and Chain Transfer Constants in the Polymerization of Methyl Acrylate II

BY

V. Mahadevan and Santappa,

Physical Chemistry Laboratory,
University of Madras, Madras-25.

(Received for publication on February 13, 1956)

ABSTRACT

A study of the bulk polymerization of methyl acrylate at 60°C to 80°C with 2,2′ Azobisisobutyronitrile, (Azo), 1,1′ Azobiscyclohexanecarbonitrile (HAzo), Hydrogen peroxide (H_2O_2), Benzoyl peroxide (Bz_2O_2), and Methyl ethyl ketone peroxide (MEKP) in 20 per cent ethyl acetate as a diluent, has been made. Rates of (a) initiation of polymerization, (b) chain transfer constants for the monomer and the catalyst have been evaluated. Catalyst efficiencies have been calculated. Certain aspects polymerization of methyl acrylate have been compared with styrene and methyl methacrylate.

In our previous publications (V. Mahadevan and M. Santappa 1955), the general nature of polymerization of methyl acrylate at 55°C to 75°C, using various initiators in 50 per cent ethyl acetate as a diluent and a non-transfering solvent was reported. The catalysts tried were Benzoyl peroxide, Methyl ethyl ketone peroxide, Ditertiary butyl peroxide and Tertiary butyl hydro peroxide. A small thermal rate and auto acceleration were also noticed under the experimental conditions. In this paper, results of polymerization with 20 per cent ethyl acetate in which thermal rate and auto acceleration are completely suppressed, are reported. Azo, HAzo, H_2O_2, Bz_2O_2 and MEKP have been used as initiators. Rates of initiation of polymerization, rates of transfer constants for the monomer and catalysts with the growing polymethylacrylate radical chain and the activation energies for these rates have been evaluated. The dependence of monomer concentration on rates has been studied and correlated to catalyst efficiencies.

The theoretical scheme relevant to this work has already been given in the first of the series of the papers (V. Mahadevan and M. Santappa 1955). For the sake of understanding of this paper, we reproduce below the three important relationships. The total overall rate R_{pt} is given by

$$R_{pt} = R_{pth} + R_p \sim R_p = [k_p (k_{df})^{1/2} / (k_{tc} + k_{td})^{1/2}] M[Cat]^{1/2}$$
$$= KM[Cat]^{1/2} \quad .. \quad (1)$$

where R_{pth} is thermal rate and R_p represents catalysed rate. k_p, k_{tc}, k_{td}, k_d represent the specific rate constants for propogation, termination by combination, termination by disproportionation and specific rate constant for spontaneous decomposition of the catalyst [Cat] respectively; f is catalyst efficiency and M represents monomer concentration.

The second relationship connecting reciprocal degree of polymerization $1/P_n$ and various rates of polymer formation by transfer with monomer C_M and rate of polymer formation by transfer with catalyst C_{cat} is given by

$$1/Pn = (ktc + 2\,ktd)\ Rp/Kp^2M^2 + CM + C_{cat}[(Cat]/(M)] \quad .. \quad (2\text{-a})$$

$$1/P_n = A'Rp/M^2 + CM + C_{cat}[cat)/(M)] \quad .. \quad (2\text{-b})$$

$$1/P_n = A\,Rp + CM + C_{cat}[(cat)/(M)] \quad .. \quad (2\text{-c})$$

It is easy to deduce the rate of initiation of polymerization R_i as

$$Ri\ (1+x)/[cat] = R_i/[cat] = 2kdf(1+x) = 2K^2A'$$

where $x = k_{td}/(k_{td} + k_{tc})$. .. (3)

From the two simple measurements of overall rates of polymerization and degrees of polymerization at these overall rates, rates of initiation, rate of transfer with monomer and rate of transfer with catalyst have been evaluated. With the known values of k_d an approximate value of catalyst efficiency and therefore the relative importance of the type of termination reaction has been arrived at.

Experimental: The method of purification and estimation of the monomer and the catalysts Bz_2O_2 and MEKP were the same as reported previously (V. Mahadevan and M. Santappa 1955). The catalysts Azo and HAzo have been prepared by the method of Thiele and Heuser (1896) as adapted by C. G. Overberger etal (1949). The general scheme of the reaction is as follows:

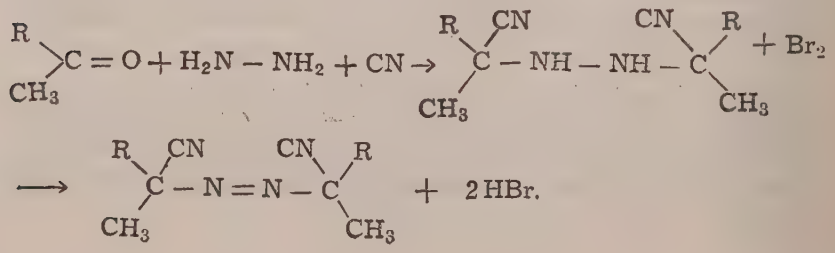

where R stands for any alkyl or aromatic group except in the case of cyclohexanone where the whole group composed of R and CH_3 is replaced by the cyclohexylring. The appropriate quantities of the ketone, hydrazine sulphate and sodium cyanide in water were shaken for two days and the substituted hydrazine compound obtained, was purified. This was then oxidised with a solution of bromine in absolute ethyl alcohol (4 gms in 100 cc). The hydrazine compound was dissolved in ethanol saturated with pure dry HCl. The bromine solution was added till absorption of bromine became very slow. The mixture was then poured into a large volume of ice water and the precipitated Azo-compound filtered and purified by repeated recrystallisation.

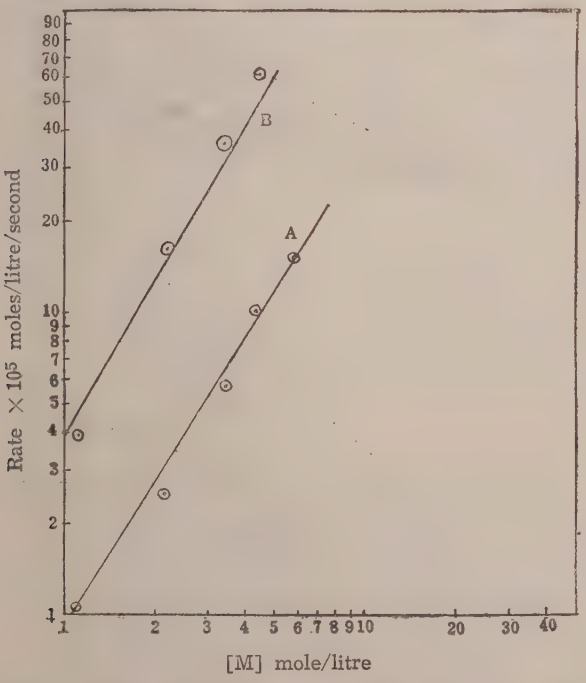

FIG. I. Plot A gives the relationship between log R_p and log M in the polymerization of methyl acrylate with Bz_2O_2 as initiator at 60°C in ethyl acetate solution. The values are plotted on the Logarithmic Scale. Plot B gives the same relationship with Azo as initiator at 70°C in ethyl acetate.

The standard solution of H_2O_2 in ethyl acetate was prepared by shaking B.D.H. H_2O_2 (~ 60 vols.) in water, with pure AR ethyl acetate, extracting the ethyl acetate layer, drying it over

anhydrous sodium sulphate, and estimating the H_2O_2 content by iodometry. This solution was then diluted to the required strength.

The details about the method of carrying out the polymerization experiments and evaluating the overall rates and degrees of polymerization have been dealt with in the previous publication (V. Mahadevan and M. Santappa 1955).

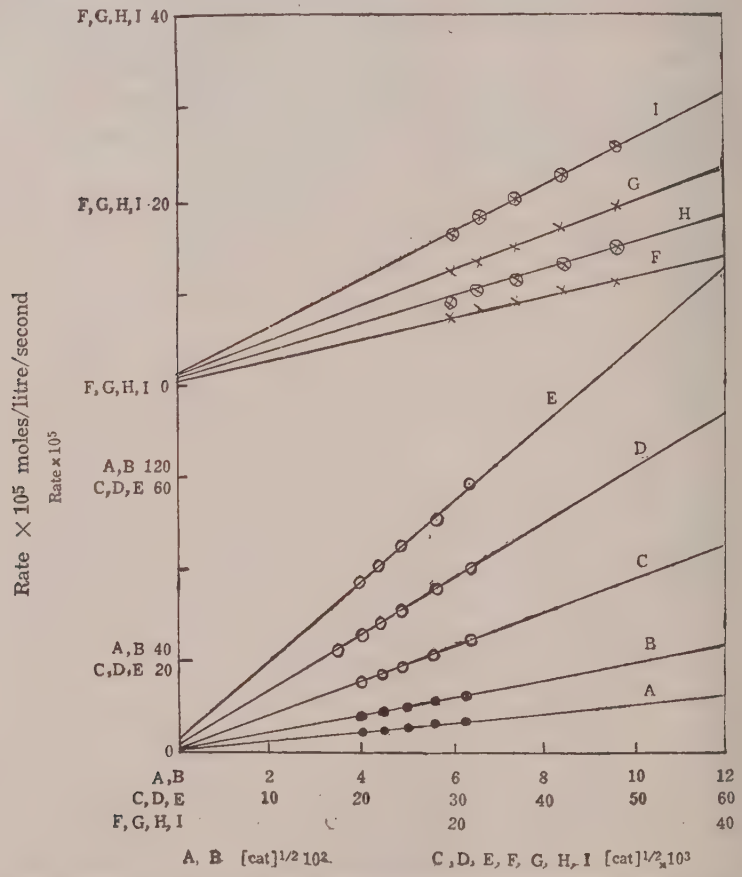

FIG. II. Plots A & B give the relationship between R_p and $(Cat)^{1/2}$ in the polymerization of methyl acrylate with HAzo as initiator at 70°C and 80°C respectively, with a 20 per cent solution of the monomer in ethyl acetate. Plots C, D & E give the same relationship with Azo as initiator at 60°C, 70°C and 80°C respectively, with a 20 per cent solution of the monomer in ethyl acetate.

Plots F & G give the same relationship with H_2O_2 as initiator at 70°C and 80°C respectively at the same monomer concentration.

Plots H & I refer to Bz_2O_2 as initiator at 60°C and 70°C respectively at the same monomer concentration.

Table 1

Rates of Initiation and Chain Transfer Constants in the Polymerization of Methyl Acrylate

Catalyst	Temp.	K	A′	Ri′/(Cat)	C cat	
Azo	60°C	$3{\cdot}182 \times 10^{-3}$	2·48	$5{\cdot}203 \times 10^{-5}$	$8{\cdot}065 \times 10^{-3}$	$12{\cdot}75 \times 10^{-5}$
	70°C	$6{\cdot}046 \times 10^{-3}$	1·94	$14{\cdot}18 \times 10^{-5}$	$1{\cdot}724 \times 10^{-2}$	15×10^{-5}
	80°C	$11{\cdot}35 \times 10^{-3}$	1·21	$31{\cdot}26 \times 10^{-5}$	$3{\cdot}125 \times 10^{-2}$	$17{\cdot}5 \times 10^{-5}$
		$3{\cdot}981 \times 10^{8}$	$2{\cdot}692 \times 10^{-6}$	$6{\cdot}918 \times 10^{12}$	$8{\cdot}511 \times 10^{9}$	·1256
		exp (-17100/RT)	exp (9154/RT)	exp (-26200/RT)	exp (-18330/RT)	exp (-4583/RT)
HAzo	70°C	$9{\cdot}09 \times 10^{-4}$	1·936	$3{\cdot}2 \times 10^{-6}$	4×10^{-3}	22×10^{-5}
	80°C	$1{\cdot}728 \times 10^{-3}$	1·2	$7{\cdot}16 \times 10^{-6}$	8×10^{-3}	24×10^{-5}
		$4{\cdot}365 \times 10^{8}$	$2{\cdot}864 \times 10^{-6}$	$1{\cdot}096 \times 10^{12}$	30548×10^{8}	·182
		exp (-18310/RT)	exp (9154/RT)	exp (-27500/RT)	exp (-17190/RT)	exp (-4583/RT)
H_2O_2	70°C	$1{\cdot}363 \times 10^{-3}$	10·75	$3{\cdot}998 \times 10^{-5}$	$6{\cdot}579 \times 10^{-3}$	$8{\cdot}3 \times 10^{-5}$
	80°C	$2{\cdot}728 \times 10^{-3}$	7·259	$10{\cdot}8 \times 10^{-5}$	$1{\cdot}921 \times 10^{-2}$	$10{\cdot}75 \times 10^{-5}$
		$6{\cdot}457 \times 10^{8}$	$1{\cdot}585 \times 10^{-6}$	$1{\cdot}479 \times 10^{11}$	$2{\cdot}188 \times 10^{15}$	1·991
		exp (-18310/RT)	exp (9154/RT)	exp (-24400/RT)	exp (-27500/RT)	exp (-6875/RT)

Table 2

Comparison of values of rates of initiation and other constants at 5·5 molar and 2·2 molar Concentration of Methyl Acrylate

(a) K, (b) A′, (c) Ri/(Cat), (d) C cat, (e) C

Catalyst	Temp	5·5 molar		2·2 molar
Bz_2O_2	60°C	(a) $1{\cdot}963 \times 10^{-3}$		(a) $2{\cdot}182 \times 10^{-3}$
		(b) 2·52		(b) 2·419
		(c) $1{\cdot}943 \times 10^{-5}$		(c) $2{\cdot}308 \times 10^{-5}$
		(d) $2{\cdot}46 \times 10^{-2}$		(d) $2\ 941 \times 10^{-2}$
		(e) $3{\cdot}25 \times 10^{-5}$		(e) $3{\cdot}5 \times 10^{-5}$
	70°C	(a) $3{\cdot}472 \times 10^{-3}$		(a) $3{\cdot}637 \times 10^{-3}$
		(b) 1·97		(b) 1·936
		(c) $4{\cdot}8 \times 10^{-5}$		(c) $5{\cdot}12 \times 10^{-5}$
		(d) 5×10^{-2}		(d) $5{\cdot}5 \times 10^{-2}$
		(e) $4{\cdot}05 \times 10^{-5}$		(e) 5×10^{-5}
MEKP	65°C	(a) $1{\cdot}325 \times 10^{-3}$	Ref. 8.	(a) $1{\cdot}386 \times 10^{-3}$
		(b) 9·456		(b) 9·679
		(c) $3{\cdot}322 \times 10^{-5}$		(c) $3{\cdot}715 \times 10^{-5}$
		(d) 5×10^{-2}		(d) 2×10^{-2}
		(e) $1{\cdot}1 \times 10^{-5}$		(e) $6{\cdot}8 \times 10^{-5}$
	75°C	(a) $2{\cdot}909 \times 10^{-3}$		(a) $2{\cdot}728 \times 10^{-3}$
		(b) 6·554		(b) 6·437
		(c) $11{\cdot}19 \times 10^{-5}$		(c) $9{\cdot}579 \times 10^{-5}$
		(d) $11\ 3 \times 10^{-2}$		(d) $3{\cdot}3 \times 10^{-2}$
		(e) $2{\cdot}5 \times 10^{-5}$		(e) $11{\cdot}8 \times 10^{-5}$

Results and Discussions:

Polymerization conditions with 20 per cent methyl acrylate monomer in ethyl acetate solution were ideal inasmuch as the thermal rate and the phase of autoacceleration were totally absent. With Bz_2O_2 as well as Azo as catalysts, it was found (Fig. I) that the rate was dependent on 3/2 powers of monomer concentration. This indicated that the catalyst efficiencies in these cases were dependent upon monomer concentration.

Polymerization experiments were conducted with the catalysts HAzo, Azo, H_2O_2, Bz_2O_2 and MEKP at temperatures ranging from 60°C to 80°C. Plots of Rate vs. $(Cat)^{1/2}$ (Fig. II) with all these catalysts were linear and passed through the origin which indicated the absence of any superimposing or disturbing reactions. The slope of each plot gave KM (Eqn 1) from which K values were evaluated. These values at various temperatures with the various catalysts with their exponential forms appear in Tables 1 and 2. An activation energy of $\sim$ 18 K cals for K would give a value of $\sim$ 26 K cals for rate of initiation with all these catalysts. The value for the frequency factor was $\sim 10^8$. If Matheson's frequency factors (Matheson etal 1951) for k_p ($\sim 10^8$) and k_t ($\sim 10^{10}$) are taken into account, a frequency factor of $\sim 10^{10}$ would be obtained for initiation.

Reciprocal degrees of polymerization versus overall rates (Fig. III A to F) were plotted after conducting polymerization of methyl acrylate with all the abovementioned catalysts. From the equations (2—a to 2—c) in the theoretical section it is obvious that the intercepts on the ordinates of these plots represent the rates of transfer of the polymethylacrylate radical chain with a monomer molecule (CM, Method 1). It was found that such a transfer did take place. It could be concluded that the specific rate of transfer with monomer was approximately 10^{-5} times as efficient as for propogation. Transfer with the monomer was highest when HAzo was the catalyst and lowest when TBHP was used (Table 3). From the slopes of the plots in Fig. III, A′ values were evaluated. These values with their exponential forms are to be found in Tables 1 and 2.

Using Matheson's values for $k_p = 2000$ and $2\ k_t = \cdot 85 \times 10^7$ in the polymerization of methyl acrylate, a value of 2·125 for $A = \frac{2k_t}{k_p^2}$ at 60°C could be obtained. Our values with Azo, and

Table 3

CM Values as obtained from the intercepts of the I/Pn vs. Rp Plot as well as [(1/Pn) — ARp] vs. [Cat]/[M] Plot

Catalyst	Temp.	Intercept of 1/Pn vs. Rp Plot		Intercept of [(1/Pn) — ARp] vs. Cat/M Plot	
Bz_2O_2	55°C	$2{\cdot}8 \times 10^{-5}$	Ref. 8 & 11	$2{\cdot}75 \times 10^{-5}$	Ref. 8 & 11
	60°C	$3{\cdot}25 \times 10^{-5}$		$3{\cdot}2 \times 10^{-5}$	
	65°C	4×10^{-5}		$3{\cdot}7 \times 10^{-5}$	
	70°C	$4{\cdot}2 \times 10^{-5}$		$4{\cdot}05 \times 10^{-5}$	
MEKP	65°C	$1{\cdot}1 \times 10^{-5}$	Ref. 8	1×10^{-5}	Ref. 8
	70°C	2×10^{-5}		$1{\cdot}8 \times 10^{-5}$	
	75°C	$2{\cdot}7 \times 10^{-5}$		$2{\cdot}5 \times 10^{-5}$	
Azo	60°C	13×10^{-5}		$12{\cdot}75 \times 10^{-5}$	
	70°C	16×10^{-5}		15×10^{-5}	
	80°C	19×10^{-5}		$17{\cdot}5 \times 10^{-5}$	
DTBP	65°C	$1\ 25 \times 10^{-5}$	Ref. 8	1×10^{-5}	Ref. 8
	70°C	$1{\cdot}8 \times 10^{-5}$		$1{\cdot}6 \times 10^{-5}$	
	75°C	$2{\cdot}75 \times 10^{-5}$		$2{\cdot}24 \times 10^{-5}$	
TBHP	60°C	$\cdot5 \times 10^{-5}$	Ref. 8	$\cdot36 \times 10^{-5}$	Ref. 8
	70°C	$1{\cdot}25 \times 10^{-5}$		$\cdot72 \times 10^{-5}$	
HAzo	70°C	$22{\cdot}1 \times 10^{-5}$		22×10^{-5}	
	80°C	24×10^{-5}		24×10^{-5}	
H_2O_2	70°C	$8{\cdot}5 \times 10^{-5}$		$8{\cdot}3 \times 10^{-5}$	
	80°C	$11{\cdot}5 \times 10^{-5}$		$10{\cdot}75 \times 10^{-5}$	

Bz_2O_2 at this temperature were 2·48 and 2·41 respectively. A value of ~ 1·9 for A′ at 70°C was also observed with Azo, HAzo and Bz_2O_2. Wide variation in the values of A′ with H_2O_2 and other catalysts (V. Mahadevan and M. Santappa 1955) remain

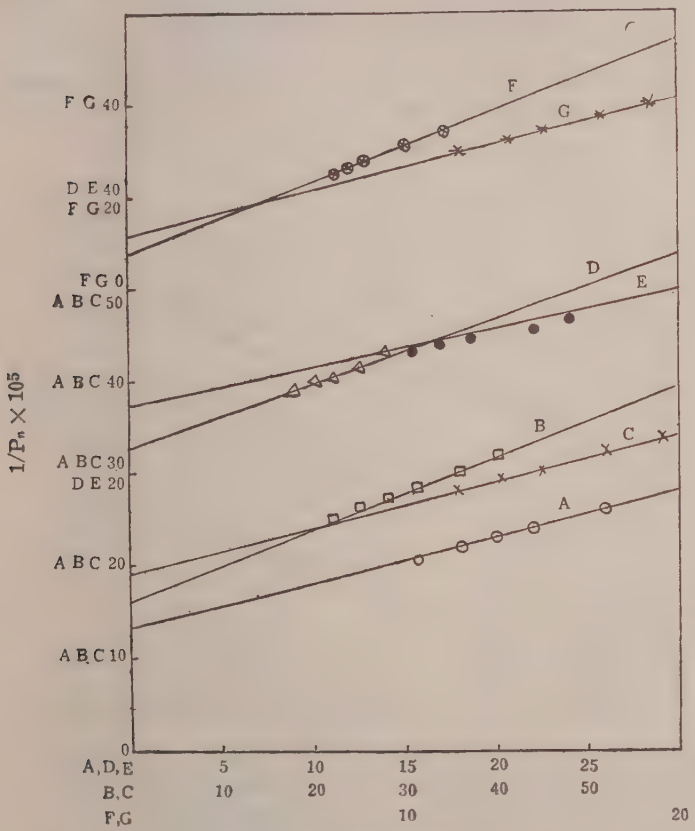

Fig. III. Plots A, B & C give the relationship $1/P_n$ vs. R_p with Azo as initiator at 60°C, 70°C and 80°C (2·2 molar monomer).

Plots D & E refer to the same relationship with HAzo at 70°C and 80°C respectively at the same monomer concentration.

Plots F & G refer to H_2O_2 at 70°C and 80°C respectively.

inexplicable at present. An activation energy of ~ 9 K cals for A′ was obtained and it was quite normal. Fig. IV (Plots A, B, C and D) represents variation of A′ with temperature when Azo, Bz_2O_2, DTBP and MEKP were used as catalysts.

Making use of the slopes in the Figures II and III, it was possible to evaluate rates of initiation of polymerization with all the catalysts under consideration at 60°C to 80°C (Eqn. 3). The $R'_i/[Cat]$ values at 70°C with Azo, HAzo, Bz_2O_2 and H_2O_2 were $14{\cdot}18 \times 10^{-5}$, $3{\cdot}2 \times 10^{-6}$, $5{\cdot}12 \times 10^{-5}$ and $3{\cdot}99 \times 10^{-5}$ respectively which indicated that Azo and Bz_2O_2 were the most efficient initiators. Further, it was found that our values for rate of initiation of methyl acrylate with Azo were much higher than the values with methyl methacrylate and styrene, the values being $5{\cdot}023 \times$

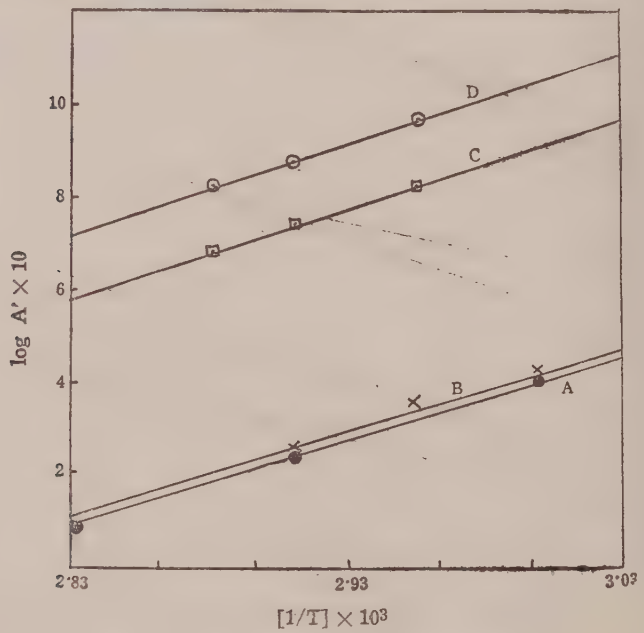

Fig. IV. Plot A log A' vs. 1/T with Azo.
Plot B log A' vs. 1/T with Bz_2O_2.
Plot C log A' vs. 1/T with DTBP.
Plot D log A' vs. 1/T with MEKP.

10^{-5}, $1{\cdot}48 \times 10^{-5}$ and $1{\cdot}77 \times 10^{-5}$ respectively at 60°C (Tobolsky and coworkers 1952 and 1953). This was in agreement with the finding by Arnett and Peterson (1952) that the rate of initiation depended upon the monomer used and not the same as had been claimed by Tobolsky and Baysal (1953). Variation of rate of initiation with temperature with the catalysts DTBP, MEKP, Bz_2O_2 and Azo are given in Fig. V. Values of initiation at various temperatures with the various catalysts with their exponential forms are given in Tables 1 and 2.

The specific rate constants for the spontaneous decomposition of the catalysts (k_d) Azo ($\cdot 0001533 \times sec^{-1}$) and HAzo ($4 \cdot 7 \times 10^{-6}$) (F. M. Lewis and M. S. Matheson 1949) being known, it was possible to calculate the catalyst efficiencies (f′) in both these cases (Eqn. 3). A catalyst efficiency of nearly 1 was obtained for Azo

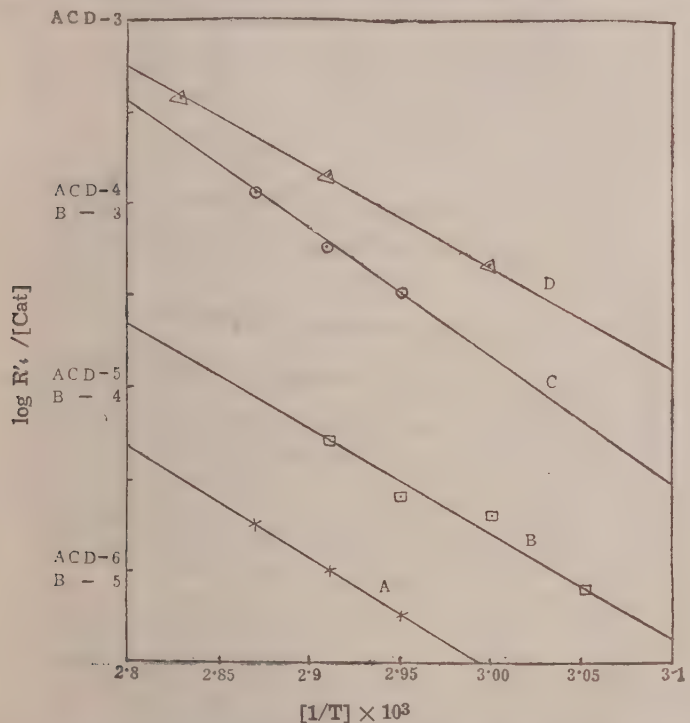

Fig. V. Plots A, B, C & D refer to the variation of $R'_i/[Cat]$ with temperature when DTBP, Bz_2O_2, MEKP and Azo respectively were used us initiators.

and approximately ·8 for HAzo. From these values, it appeared as though that termination by combination was more predominant in methyl acrylate polymerization and the monomer conformed to methyl methacrylate rather than styrene in the type of termination in its polymerization.

Values of $[(1/Pn) - AR_p]$ were plotted against [Cat]/[M] (Eqn. 2—c) and from the slope and the intercept of these plots were evaluated rates of transfer of the chain radical with the catalyst C_{cat} and with monomer C_M (Method 2) respectively. C_{cat} values for all the catalysts were $\sim 10^{-2}$ to 10^{-3}. These values with their exponential forms for all the catalysts are given in Tables 1

and 2. It was interesting to observe that in all cases catalyst was more efficient by hundred to thousand times than monomer for transfer. Further, wherever transfer was more efficient with catalyst, transfer with monomer in the same reaction was comparably less efficient.

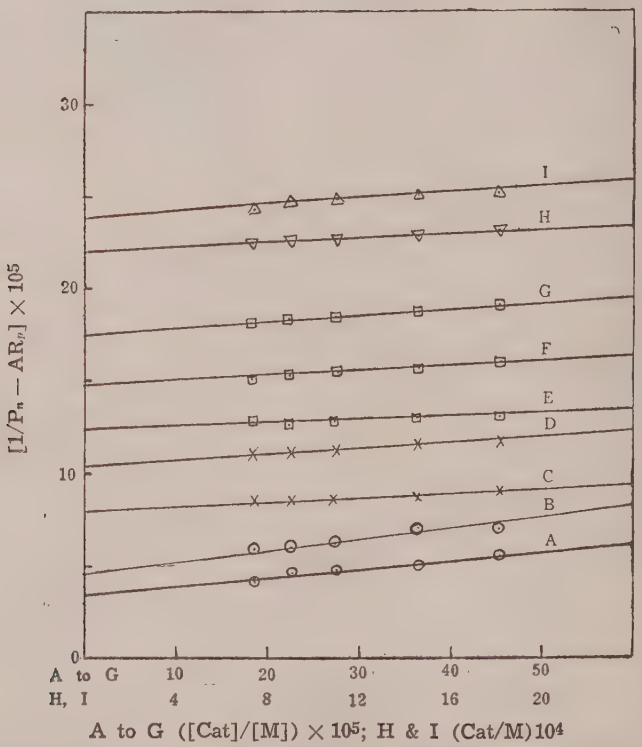

Fig. VI. All the Plots give the variation of $[(1/P_n) - AR_p]$ with [Cat]/[M] in the polymerization of methyl acrylate with a 20 per cent solution in ethyl acetate.

Plots A & B refer to Bz_2O_2 at 60°C and 70°C.
Plots C & D refer to H_2O_2 at 70°C and 80°C.
Plots E, F & G refer to Azo at 60°C, 70°C and 80°C respectively.
Plots H & I refer to HAzo at 70°C and 80°C.

The C_M values evaluated by the methods (1 and 2) indicated above are compared in Table 3. It was found that the values differed very little when either of the methods was used for calculating this quantity. It was further found that the values of K, A', $R_i'/[cat]$, C_{cat} and C_M differed very little when either 5·5 molar monomer or 2·2 molar monomer was used for polymerisation. These

Table 4

Rates of Initiation in the Polymerization of Methyl Acrylate, Methyl Methacrylate and Styrene

(a) K, (b) A', (c) R'i/(Cat), (d) C_{cat}, (e) CM

Monomer	Azo		HAzo		MEKP	
Methyl acrylate	(a) $3{\cdot}182 \times 10^{-3}$		(a) $1{\cdot}728 \times 10^{-3}$		(a) $1{\cdot}447 \times 10^{-3}$	
	(b) 2·48		(b) 1·2		(b) 7·563	
	(c) $5{\cdot}023 \times 10^{-5}$	at 60°C	(c) $7{\cdot}164 \times 10^{-6}$	at 80°C	(c) $5{\cdot}733 \times 10^{-5}$	at 70°C
	(d) $8{\cdot}065 \times 10^{-3}$		(d) 8×10^{-3}		(d) $7{\cdot}698 \times 10^{-2}$	Ref. 8
	(e) $12{\cdot}75 \times 10^{-5}$		(e) 24×10^{-5}		(e) 18×10^{-6}	
Styrene	(a) $8{\cdot}61 \times 10^{-5}$		(a) $1{\cdot}17 \times 10^{-5}$		(a) $5{\cdot}909 \times 10^{-4}$	
	(b) 900 & 861	at 60°C	(b) 399		(b) 1085	
	(c) $1{\cdot}77 \times 10^{-5}$	Ref. 4	(c) $1{\cdot}08 \times 10^{-7}$	at 80·3°C	(c) $10{\cdot}68 \times 10^{-6}$	at 70°C
	(d) 0		(d) No data	Ref. 4	(d) $21{\cdot}714 \times 10^{-2}$	Ref. 13
	(e) 6×10^{-5}		(e) No data		(e) No data	
Methyl methacrylate	(a) $3{\cdot}28 \times 10^{-4}$		(a) $2{\cdot}9 \times 10^{-4}$		(a) $1{\cdot}086 \times 10^{-4}$	
	(b) 67·3	at 60°C	(b) No data		(b) 103·3	
	(c) $1{\cdot}48 \times 10^{-5}$	Ref. 4	(c) $5{\cdot}57 \times 10^{-6}$	at 77°C	(c) $2{\cdot}44 \times 10^{-6}$	at 70°C
	(d) 0		(d) No data	Ref. 4	(d) 5×10^{-3}	Ref. 5
	(e) 1×10^{-5}		(e) No data		(e) 2×10^{-5}	

various values for the catalysts Bz_2O_2 and MEKP are given in Table 2. All these values for methyl acrylate with Azo, HAzo and MEKP are also compared with the values for methyl methacrylate and styrene polymerizations with the same catalysts (Table 4). From a glance at these values, it is obvious that methyl acrylate conforms to the other normal monomers for polymerization in spite of its abnormal tendency for autoacceleration.

REFERENCES

Arnett, L. M.	(1952)	Kinetics of the polymerisation of methyl methacrylate with aliphatic azobisnitriles as initiators. *J. Amer. chem. Soc.* **74**: 2027.
Arnett, L. M. & Peterson, J. H.	(1952)	Vinyl polymerisation with radioactive aliphatic azobisnitriles as initiators. *J. Amer. chem. Soc.* **74**: 2031.
Baysal, B. & Tobolsky, A. V.	(1952)	Rates of initiation in vinyl polymerisation Methyl methacrylate. *J. Polym. Sci.* **8**: 529.
Baysal, B. & Tobolsky, A. V.	(1953)	A Review of Rates of Initiation *J. Polym. Sci.* **11**: 471.
Gopalan, M. R. & Santappa, M.	(1956)	Methyl ethyl ketone peroxide as initiator in the polymerisation of methyl methacrylate. *J. Madras. Univ.* (In press).
Johnson, D. H. & Tobolsky, A. V.	(1952)	Monoradical and Diradical Polymerisation of styrene *J. Amer. chem. Soc.* **74**: 938.
Lewis, F. M. & Matheson, M. S.	(1949)	Decomposition of Aliphatic Azo compounds" *J. Amer. chem. Soc.* **71**: 747
Mahadevan, V. & Santappa, M.	(1955)	Rates of initiation and chain transfer constants in the polymerisation of methyl acrylate. *Makromol. chem.* **16**: 119.
Matheson, M. S., Auer, E. E., Bevilacqua, E. B. & Hart, E. J.	(1951)	Rate constants in freeradical polymerisation. IV. Methyl acrylate. *J. Amer. chem. Soc.*, **73**: 5395.
Overberger, C. G, O'Shaughnessy, M. T., & Shalit, H.	(1949)	Preparation of Aliphatic Azobisnitriles *J. Amer. chem. Soc.*, **71**: 2661.
Santappa, M. & Mahadeva Ayyar, V.	(1955)	Rates of initiation in the polymerisation of methyl acrylate. *Curr. Sci.* **24**: 173.
Thiele, J. & Heuser, K.	(1896)	Ueber Hydrazinderivate der Isobuttersaure *Liebigs, Ann.* **290**: 1.
Vaidhyanathan, V. S.	(1956)	M. Sc. Thesis to the University of Madras January, 1956.

J. Madras Univ., B, XXVI, No. 1, pages 93-115, 1956

Charnockites and Associated Rock Types of the Type Area of Sir Thomas Holland—Part I

BY

N. Leelananda Rao,
Department of Geology and Geophysics,
University of Madras-25 *

(Received for publication on January 31, 1956)

ABSTRACT

In this paper is presented a detailed map of the "Charnockite Series" of the type area of Sir Thomas Holland. The structural elements have been evaluated and the mutual field relationships of the rock types indicated. The area consists of psammitic, pelitic, semi-pelitic, calcareous and igneous members which had attained earlier the sillimanite grade of metamorphism. These metamorphosed rocks have been later subjected to a Regressive Metamorphism, by the intrusion of the charnockite (acid member of the 'Charnockite Series' of Sir Thomas Holland).

Introduction

An interesting suite of rocks called Charnockites were first found in full variety by Sir Thomas Holland at St. Thomas' Mount and Pallavaram which are about 10 miles south of Madras and have since come to be regarded as the type area of charnockites. Subsequently he found occurrences of these rocks in great force throughout South India, and laid the foundations for the study of Charnockites in his classical Memoir published in 1900. Rajagopalan (1946, 1947) made critical studies on the Petrography and Petrochemistry of the Charnockites of St. Thomas' Mount; and recently Naidu (1954) and Howie (1955) made unique contributions to the mineralogy of Charnockites. Though important aspects of the charnockitic rocks of the type area have been engaging the attention of research workers from time to time, it has to be noted that a geological map and structural map of this important area, which are so essential for a closer understanding of the problem of Charnockites, have been lacking up-to-date. To supply the long felt want, therefore, geo-

* Now in the Department of Geology, Presidency College, Madras-5.

logical and structural maps have been prepared and appended to this paper which deals with the field and structural aspects of the Charnockites and associated rocks of the type area of Sir Thomas Holland.

Classification and Occurrence

The principal rock types of the type area of Holland can be divided into:

(1) Khondalites,
(2) Charnockites,
(3) Leptynites,
(4) Granites, Pegmatites and Aplites
and (5) Dolerites.

Khondalites which are undoubtedly the oldest formations occur as disconnected patches and lenses associated with charnockites and leptynites, and comprise a series of psammitic and pelitic gneisses which show lateral compositional variation in the direction of persistent strike and dip. The components of the khondalites are garnetiferous—sillimanite gneiss, cordierite gneiss, garnetiferous-biotite gneiss and quartz magnetite rocks. They are perfectly gneissose and bedded in character.

Garnetiferous-sillimanite gneiss which is greyish white rock of banded appearance is principally made up of quartz with subordinate amounts of needles of sillimanite and pink garnets, and forms the main bulk of khondalites. Distinct bands of these rocks occur in force in Pachaimalai and in low mounds east of Nagalkeni and north-east of Cowl Bazaar, surrounded by leptynites or charnockites.

Cordierite gneiss comprised of deep blue cordierite and white quartz occurs at the contact of these rocks with charnockites in a low mound south-west of St. Thomas' Mount.

Garnetiferous-biotite gneiss appears as intercalated bands varying in width from 10-20 feet in the sillimanite gneisses of Pachaimalai and is highly siliceous in character. Thin layers of biotite separate the layers of quartz with felspar and garnet.

In the western portions of Pachaimalai quartz-magnetite rocks occur as thin bands both in sillimanite gneisses and leptynite. In

the sillimanite gneiss these bands are enriched with deep green hedenbergite, red garnet and magnetite with subordinate amounts of quartz. But in the leptynite they show perfect banded structure due to the presence of alternating layers of quartz and magnetite, with or without very subordinate amounts of hedenbergite and garnet.

Charnockites which are the predominant rock types of the area comprise ultra-basic, basic, intermediate and acid types.

The Ultra-basic Charnockites are mainly represented by granulitic pyroxenites which are characterised by hypersthene, greenish brown hornblende and augite together with small quantities of green and black spinelloids and occasional apatite. They occur on the summits of the low hill south-west of Pammal as minute lenticular ultra-basic segregations in the basic charnockites with interlocking contacts. Segregations of pyroxenites and amphibolites with subordinate amounts of plagioclase occurring as autoliths in the basic charnockites in a long hill east of Trisul and in the plains east of Nanmangalam can also be included under this division.

Basic Charnockites occur as imperfect bands associated with subacid and acid charnockites, and the largest of the bands ex-

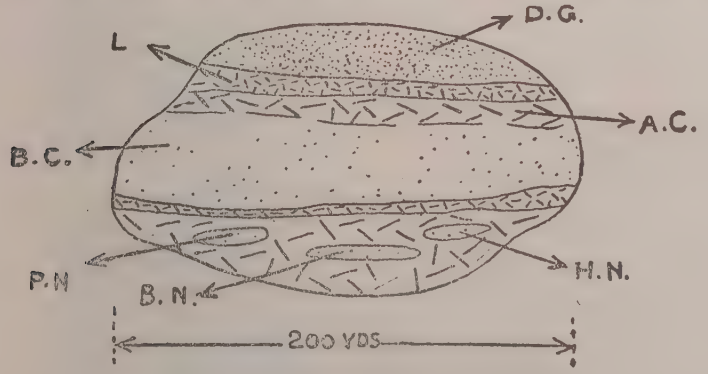

Fig. 1

B.C. Basic Charnockite. H.N. Hornblende Norite. A.C. Acid Charnockite. P.N. Pyroxene Norite. B.N. Biotite Norite. L. Leptynite. D.G. Diopside Granulite.

tends from Pammal Hill to south-west of Tirunirmalai. The small masses possess a lenticular habit and show a directional disposition of the constituents parallel to the long axis of the lens. Fine-grained, dark-coloured basic charnockites rich in hornblende and

biotite and sometimes garnet occur in the form of schlieren and autoliths (Plate i. Fig. 1) throughout the acid charnockites east of Pallavaram. At Cherimalai the autoliths of granulitic pyroxene-bearing basic charnockites enveloped in the acid charnockites show a gradational passage through hornblende norites to biotite norites (Fig. 1), which are characterised by a gneissose texture due to the directional orientation of hornblende, biotite and hypersthene. At the southern end of the Rifle Range the basic charnockites occurring as subangular fragments in the acid charnockitic base (Fig. 2) induce in the rock the appearance of a flow breccia.

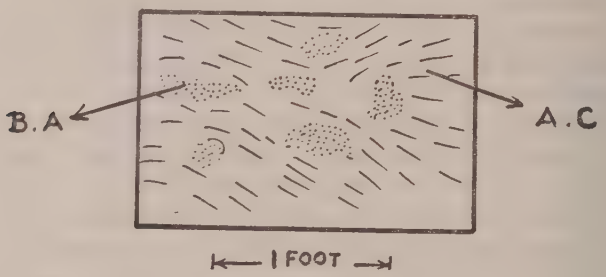

Fig. 2

B.A. Basic autoliths.
A.C. Acid charnockite.

About one furlong south-east of Meenambakkam Railway Station, basic charnockite occurs as thin, distorted and drawn out lens in the acid charnockite (Fig. 3) giving the rock a striking appearance on the weathered surface.

Fig. 3

B.C. Basic charnockite.
A.C. Acid charnockite.

The basic charnockites comprise a series of norites enriched either with augite, hornblende or biotite. There is also a garnetiferous variety.

FIG 1. Field photograph of Basic autoliths in Acid Charnockite, Thattan Kunnu quarry north-east of Trisul.

The perthitic types of acid charnockites show variations with respect to their mafic constituents. Though hypersthene is the normal mafic member, we also come across types west of Cowl Bazaar which are characterized by only biotite, garnet or magnetite as the principal mafic constituents in one and the same mass. Of course all these minerals are secondary after hypersthene.

Coarse-grained quartz-felspar veins of bluish grey colour run in diverse directions in the acid and basic charnockites. In a hill north-east of Trisul the coarse grained bluish grey veins which are one foot thick cut across the charnockites as shown in Fig. 4.

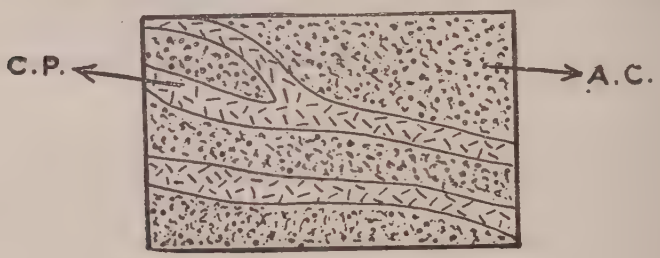

Fig. 4

C.P. Charnockitic pegmatite.

A.C. Acid charnockite.

Sometimes coarse grained microcline perthite with very subordinate amounts of quartz occurs as clots and patches in the charnockites in the south-western portion of Trisul. Larger masses of coarse grained variety with quartz and microcline perthite occur to the west of Cowl Bazaar as an intimate member of the charnockites. These rocks without mafic constituents can be called Alaskitic charnockites and perhaps these represent the last phase in the consolidation of charnockitic magma.

Besides autoliths of acid charnockites in the basic charnockites and a basic type in the acid variety there are also fragments of xenoliths present in the basic charnockites of Trisul and Cherimalai. At Cherimalai (Fig. 5) there are xenoliths of calc-diopside granulites in the garnetiferous diopside granulites; and the intermediate zone between them is enriched with diopside, plagioclase, scapolite and calcite with sphene as an important accessory. The diopside granulite passes outwards to diopside bearing norites. At Trisul the calc silicate xenolith, characterized by wollastonite, diopside, grossularite, sphene and calcite occurs as a caught up patch

(Fig. 6) in the acid charnockites. Besides these calc-xenoliths there are also cordierite-hypersthene-sillimanite bearing xenoliths in the acid charnockites at the south-eastern portion of Tambaram Hill (Fig. 7).

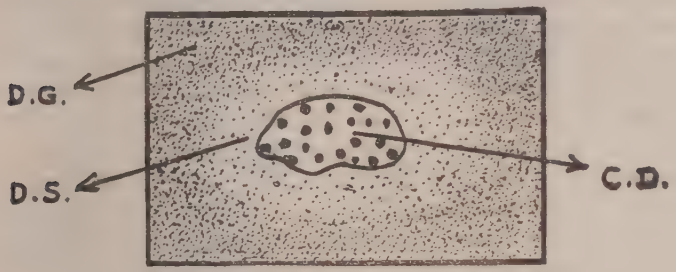

Fig. 5
C.D. Calc-Diopside granulite.
D.S. Diopside-scapolite granulite.
D.G. Diopside granulite.

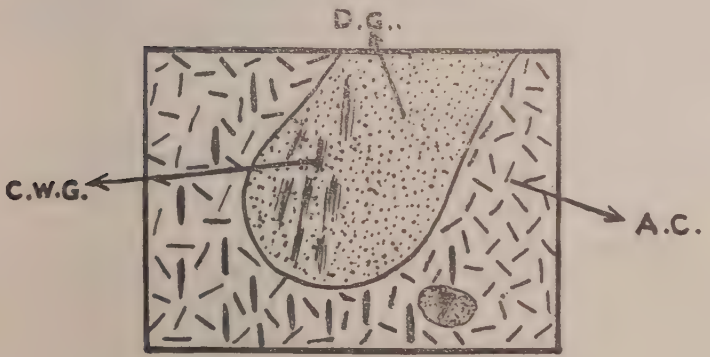

Fig. 6
C.W.G. Calc-Wollastonite granulite.
D.G. Diopside granulite.
A.C. Acid charnockite.

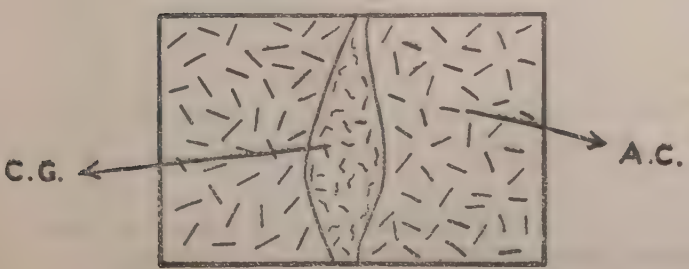

Fig. 7
C.G. Cordierite gneiss.
A.C. Acid charnockite.

Leptynite is a friable cream-coloured rock sprinkled with garnets and occurs as distinct bands and lenses associated with khondalites and charnockites. Holland (1900 p. 143) considers these leptynites as metamorphosed members of the acid charnockites and observes, "The rocks now referred to present the characters of those known to German petrographers as 'normal granulites', but the minerals rutile, kyanite, sillimanite, etc., so frequently found in the Saxon Granulites do not occur in these rocks at Pallavaram." The detailed survey of the area by the author discloses that very often lenses and patches of highly siliceous sillimanite gneiss occur as relics in the leptynites of the eastern and western portions of Pachaimalai. Similarly relics of sillimanite gneisses and radiating needles of sillimanite are found in the leptynites east of Pallavaram (Fig. 8). It also occurs as bands of considerable length in between the khondalites and charnockites and it grades often into the khondalites on the one hand and into the charnockites on the other. At the contacts of the charnockites there is gradation of colour from greyish white to grey. It shows faint banding approaching that of migmatite. In brief, these rocks present the characteristics of Saxon Granulites.

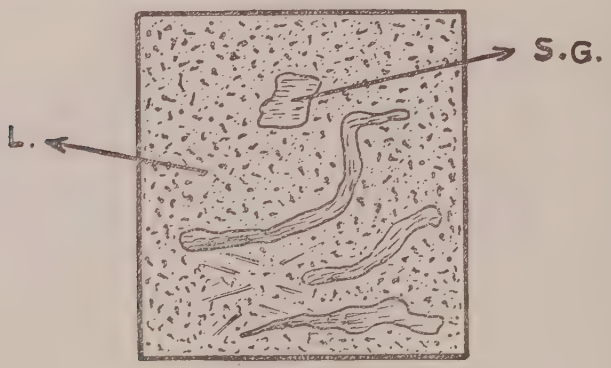

Fig. 8

S.G. Sillimanite gneiss.
L. Leptynite.

There are highly crushed bluish grey garnetiferous leptynites derived from charnockites in the highly disturbed zone east of Pallavaram.

The cream coloured garnetiferous leptynites are extensively ramified by quartz felspar veins genetically connected with later granite intrusives.

The *coarse and medium grained granites* principally made up of felspar and quartz with subordinate amounts of hornblende, biotite and chlorite show discordant relation to the charnockites in Cherimalai, in the long hill east of Trisul and in the northern portion of Tambaram Hill. Pegmatites of granitic composition without mafic minerals cut through the charnockites east of Pallavaram, and *aplites* of the same composition displaying discordant relation to the charnockites are found along the western portions of the hill south-west of Pammal.

Dolerite dykes of diverse composition are the youngest formations in the type area of Holland and their field and structural characters were described in detail in a previous paper by the author (1956).

Structural Elements

Structural map (Fig. 22) of the type area of Holland has been prepared on the lines initiated by Hans Cloos (1936). The symbols on the map refer to structures occurring in groups and variations in strike or dip. Any structural element within the area covered by the symbol is not more than 5° from the plotted direction. As there is consistency of orientation of structural elements within suitable areal limits the same symbol has been recorded on the map to show their average strike and dip.

This technique was applied to all the rocks occurring in the area, and some 600 readings were plotted involving over 1000 individual compass-clinometer readings.

The rocks are characterized by foliated structure to which all joints and other structures are geometrically related.

Foliation: The pelitic and psammitic gneisses are strongly foliated, and in these rocks the primary bedding is entirely subordinate to foliation. The foliation planes are 2 to 3 mm. across in fine grained sillimanite gneisses. The strike of foliation varies from N 35° E to N 45° E, and they are either vertical or dip at high angles towards south-east. On the surface of foliation plane quartz and sillimanite show distinct lineation, the pitch of which is 20° in the N 35° E—N 45° E direction (Fig. 9). The sillimanite gneiss of the summit of Pachaimalai shows a perfect bedding plane schistosity and cleaves readily along that direction. With the increase in grain size the foliation planes are faintly visible or not visible at all.

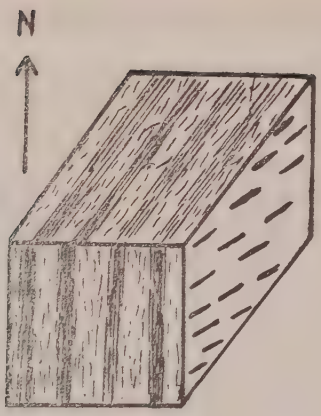

FIG. 9

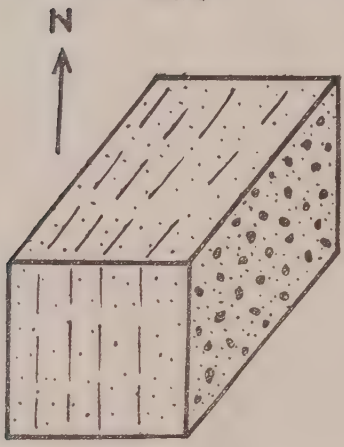

FIG. 10

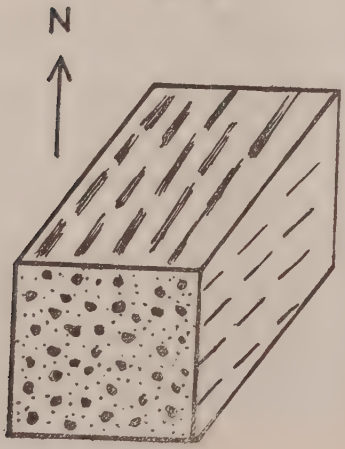

FIG. 11

In garnetiferous biotite gneiss the individual folia are very much thinner, and the dark thin folia which are enriched with oriented biotite flakes alternate with thin layers of quartz and felspar.

Foliation and lineation of charnockites are marked on the map where they could be measured in the field. As a rule the centres of charnockite massifs are structureless on fresh surfaces but in a few localities lineation is distinctly seen on weathered surfaces due to the directional orientation of hypersthene, hornblende and biotite. In the rocks the faint foliation parallels the strike of foliation of the meta-sediments. Fig. 10 shows the characteristic foliation displayed by a norite south-west of St. Thomas' Mount. Due to the parallelism of hypersthene the rock shows distinct foliation, but the surface parallel to the foliation displays granulitic texture and this is a common feature of charnockite quarries opened along the strike of foliation. Acid and enderbitic charnockites also show faint and discontinuous foliation due to the parallel orientation of hypersthene along their contacts with basic charnockites and meta-sediments. Perhaps the discontinuity is due to the presence of meagre amounts of hypersthene. Some of the leptynites show distinct foliation on the weathered surfaces due to the horizontal lineation of quartz. The sections perpendicular to visible foliation exhibit a granulitic texture as shown in Fig. 11.

The foliation planes of the majority of the rocks strike from N 20° E — S 20° W to N 45° E — S 45° W.

Though the strike of foliation of metasediments, charnockites and leptynites is roughly towards a N. E.-S. W. direction, it shows a sudden swing in its trend towards E-W direction to the east of Pallavaram. This fact is shown in Fig. 12 which is the projection of the poles of 430 foliation planes plotted without selection. There are two maxima, the best of which lies in the N-W quadrant and the minor one in the north pole. It is therefore concluded that the forces in the area operated from the north-west to induce the foliations in a north-east to south-west direction in all the rock types. The minor deviation of strike of foliation towards E-W may be either due to an independent strike of deposition of the rock types, or alternately, the rocks which had a concordant strike of deposition in N. E.-S. W. direction may have been titled into their present position by a shear couple.

Joints: The joints have been analysed by considering their relation to the foliation planes of the rocks. There are two major sets of joints. one parallel or nearly parallel to the foliation and the

other at 70° to 90° to the foliation. In addition to these two there is a third type which is nearly at 45° to the foliation planes with a very variable dip. Of these the two major sets constitute 85% of the recorded observations. Although essentially similar, the jointing in the meta-sediments is not so regularly developed as that in the charnockites. Even amongst the charnockites the regularity of the joints is present in the acid types.

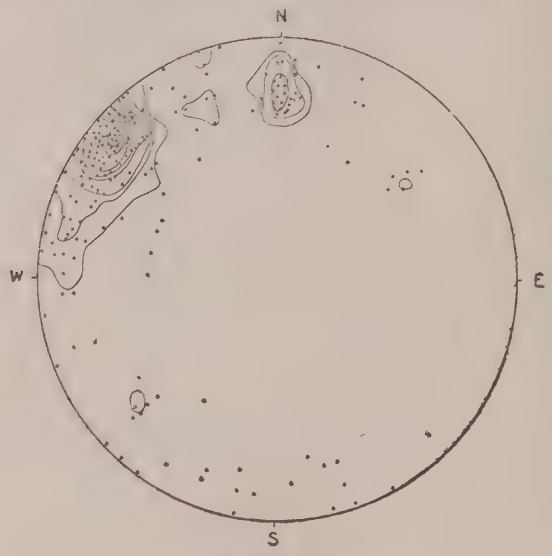

Fig. 12
Contours at 0-1-2-3-4-5-6-7-8%

Besides these, sheet joints which have resulted due to the release of load are present and follow the topography.

The field observations were checked by analysing the joints on a Schmidt equal-area projection. As the joint patterns of the meta-sediments and charnockites are closely similar, the poles of the joints were plotted on the lower hemisphere and they are shown in Figs. 13, 14, and 15. In Fig. 13 the contours of cross joints perpendicular to foliation culminate in two maxima which are due to N. E. and E. W. foliation displayed by the rocks. The predominance of joints perpendicular to North-East foliation is shown by the wider area of the contours. Similar behaviour of joints is shown in Fig. 14 by the joints parallel to foliation. Fig. 15 shows two well developed maxima and one subsidiary maximum. The two major maxima correspond to the joints present at approximately 45° to the E-W and N. W.-S E. foliation planes and the subsidiary maxima to the predominant N. E.-S. W. foliation.

FIG. 13
Contours at 0-1-2-3-4-5-6-7-8-9-10-11%
(513 Poles).

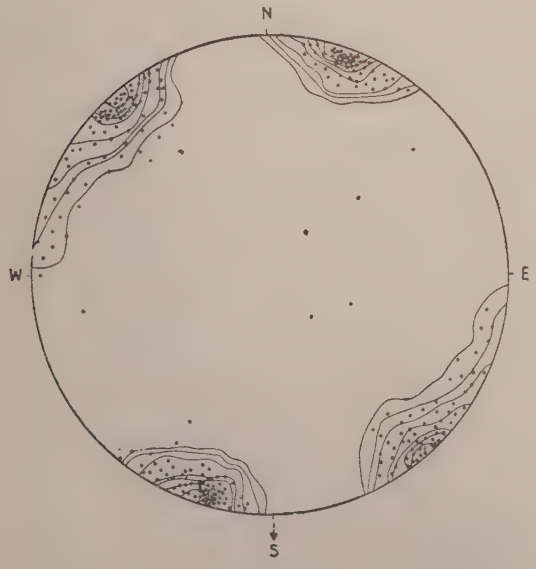

FIG. 14
Contours at 0-1-2-3-6-9-12-15%
(282 Poles).

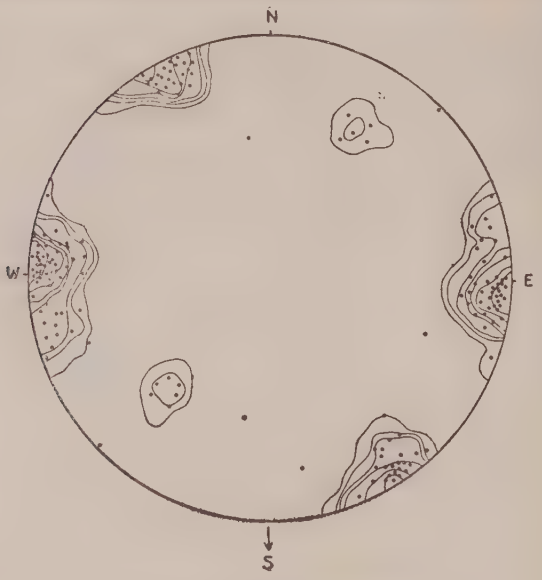

FIG. 15
Contours at 0-1-2-3-6-9-12-15%
(163 Poles).

The joint surfaces vary from smooth to hackly and apart from a brownish stain they are generally free from mineral deposition. Sometimes pyrite is present. The joints of metasediments are hackly and usually limonitized to a great extent.

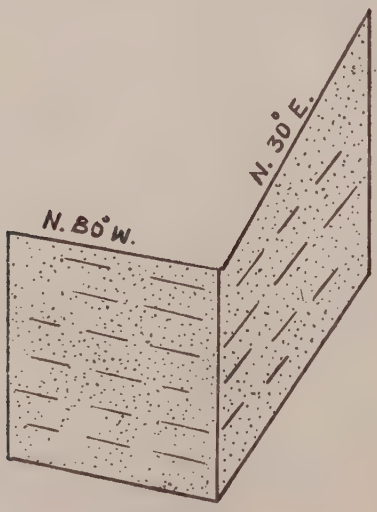

FIG. 16

At the southern end of the Rifle Range the joints are highly polished and slickensided, and one joint strikes N 80° W and the other N 30° E. Their highly polished joint surfaces show lineation of the mineral constituents as shown in Fig. 16. On detailed examination it was found that there are several such joints in that area, and by resolving the forces in the field it appears that couples have acted along the directions indicated in Fig. 17. The rocks adjacent to these joints show their highly crushed and mylonitised nature.

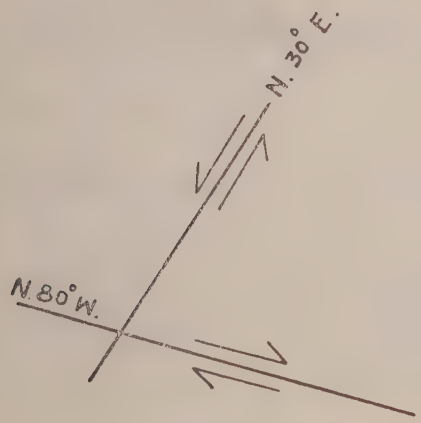

Fig. 17

Deformation Breccia: Adjacent to the zone, just south of the Mosque on the summit of the Mosque Hill, there are black compact strings, lenses and dykes of greyish black dense compact material in the basic and acid charnockites and in charnockitic leptynites to which King and Foote (1865) have suggested the name "trap-shotten gneiss". Some of these lenses are characterised by two sets of cleavages which strike N 75° W — S 75° E and N 20° E —S 20° W, and these closely parallel the directions of the slickensided joint planes. The breccia has a steep dip and definite walls, and sends several branches in different directions into the rocks in which it occurs as shown in Fig. 18.

Under the microscope the greyish black compact mass is composed of black dust through which angular fragments of quartz, felspar and mafic minerals are disseminated and the whole rock is highly crushed and mylonitized.

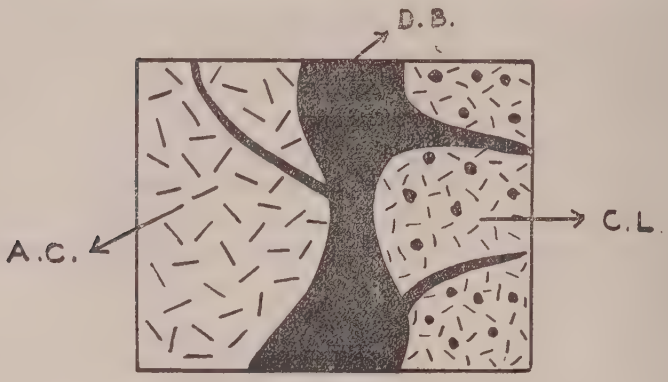

Fig. 18

D.B. Deformational Breccia. A.C. Acid Charnockite. C.L. Charnockitic Leptynite.

The matrix varies considerably but has some relation to the rocks in which it occurs. In basic charnockite it is black, in acid charnockite brown and in leptynite somewhat greyish. The matrices of these breccia display flow texture. Sharp contacts of the fine grained matrix with uncrushed but strained portions confirm the plastic flow of the breccia. Sometimes veins of this finely crushed matrix shoot into the highly crushed portions in different directions.

The matrices have the same mineral composition as the rocks in which they occur. The fragments are usually angular to subangular with shapes which can endure flow.

In the southern portion of Rifle Range the charnockites are highly crushed. Angular fragments of charnockites, porphyroblasts of felspar and quartz, variations in grain size of the gound mass, bent plagioclase crystals along the borders of a few of the fragments, and drawn-out appearance of small fragments are evidences of their highly disturbed and crushed nature. In the Mosque Hill and Rifle Range garnets occur in the crushed charnockites.

Faulting: East of Pallavaram in the highly disturbed zones of the charnockitc complex the strike of foliation suddenly swings to N. W. — S. E. to E —W. from the normal N. E. — S. W. trend, and dips towards south-east or south at angles varying from 50° to 70°. North-east of Rifle Range some of the masses dip towards north-west. These sudden and abrupt changes in strike and dip

indicate dislocation and rotation of the block east of Pallavaram from its normal position. This is also supported by slickensided joint surfaces, mylonitic and cataclastic structures displayed by the rocks in that portion. The rotation of the block appears to have been brought about due to the movement of the rocks along the complementary fractures which parallel closely the trend of major joints that are either parallel or perpendicular to the dominant N. E. — S. W. foliation of the type area. It is also interesting to note that the trend of the major leptynitic bands are also parallel to the fractures.

After the formation of charnockites the rocks were apparently subjected to severe compression, and in the charnockitic massif east of Pallavaram the deformation was most severe with the result that the mass was blocked out.

Petrofabrics: The petrofabric study of the various rock types in the area, charnockites, leptynites and sillimanite gneisses has been undertaken.

Petrofabric diagrams prepared on sections cut perpendicular to the strikes of visible foliation of these rocks are represented in Fig. 19 a-d. It is obvious in these diagrams that the plane of foliation is coincident in all the 4 diagrams. The petrofabric patterns, however, are different.

Fig. 19-a
Contours at 0-1-2-3-4-5-6-7-8-9%
(235 Quartz axes).

FIG. 19-b

Contours at 0-1-2-3-4-5-6-7-8-9-10%
(242 Quartz axes).

FIG. 19-c

Contours at 0-1-2-3-4-5-6-7-8-9%
(204 Bi-cleavage Poles)

Fig. 19-d
Contours at 0-1-2-3-4%
(234 Quartz axes).

The sillimanite gneiss (Fig. 19a) has a prominent maximum near the periphery of the diagram. This maximum looked at from b-c plane would correspond to the central maximum type 1 of Sander. According to him this is the maximum around a- axis, the direction of movement. Fig. 19b which is that of leptynite adjoining the sillimanite gneiss shows an identical maximum of quartz axes.

The biotite diagram of the norite (Fig. 19c) shows the characteristic double maxima of the biotite diagram, and the foliation plane runs in between them. Fig. 19d is a quartz diagram of acid charnockite of St. Thomas' Mount. Here the pattern is slightly different. There is a weak central maximum with four better maxima developed on either side of the c-axis and barrenness at the end of 'a', with an almost complete a-c girdle. The diagram seems to correspond to a typical granulite diagram. The peripheral maxima, however, do not make an angle of 45° with each other but make an angle of 30°.

It is, therefore, seen that though all these rock types have a consistent foliation referrable to the same force their petrofabric patterns are not always the same. Therefore, the two features,

foliation and petrofabric patterns, are referrable to two different causes. The first is due to deformation and the second due to crystal growth during or after deformation.

Petrofabric diagrams (Fig. 20a, b, c) illustrate the central maxima in granulite diagrams, and the discussions that have been introduced in interpreting them. Fig. 20a is that of leptynite cut perpendicular to the strike of foliation. Here there is a complete girdle with several minor maxima within the girdle. Since a-c girdle is interpreted as being perpendicular to b-axis of Sander, one should interpret this diagram so that the central maximum corresponds to the b-axis and the girdle as rotatoin around it. But in the rock section there is no lineation parallel to 'b'. In these circumstances the central maximum is interpreted as the 'a' direction of movement of Sander.

Fig. 20b is again a diagram of leptynite in the plane perpendicular to strike of foliation. Here there is a single maximum in the centre and incomplete and dispersed a-c girdle. There is no difficulty in interpreting the central maximum as a direction of movement.

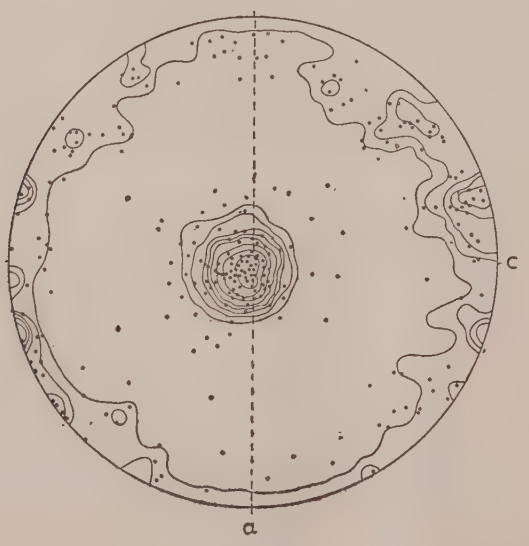

Fig. 20-a

Contours at 0-1-2-3-4-5-7-9-11%
(231 Quartz axes).

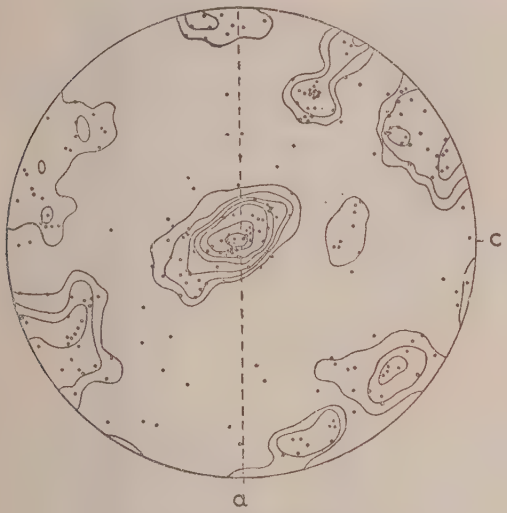

FIG. 20-b

Contours at 0-1-2-3-4-5-6-7%
(266 Quartz axes).

FIG. 20-c

Contours at 0-1-2-3-4-5-7%
(284 Quartz axes).

Fig. 20c represents b-c plane of an acid charnockite; and again the central maximum indicates the 'a' direction of movement. From this diagram it is evident that acid charnockites intruded vertically.

Conclusion

In this paper is presented the results of detailed mapping of the rock formations of the type area of Sir Thomas Holland. The descriptions of the rock types have been confined to their magoscopic characters and mutual field relationships. Structural elements in the rocks have been evaluated. Detailed microscopic and chemical characters are to follow.

The rock types comprise pelitic, semipelitic, calcareous and igneous members which had been subjected to an earlier metamorphism. The pelitic and semipelitic elements attained the sillimanite grade with biotite grade persisting. The igneous elements had attained the hypersthene-diopside-garnet grade. The calcareous elements had attained the pyroxene-hornfels grade. These metamorphic grades were then subjected to wet conditions by the intrusion of the acid charnockite magma surcharged with water and volatiles. This was the period of the amphibolization of the basic charnockites and the biotitization of the shear zones with the introduction of potash. This was also the period of formation of the migmatites. We have therefore in the type area of Sir Thomas Holland rocks of an earlier age of high grade metamorphism which have been subjected to later retrograde metamorphism.

Acknowledgement

I avail this opportunity of placing on record my deep indebtedness to Dr. P. R. J. Naidu for his suggestions and guidance.

REFERENCES

Cloos, H. (1936) Plutone und ilvre stellung in Rahmen der Krustenbewegungen. 16th *Int. geol. Congr., Rep.*, **1**: 235-253.

Holland, T. H. (1900) The charnockite series, a group of archaen hypersthenic rocks in peninsular India. *Mem. geol. Surv. India*, **30**.

FACT MAP OF THE TYPE AREA OF CHARNOCKITES OF HOLLAND.

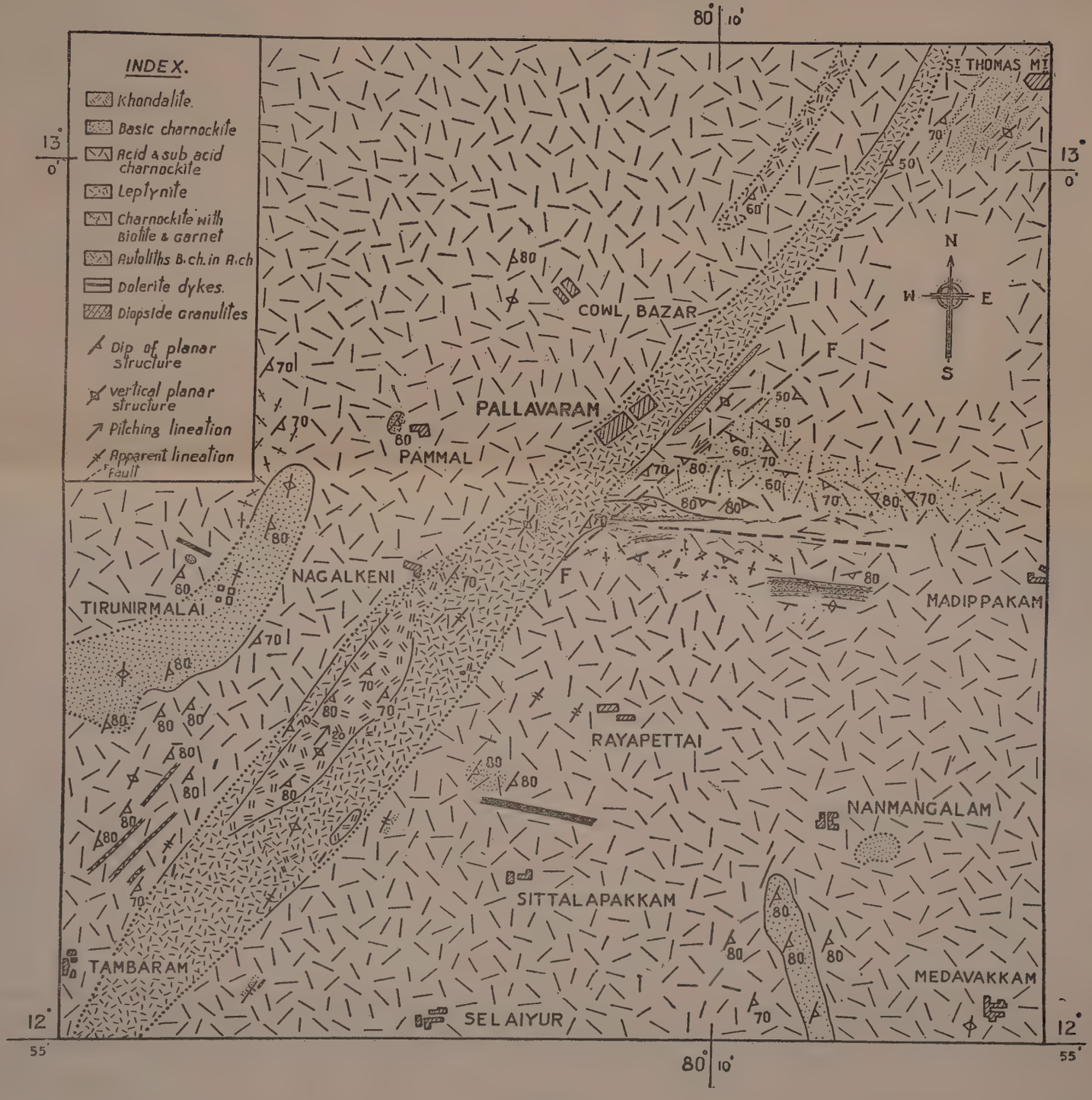

SCALE

FURLONGS 8 6 4 2 0 1 2 MILES

FIG. 21.

STRUCTURAL MAP OF THE TYPE AREA OF CHARNOCKITES OF HOLLAND.

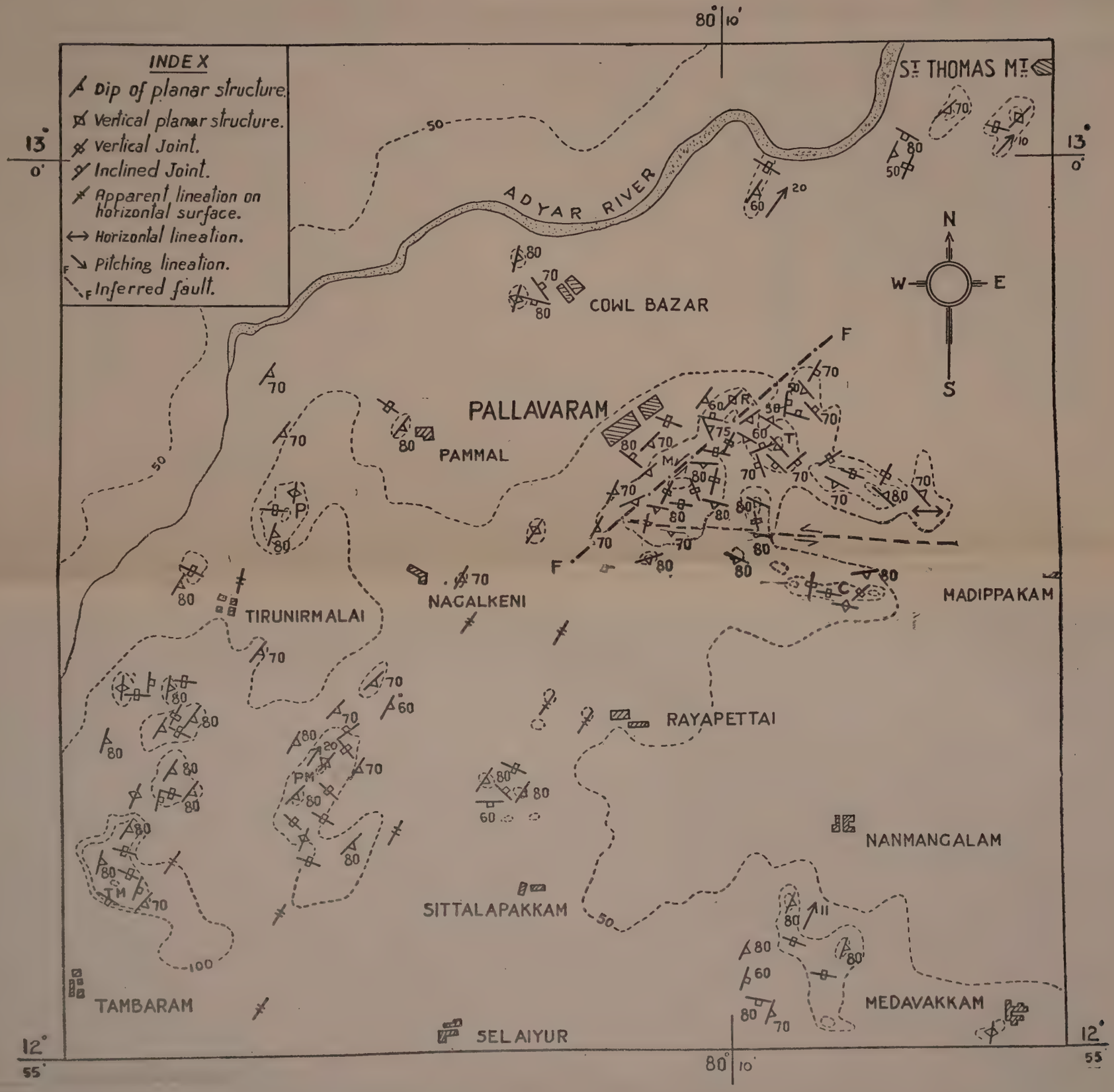

SCALE

FURLONGS 8 6 4 2 0 1 2 MILES

FIG. 22.

INDEX TO LOCALITIES

C. Cheri Malai; M. Mosque Hill; P. Pammal Hill; P.M. Pachai Malai; R. Rifle Range; T. Trisul; T. M. Tambaram Malai.

Howie, R. A. (1955) The Geochemistry of the charnockite series of Madras, India. *Trans. roy. Soc. Edinb.*, **62**: 725-768.

King, W. & Foote, R. B. (1865) The Geological structures of portions of the districts of Trichinopoly, Salem and South Arcot, Madras. *Mem. geol. surv. India*, **4**:

Leelananda Rao, N. (1955) Further studies on dyke rocks of Pallavaram. *J. Madras, Univ.*, B. **25**: 323-339.

Naidu, P. R. J. (1954) Minerals of charnockites from India, *Schweiz, min. petrogr. Mitt.* **34**: 204-275.

Rajagopalan, C. (1946) Studies in Charnockites from St. Thomas' Mount, Madras. Part-I. *Proc. Indian Acad. Sci.*, A, **24**: 315-331.

Rajagopalan, C. (1947) Studies in charnockites from St. Thomas' Mount, Madras-II, *Proc. Indian Acad. Sci.*, A, **26**: 237-260.

J. Madras Univ., B, XXVI, No. 1, pages 117-159, 1956

On the Hypersthene-bearing Rocks of Salem—I

BY

S. Ramanathan,
Department of Geology and Geophysics,
University of Madras, Madras-25

(Received for publication on January 27, 1956)

ABSTRACT

The ultra basics and hypersthene-bearing rocks of Salem have been geologically mapped and a brief account of the texture, mineralogy and chemistry of the hypersthene bearing rocks given. The hypersthene-bearing rocks are found to be of more than one age. The Pertrogenesis of these rock types is indicated.

Introduction

Holland described in 1900, the charnockite series of rocks. Since then, excellent papers have been published on these rocks all over the world. Quensel (1951) has brilliantly summarized the various views on the origin of these rocks. Pichamuthu (1953) has also given an exhaustive summary and a bibliography. Howie (1955) has said the last word on the chemistry of these charnockite series of rocks and the minerals contained in them. Naidu (1955) has discussed the relationship of these minerals to the rocks. A review of this vast literature on this series reveals that the charnockite series have different geological settings in the several countries wherefrom they are reported.

Charnockites from Dangin, Western Australia, are reported (Prider 1945) to be set in a terrain of metasediments, belonging to an older series of paraschists. The hypersthene bearing rocks of Meru district, Kenya, described as norites, hyperites, bojites, and pyroxenites by Pulfrey (1946) are considered by him as plutonic rocks set in a basement of biotite-schists and gneisses. Dixey (1921) records the occurrence of the magnesian group of igneous rocks in Sierra Leone Peninsula, West Africa, associated with talc-schists and amphibolites. The same author quotes Lacroix's authority for the occurrence of gabbro-peridotite series in French Guinea, "analogous to the igneous rocks in West Africa." Groves (1935) describing the charnockites from Uganda reports the "discovery" by Simmons of a small area composed entirely of anthophyllite and actinolite, forming the original basement. Mikkola and Sahama

(1936) have described the granulites of Lapland, passing on to "norite-bands" often, in a setting of ultrabasics.

In India, the charnockites of Eastern Ghats have a Khondalite setting (Crookshank, 1938). "The basic and ultrabasic members of the charnockite series" of the Central Provinces are found "intruded" into the biotite—and hornblende-gneisses (Hallowes, 1924). Ghosh (1941) while marshalling evidences to prove the metamorphic origin of the charnockites of Bastar State, points out their association with banded, streaky or composite gneisses. Rama Rao (1945) in his memoir on the charnockites of Mysore describes the associated rocks as schists, ferruginous Quartzites and gneisses.

The charnockites of the type area of Holland, in Pallavaram, are again found to have a khondalite setting (Leelananda Rao, 1955). In Vellore, North Arcot district, the Charnockites have a setting of granitic-gneisses and basalts (unpublished).

In Salem, the charnockites, though they have a basement of older para-schists, have a dunite-association with them (Holland, 1900). A similar charnockite-dunite association is found on the other side of the Nilgiris (Rama Rao, 1945). A study of these two areas has been undertaken to find out the relationship of these ultrabasics to the charnockites. In this paper, the hypersthene-bearing rocks of Salem are described.

The literature reviewed above shows that Charnockites of different areas have different geological settings. Any discussion on the origin of charnockites should depend on the particular geological setting and associated rocks. Geological maps of the charnockite areas in India (which have been reported all over India) showing the charnockites and their associated rocks have been felt necessary (Howie, 1955). The author has prepared a map of the area around Salem, showing the ultrabasics, charnockites, and associated rocks (Map 1).

A brief summary of the lithology follows:

Geology around Salem

The following rock types have been identified in this area.

Dolerites
Potassic rocks
Dunites
Intermediate Charnockites
Variegated gneisses

THE ULTRABASICS & CHARNOCKITES AROUND SALEM.

SCALE

FURLONGS 8 6 4 2 0 1 2 MILES

78° 0′ 5′ 10′ 78° 15′

11° 45′ 11° 40′

Omalur

Pakalpatti

Toppur

NAGARA MALAI R.F.

KUSA MALAI

KANJA MALAI

SALEM

NAMAM HILL

SHERVAROYS

JARUGA MALAI

1107 1061 1245 1383 1332 1226 1441 1426 2030 1478 1023 1797 1016 3087 3389 1446 1342 1572 1749 1510 3236 2201 1912 1181 3466 1821

N S

INDEX.

- Dolerites.
- Potassic rocks.
- Dunite.
- Intermediate charnockite.
- Variegated gneiss.
- Basic granulite.
- Amphibolite.
- Eclogite.
- Hornblende-granulite.
- Actinolite-talc schist.
- Magnetite quartz rock.
- Andalusite schist.
- Dip of foliation
- vertical dip of foliation.

MAP 1.

Basic granulites
Amphibolites

Garnet-pyroxene rocks

Hornblende-granulites
Actinolite-talc schists
Magnetite-Quartz-rock
Andalusite-hornblende-schists

The structure of the region is a broad syncline, the general strike of the region being NE-SW. The formations on the northern side have a dip towards SE and the southern formations towards NW.

A reference to Map 2, which is an enlarged-map of the portion shown inside the square in Map 1, shows the quartz-magnetite-band and associated rocks near the centre to have a vertical dip, which may represent the general axis of the fold.

In Kanjamalai, the structure is a basin, as also reported by Iyengar (1941). This basin structure does not seem to fit in with the general syncline of the area, unless the basin is due to the sagging of the rocks inwards due to the weight of the iron-ore, or withdrawal of the dunite magma from underneath, or the deposition of sediments in a basin. This leads on to the question of the age relationships of the rock types occurring in this area.

Age relationships: The geological Survey of India regard the variegated gneisses as the oldest rock of the area (Holland, Mem. G.S.I. 30). The paraschists consisting of the Andalusite-schists, Actinolite-talc schists and the hornblende-granulites along with the iron-ore series are regarded as the Dharwars laid on this basement of gneisses. The charnockite series are intrusions into these schists and gneisses. Then come the dunite mass and the younger dykes.

According to the Geological Survey of India, therefore, the following succession of events holds good for the area here mapped.

Dolerites
Dunites
Charnockite series (including the garnet-pyroxene rocks, regarded as ultrabasic members of the Charnockite-series)
Schists and the iron-ore series (Dharwars)
Variegated gneisses (Fundamental gneiss).

The difficulties in accepting this succession are as follows: —

(1) The iron-ore series are interbedded with garnet-hypersthene-augite granulites, which are regarded by Holland (1900) as the ultra basic members of the charnockite series. These granulites therefore should be contemporaneous with the iron-ores and must be Dharwarian in age, whereas the charnockite series have been regarded as very much younger than the Dharwars.

(2) The iron-ore series do not have any relict structures of sedimentary rocks, which are found in the other Dharwarian iron-ores. Holland (Mem. G.S.I. 30) explains this as due to the high-grade of metamorphsim that the Kanjamalai Dharwars have undergone. The sedimentary nature of these iron-ores is mainly inferred from their basin-structure but the iron-ores can be traced from the iron-ore-beds to the garnetiferous rocks.

(3) The Intermediate charnockites, which are banded, have thin magnetite-quartz bands which alternate with mafic bands containing crushed hypersthene, biotite and hornblende. Therefore, there is some relation between the Intermediate charnockites and the iron-ore series.

(4) The basic granulites (basic members of the charnockite series) are regarded as intrusives into the variegated gneisses. But, it is very difficult to establish in the field their intrusive nature. They are rather in the form of lenticles. Their lenticular nature has been commented upon by Prider (1945) in his study of Australian charnockites. There is therefore a possibility that these basic granulites are older than the variegated gneisses.

(5) The intermediate charnockite and the variegated gneisses intermix at their borders, the xenoliths of one being found in the other. Opinions are current that the biotite-gneisses have been converted over to charnockites and vice versa (Pichamuthu, 1953, Narayanan, 1955).

The age-relationship of these rocks, in view of these difficulties, is discussed at the end, after all the field, textural, mineralogical and chemical relationships of the various rock types have been enumerated.

PETROGRAPHY

1. *The Paraschists*

Andalusite-hornblende-schists and Actinolite-talc-schists with hornblende-granulites comprise the oldest series of rocks. There

78° 10'

ENLARGED PORTION OF THE AREA SHOWN IN MAP 1

SCALE

FURLONGS. 4 3 2 1 0 MILE 1

Vellalappatti

Tyagampatti

Mungilpadi

Sanekavundanur

1503

1332

1226

1426

1665

1645

1953

NAGARAMALAI R. F.

2030

1797

1023

1478

Chinna kallappatti

Paraleruvu

Periya kallappatti

1016

N

S

78° 10'

MAP 2

are also types linking these rocks as is evidenced in the field and under the microscope.

The andalusite-hornblende schists consist of blue-green hornblende, stumpy needles of andalusite, granular pieces of Zoisite and epidote, oligoclase (An_{20} to An_{28}), a little iron-ore and biotite with a small amount of magnesian spinel? In some cases, they also have a little actinolite and a few grains of released quartz. The blue-green hornblende has a needle-like inclusion arranged parallel to (100). The microscopic evidences suggest an original chlorite-schist epidotised and then recrystallised into a blue-green hornblende. At contacts, andalusite, epidote and Zoisite become very abundant. These granules can be traced into sections wherein the andalusite and blue-green hornblende tend to be porphyroblastic. Both andalusite and epidote are elongated in schistose planes. The almost complete absence of twinning in the plagioclase and its simultaneous extinction in the base between the mafic minerals suggests a salic infusion (originally albitic) into the chlorite-schist.

The first stage of the metamorphic history of this rock type is one of complete crushing and mylonitisation of the chlorite and then recrystallisation into zoisite, epidote and blue-green hornblende, as evidenced by slide R. 74. The next stage is the conversion to an andalusite-hornblende schist. A retrograde metamorphic effect is also marked by the leaching out of iron-ore in the blue-green hornblende and its paler tint as seen in slide R. 36, resulting in the conversion of the amphibole to edenite ($-2V = 87° - 88°$), and then to chlorite.

Optical characters:

Andalusite: Andalusite occurs as colourless, stumpy prisms, with negative elongation.

$$-2V = 81°-83°,\ \gamma-\alpha = \cdot016,\ \gamma-\beta = \cdot007.$$

Zoisite and epidote: Zoisite is orthorhombic and occurs in the form of granules. It shows abnormal blue interference colour and the optic axial angle varies from very low (positive) to uniaxial. It is also characterized by negative elongation. It is often found intergrown with granules of monoclinic epidote and looks as though one passes on to the other. The birefringence ($\gamma-\alpha$) of Zoisite is 0·006.

The epidote granules are distinguishable from zoisite in their optic axial angle, $-2V = 78°$.

$Z\Lambda$ (001) cleavage = 24°—25°.

$(\gamma-\alpha) = 0{\cdot}043$.

These optical data agree closely with an epidote containing 9·68% Fe_2O_3 and 9·99% MnO (Winchell, 1951).
Blue-green amphibole:

$-2V = 72°-74°$	X = Yellowish green
$Z\Lambda C = 14°-15°$	Y = green
$\gamma-\alpha = 0{\cdot}021$	Z = greenish blue.

Actinolite: The mineral is pleochroic from yellowish green (X) to green (Z).

$-2V = 81°-83°$
$Z\Lambda C = 15°$
$\gamma-\alpha = {\cdot}023$.

The average modal composition of the rock is as follows:

Plagioclase	.. ..	13·9%
Andalusite, Epidote, Zoisite	.. ..	23·8%
Actinolite	.. ..	41·9%
Blue-green hornblende	.. ..	18·5%
Accessories	.. ..	1·9%

Actinolite-talc-schists: This group is characterized by the presence of actinolite and tremolite with a little muscovite and foliated chlorite. Actinolite is pleochroic from yellowish brown to green while tremolite is colourless. $-2V = 86°-88°$, $Z\Lambda C = 21°$.

The actinolites are rich in released grains of iron-ore arranged parallel to their foliae and are altered to talc. In some places, they have been completely altered to Steatite. The amphiboles are of the Dharwarian type and the rock occurs as lenticles in the variegated gneisses.

Magnetite-grunerite-leptites and Magnetite-Quartz rocks: The magnetite-Quartz rocks form prominent bands in Kanjamalai, a detailed account of which is given, among others, by Iyengar (1941). Similar magnetite-quartz band occurs in the dunite area also. This is found associated with magnetite and grunerite bearing leptites. The grunerite grains keep to the plane of schistosity of the rock. The quartz grains are of the infiltrated type and are clustered with

iron-ore. Quite a good number of grains of iron-ore are octahedral in shape. There are also a few grains of plagioclase. (Ab_{75} An_{25}).

The grunerite is colourless, and shows multiple twinning parallel to (100). The optic axial plane is parallel to (010).

$+2V = 80°$, $\gamma - \alpha = 0{\cdot}032$, $Z\Lambda C = 8°$.

The modal composition of this rock is as follows:

Quartz, Felspar	.. ..	62·1%
Grunerite	.. ..	11·6%
Magnetite	.. ..	26·3%

There are leptite bands (R. 76) occurring both in Kanjamalai and adjoining hillocks, containing crushed grains of quartz, antiperthite, biotite, muscovite and epidote. The quartz is mosaic and the antiperthitic inclusions are restricted only to the centre of the plagioclase grains. There are tufts of big flakes of biotite and muscovite occurring in clusters with epidote, apatite and a few grains of club-shaped Zircon. The plagioclases are studded with needles and grains of muscovite, sericite and epidote and their An. content varies from An_{20} to An_{25}.

These pass on to types that may be called migmatites, as for instance, R. 65, collected from Kanjamalai. The plagioclase grains here are disintegrated and contain "vein" antiperthites. The biotite occurs in tufts and rarely grows into a big flake and is more of a greenish type. Original diopside grains are seen altering to green amphibole and actinolite which pass on to chlorite. Granules of epidote and apatite form the chief accessories with a few grains of club-shaped Zircon. The modal percentage of minerals is given below:

Felspar	.. ..	43·4%
Quartz	.. ..	5·6%
Diopside	.. ..	2·5%
Actinolite, chlorite	.. ..	28·6%
Biotite, Apatite, Magnetite, and Zircon.	.. ..	19·9%

The pure leptite variation from these types is characterized by the absence almost of any mafic mineral. The plagioclase (An_{25}

to An_{30}) in these rocks is sericitised and kaolinised. Quartz grains have undulose extinction and are clouded with dusts of iron-ore. They are vermicular and of the infiltrated type. (R. 78). The modal composition of this leptite is given below:

Quartz	.. ..	25%
Felspar	.. ..	63%
Others	.. ..	12%

The association of the magnetite-quartz rocks and the leptites, their age relationships and their petrogenetic significance are discussed in the last section.

The hornblende-granulites are found to occur mostly in the form of lenses in the variegated gneiss, as near Toppur. They are granulitic in texture and contain plagioclase (An_{25} to An_{30}), Quartz, blue-green hornblende and brown biotite. The biotite is found to be intergrown along its lamellae with iron-ore. A little epidote and apatite form the accessories. Optically, the blue-green hornblende has the same characters as the blue-green amphibole occurring in the andalusite-hornblende schist. The volumetric percentage of the mineral constituents are:

Plagioclase	.. ..	51·5%
Quartz	.. ..	3·2%
Actinolite	.. ..	10·5%
Blue-green hornblende	.. ..	25·2%
Biotite and accessories	.. ..	9·6%

2. *Garnet-Pyroxene Rocks*

In the immediate neighbourhood of Salem, there are several prominent, bare, rocky hill-masses like the Nagaramalai, Kusamalai, Karankaradu and the hills of Kanjamalai and adjoining hillocks which are composed mainly of this garnetiferous rock referred to as "the garnetiferous basic members of the charnockite series" by Holland (1900). These rocks are mostly coarse-grained. The granularity, especially of the garnet varies from sizes bigger than one's fist to minute specks. The main rock-type looks in a hand-specimen, coarse-grained, granulitic and contains garnet, amphibole and pyroxene. This varies to a finer-grained type on the one hand and to schlieren, patches and lenses of almost pure amphibolites, or pyroxenites, on the other. When finer-grained, they pass on to a hornblende gneiss containing clinopyroxene,

hypersthene and amphibole. There are also felspathic schlieren, composed of Quartz and felspar, forming veins in the rock. Similar rock types noticed by Rama Rao (1945) have been described by him as follows: "In some of the hand-specimens of these rocks, if based purely on the mineral composition, the garnetiferous melanocratic portions may be termed eclogites whereas the leucocratic portions can be called the garnetiferous hypersthene or hornblende-granulites, or the basic or intermediate charnockites, according to their texture and other characters". A similar description would hold good for the Salem rocks as well.

Among the different types studied, three have been chosen as representative, and they are chemically analysed (R. 43, R. 32 and R. 64).

In thin section, R. 43 is found to consist of coarse-grained subhedral plates of green clino-pyroxene (of 2 mm. size), hypersthene (of 2 mm. size) garnet (2 to 3 mm. size), hornblende (0·5 to 5 mm. size) and plagioclase (1 to 2 mm. size). Quartz, a little apatite and iron-ore form the accessories. The texture is distinctly granulitic. The plagioclase grains are quite as large as the mafics. This is taken to represent a type garnet-pyroxene rock.

R. 32, in thin section consists of coarse to medium-grained subhedral grains of green clino-pyroxene (about 1 mm. size), hypersthene (1 mm. size), hornblende (1 mm. size) and plagioclase (1 mm. size). Iron-ores form the main accessories. Garnet is absent and plagioclase is smaller in grain-size than the mafics. This is taken to represent a garnet-free variation of the type R. 43.

Clinopyroxene (2 mm. size), hypersthene (2 mm. size) and hornblende (2 to 4 mm. size), together with iron-ore form the main constituents in thin section of R. 64 which represents a pyroxenic variation of the type.

Besides these, there are variations to pure amphibolites, as for e.g. R. 39, which contains brown hornblende, clinopyroxene and hypersthene, R. 160 with only actinolite altering here and there to chlorite with a little apatite and iron-ore and R. 44, with actinolite and tremolite altering quite a good amount to chlorite; the texture in these cases is granoblastic.

Mineralogy

Plagioclase: The twin-laws of the plagioclase felspars of these rock types and their anorthite content have been published earlier (Ramanathan, 1954). The plagioclase grains are often porphyritic, as in R. 43 and R. 77. A good many of them have got well deve-

loped cleavages, and the cleavages disappear when there are discontinuous lamellae appearing. But, the anorthite content of both the twinned and untwinned, well-cleaved grains, is the same, as in R. 43, where it ranges from An_{45} to An_{50}. The plagioclase in this is andesine. In R. 32, the plagioclase varies in its anorthite content from An_{60} to An_{70}, while the amphibolite and pyroxenic variations are free of felspar. The plagioclase is clear and not clouded, but most grains are surrounded by veins of an amorphous material. This can be traced on to a Zone of the same material surrounding the mafics, implying thereby, that an infusion of salic liquid has dissolved the earlier mafics and converted them. The plagioclase grains, in some cases as in R. 77, have a tendency to be elongated along with hypersthene; then, the mineral is untwinned, and the untwinned grains show undulose extinction.

Pyroxenes: The mafic minerals occur in clots and are often surrounded by veins of he same amorphous material as seen in plagioclases. The clino-pyroxene occurs in big plates, is green in colour and non-pleochroic. The green colour of the clino-pyroxene matches with the green colour of hypersthene parallel to Z. It is one of the primary minerals and is present in all the varieties. It is lamellar parallel to (100) and has good partings parallel to (010) (continental setting). The optical characters are as follows:

R. 43.

$+2V = 58°—61°$	$\gamma-\alpha = \cdot024—\cdot025$	$\beta = 1\cdot706$
$Z\wedge C = 41°—43°$	$\gamma—\beta = \cdot017—\cdot018$	

R. 32.

$+2V = 57°—59°$	$\gamma—\alpha = \cdot021—\cdot022$
$Z\wedge C = 43°—44°$	$\gamma—\beta = \cdot017—\cdot018$

R. 64.

$+2V = 55°—57°$
$Z\wedge C = 43°—44°$

The above characters are those of augite. The augite is found altering to amphibole, and often there are grains of augite at the centre, altering on to an amphibole all around. (Sketch 1)

The first stage of alteration is the development of chlorite with iron-ore released, and then on to well-developed grains of yellowish green amphibole. Augite is also found to have reacted with plagioclase resulting in the development of garnet.

Augite, occurring in the form of small and occasional schlieren in the garnet-pyroxene rock has been collected from Karankaradu.

It was crushed to 80 mesh and separated in bromoform and different dilutions of clerici from amphibole and a little hypersthene, and was analysed. The approximate modal composition of the specimen from which the clino-pyroxene was separated is

Clino-pyroxene	—	85·3%
Hypersthene	—	8·1%
Amphibole	—	4·2%
Ores	—	2·4%

The analysis is set below in Table I.

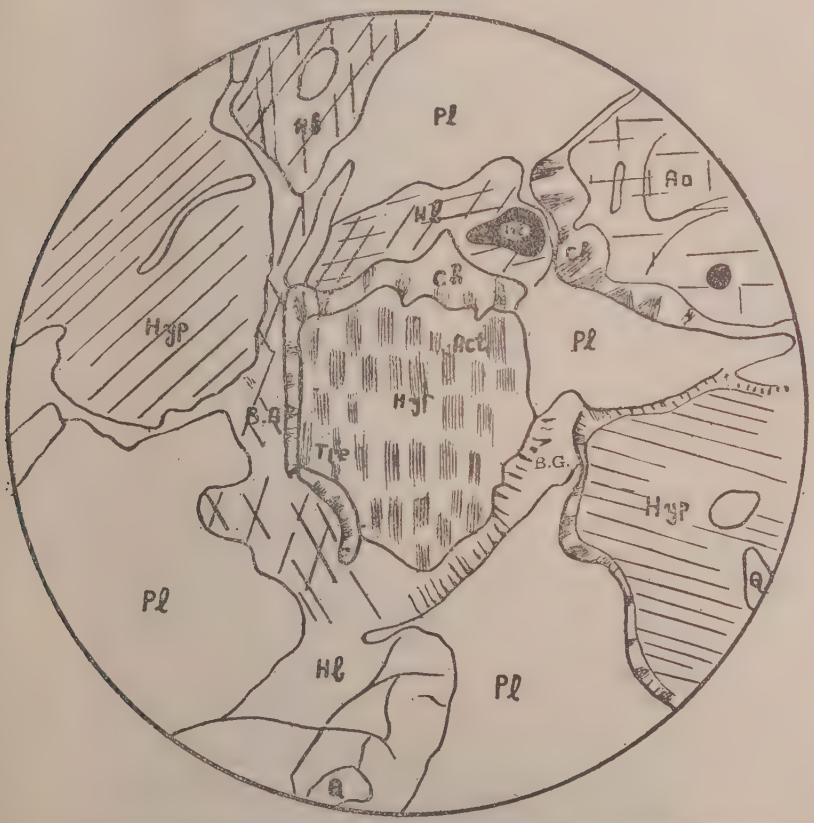

Sketch 1: Hypersthene completely replaced by actinolite and tremolite. Augite and hypersthene grains are surrounded by a rim of chlorite and blue green hornblende. At contacts with hypersthene and plagioclase, brown amphibole developes.

Hyp—Hypersthene. Act—Actinolite. Tre—Tremolite. Au—Augite. Ch—Chlorite. Pl—Plagioclase. B.G.—Blue green amphibole. Hb—Hornblende. Q—Quartz. Mt—Magnetite. B.A.—Brown amphibole.

Table I

Chemical Analysis of Clinopyroxene, S. 1

Oxides	Wt %	Mol. No.	Metal. atoms.	O, OH, F atoms	Basis 6 (O, OH, F)		Valency check	
SiO_2	45·87	765	765	1530	1·76		Si^{++++}	7·04
TiO_2	0·44	5	5	10	0·01	1·98	Ti^{++++}	0·04
Al_2O_3	4·67	46	92	138	0·21		Al^{+++}	0·63
Fe_2O_3	2·22	14	28	42	0·06		Fe^{+++}	0·18
FeO	13·93	193	193	193	0·45	1·24	Fe^{++}	0·90
MgO	12·59	315	315	315	0·73		Mg^{++}	1·46
CaO	19·48	349	349	349	0·80		Ca^{++}	1·60
Na_2O	0·53	8	16	8	0·04	0·84	Na^{+}	0·04
K_2O	0·14	1	2	1				
H_2O	0·28	17	34	17	0·08	0·08		11·89
	100·15			2603			OH	0·08
							O	11·84
Sp. Gr.	3·41							11·92

Formula :

$(OH)_{0·08}$ $(Na, K, Ca)_{0·84}$ $(Mg, Fe'', Fe''')_{1·24}$ $(Si, Ti, Al)_{1·98}$ $O_{5·92}$

$Mg\ SiO_3$: $Fe\ SiO_3$: $Ca\ SiO_3 = 36·8: 22·5: 40·7$.

Analyst: S. Ramanathan

Titanium and aluminium are in this analysis regarded as replacing silica. The bases are slightly in excess of the ideal 2 atoms by 0·008 and the silica falls short of it by 0·002.

The analysis is given in Table II, with four others for comparison.

Table II

Oxides	I	II	III	IV	V
SiO_2	45·87	54·49	48·52	48·0	42·70
TiO_2	0·44	Tr	0·70	0·7	0·42
Al_2O_3	4·67	2·50	5·87	4·9	8·55
Fe_2O_3	2·22	1·63	2·58	2·1	1·80
FeO	13·93	1·98	9·76	14·1	6·52
MnO	—	0·06	0·20	—	0·16
MgO	12·59	16·74	11·59	14·0	13·41
CaO	19·48	21·40	19·66	16·2	24·52
Na_2O	0·53	0·83	1·04	—	1·02
K_2O	0·14	0·40	0·19	—	0·48
H_2O+	0·28	0·12	0·13	—	0·58
H_2O-	—	—	0·05	—	0·17
Total	100·15	100·15	100·29	100·0	100·33

I. Clino-pyroxene from Garnet-pyroxene rock, Karankaradu, Salem. Analyst, S. Ramanathan.
II. Pyroxene from eclogite, Eskola. Quoted from "Petrography, Vol. IV" by Johannsen, p. 462.
III. Augite, Norite, Nagaramalai, Salem. Analyst, R. A. Howie.
IV. Clino-pyroxene from s22, Basic charnockite, Uganda. Analyst, A. W. Groves.
V. Clinopyroxene, Sittampundi. Analyst, C. E. Nehru.

It is seen from the table that the analysed clino-pyroxene does not resemble the pyroxene from eclogite, reported by Eskola. The clino-pyroxene from Sittampundi, occurring in a garnet-pyroxene rock, is richer in alumina and calcium and poorer in iron and silica. It is however, close to the augite from Norite, Nagaramalai, Salem (analysed by Howie) and to the clino-pyroxene reported by

Groves from a basic charnockite. When the Q L M values of the mineral are plotted in Niggli's diagram for pyroxenes, the point falls inside the field of pyroxenes just below common augites, and not inside the omphacite field. Under these circumstances, the author is inclined to call this mineral as common augite and not as omphacite which is the pyroxene typical of eclogites.

Orthopyroxenes occur in all varieties of this rock type and this is perhaps the reason for Holland to have regarded them as "garnetiferous basic members of the charnockite series". They are granular and have pleochroism from pink to green.

X = pink
Y = greenish
Z = green

The hypersthenes are clearly lamellar, parallel to (100) and they are discussed more in detail under the "Intermediate Charnockites". They are found to occur as primary minerals.

The optical characters of the hypersthene from different varieties are listed below:

	R. 32.	R. 43.	R. 64.
$-2V$.	68° — 72°	55° — 61°	71° — 75°
$(\gamma - \alpha)$	0·012 — 0·013	0·014	0·011 — 0·012
$(\gamma - \beta)$	0·004	0·004	0·004
β	1·683	1·702	1·686

All the three are pleochroic but the pinkish tinge increases with the decrease in the optic axial angle. The optical characters place them in the Hypersthene-Ferrohypersthene range of Poldervaart (1947).

The hypersthene and augite are surrounded by a rim of amorphous material, when they are altered. They alter to amphibole. The first stage is the formation of chlorite with its fibres across the boundary of the mineral with released iron-ore. The chlorite

is next converted to green actinolite, and in contact with plagioclase, a rim of blue-green amphibole develops (Sketch 1). In some cases, hypersthene is entirely surrounded by a brown amphibole when it is in contact with plagioclase. Again, there are cases where the whole hypersthene grain is replaced by actinolite and tremolite, surrounded by a corona of green amphibole (Ref. Sketch 1).

Hypersthene and augite occur in separate clots suggesting that they may have crystallised separately.

Amphiboles: The amphibole is secondary and all stages can be traced from the process of conversion of augite and hypersthene to the stage when the green and brown hornblendes become the major constituents of the varieties, as for eg., R. 160 and R. 39. The process of conversion seems to be

Augite, Hypersthene } → Chlorite + iron-ore → Actinolite → Brown Amphibole → green Amphibole.

These amphiboles are seen spreading freely at the expense of both augite and hypersthene. Most amphiboles have got released iron-ore and a little Quartz. Some of the green amphiboles have got schiller inclusions parallel to (001).

In some cases, the garnets have suffered retrograde metamorphism and are converted to blue-green amphibole and then on to chlorite. The blue-green amphibole is seen to grow into garnet in such cases.

The optical characters of the different amphiboles are listed below:

Yellowish green amphibole occurring in R. 32, R. 43, S. 77:

$+2V = 85°—87°$ $\quad \gamma—\alpha = \cdot017—\cdot018$

$Z\wedge C = 15°—17°$ $\quad \gamma—\beta = \cdot009—\cdot010$

X = pale yellow

Y = greenish yellow

Z = pale green

$X < Y < Z$

The mineral has positive optic axial angle, having an affinity towards pargasite, but the pleochroism is from yellow to green and

not to blue. Since Z^C =15°—17°, the mineral cannot tend towards Hastingsite. The optic axial angle is not very low to be grouped with edenite. Following Buddington (1952), the mineral is named common hornblende.

Green Amphibole occurring in R. 43:

$-2V = 74°—76°$ $\quad \gamma—\alpha = \cdot 021$
$Z\wedge C = 18°—19°$ $\quad \gamma—\beta = \cdot 007$

X = light green
Y = light green
Z = dark green
X = Y < Z

The optical characters group this mineral as common hornblende.

Actinolite occurring in R. 43, R. 160, R. 44:

$-2V = 81°—83°$
$Z\wedge C = 14°—15°$ $\quad \gamma—\alpha = \cdot 023—\cdot 024$

X = yellowish green
Y = colourless
Z = dark green
Y < X < Z

Blue-green Amphibole: R. 43.

$-2V = 72°—74°$ $\quad \gamma—\alpha = \cdot 017—\cdot 018$
$Z\wedge C = 14°—15°$ $\quad \gamma—\beta = \cdot 006—\cdot 007$

X = Yellow
Y = green
Z = bluish green

This bluish-green amphibole occurring in the amphibolites of Kusamalai, Salem, have been separated and analysed by Naidu (1955) and its optical characters reported in detail. The analysed amphibole lies within the field of common hornblende and represents a type rich in iron.

Brown Hornblende: R. 39.

$-2V = 78°—80°$ $\quad n_\beta = 1{\cdot}692—1{\cdot}694$

$Z \wedge C = 10°—11°$ $\quad n_\gamma' = 1{\cdot}701—1{\cdot}703$

$n_\alpha' = 1{\cdot}705—1{\cdot}707$

X = yellowish brown
Y = pale brown
Z = dark brown
X < Y < Z

This and some other similar amphiboles have high absorption making it impossible to measure the extinction angles, accurately. In such cases, two methods after Naidu (1955) have been employed, wherein reasonable accuracy was available. The methods eliminate difficulties arising out of strong absorption parallel to Z and consists in getting the emergence of both the optic axes, locating the acute bisectrix and the optic axial plane, drawing the cleavage trace and applying the Biot-Fresnel law of extinction.

This brown hornblende occurring in the amphibolite, R. 39 at Karankaradu was separated first in bromoform and then in methylene iodide. Methylene iodide is found to be an excellent liquid for separation of amphiboles since almost pure amphibole grains are separated from co-existing augite and hypersthene. Repeated separations in methylene iodide and various dilutions of clerici, gave an almost hundred percent pure amphibole for analysis.

The approximate modal composition of the specimen from which the brown amphibole was separated is given below:

Brown amphibole	..	78·4%
Pyroxene	..	18·6%
Chlorite and iron-ore	..	3·0%

The analysis is set in Table III.

The Warren's formula for the mineral is

$$(OH)_{0\cdot51}\ (Na, K, Ca)_{3\cdot36}\ (Mg, Fe'', Fe''', Al)_{5\cdot22}\ (Si, Ti, Al)_8\ O_{23\cdot49}$$

According to Berman (1937) the formula of the mineral is

$$(WXY)_{8\cdot58}\ Z_8\ O_{23\cdot49}\ (O, OH, F)_{0\cdot51}$$

In the allotment of atoms, Ti is reckoned with Si, after kunitz (1930). Berman's formula indicates a slight excess of the bases and deficiency in (O, OH, F). The Warren's formula, however,

Table III

Chemical Analysis of Brown Amphibole from R. 39

Oxides	Wt %	Mol. No.	Metal. atoms.	(O, OH, F) atoms	Basis 24 (O, OH, F)			Valency check		
SiO_2	40·44	674	674	1348	6·16	}	8 00	Si^{++++}		24·64
TiO_2	0·56	8	8	16	0·07			Ti^{++++}		0·14
Al_2O_3	15·61	153	306	459	2·80	1·77		Al^{+++}		8·40
Fe_2O_3	2·63	16	32	48	0·29	1·03		Fe^{+++}		0·87
FeO	12·40	172	172	172	1·55	}	5·22	Fe^{++}		3·10
MnO	Tr	—	—	—	—			Mg^{++}		4·70
MgO	10·29	257	257	257	2·35			Ca^{++}		4·16
CaO	12·68	227	227	227	2·08	}	3·36	Na^{+}		1·21
Na_2O	4·06	66	132	66	1·21			K^{+}		0·07
K_2O	0·42	4	8	4	0·07					47·29
H_2O^{+}	0·53	28	56	28	0·51		0·51		OH	0·51
H_2O^{-}	0·16								O	46·98
	99·78			2625						47·49
Sp. Gr.	3·31									

Analyst: S. Ramanathan

shows a slight excess of the (Na K, Ca) group, over the normal for the formula.

The analysis of the mineral is set in Table IV with a few others for comparison.

Table IV

Oxide	I	II	III	IV	V
SiO_2	40·44	38·84	43·08	39·78	41·06
TiO_2	0·56	3·90	0·17	1·47	1·85
Al_2O_3	15·61	7·91	7·48	11·39	15·47
Fe_2O_3	2·63	3·89	3·01	5·93	2·47
FeO	12·40	9·42	15·37	14·21	13·20
MnO	Tr	0·25	1·18	0·68	0·18
MgO	10·29	14·60	9·42	9·62	10·85
CaO	12·68	13·86	11·82	9·68	10·00
Na_2O	4·06	2·69	3·85	1·57	2·27
K_2O	0·42	0·97	0·53	1·60	0·61
H_2O+	0·53	3·67	4·09	0·25	1·75
H_2O-	0·16			2·59	0·01
Total	99·78	100·00	100·00	98·77	99·72
Sp. Gr.	3·31	3·33	3·418	3·211	3·236
ZΛC	10° — 11°	10°	16°	21° ± 5°	16°

I. Brown Amphibole, Karankaradu, Salem. Analyst, S. Ramanathan.
II. Barkevikit, Fuerteventura (Essek), Analyst, W. Kunitz.
III. Barkevikit, Skuttersundskjar (Foyait), Analyst, W. Kunitz.
IV. Femaghastingsite, Tupper lake quadrangle, Analyst, E. K. Oslund. (Buddington and Leonard, 1953).
V. Hornblende from almanditic amphibolite-gneiss with porphyroblastic garnet, 2·5 miles E. S--E. of St. Regis Falls (Nicholville Quad). Analyst, L. C. Peck (Buddington, 1952).

It is seen from the above table that the brown amphibole from Salem lies in between the two barkevikites set for comparison. The optical characters agree well, while chemically, the Salem amphibole is richer in alumina and slightly poorer in silica and deficient in water. The Femaghastingsite of Buddington and Leonard (1953) is alkali—poor and ZΛC is large. The hornblende from Adirondack closely resembles the analysed mineral in chemical

composition but its sp. gr. is only 3·236 and $Z\Lambda C = 16°$. Also, it is pleochroic from straw yellow to green.

The Q L M values of the amphibole were calculated and plotted in Niggli's diagram for amphiboles (Fig. 1). It is seen that this amphibole (A), falls inside the field for Barkevikite, hastingsite and basaltic hornblendes. So, on the evidence of Niggli's diagram, Kunitz's analyses and the optical characters determined, this mineral is named Barkevikite.

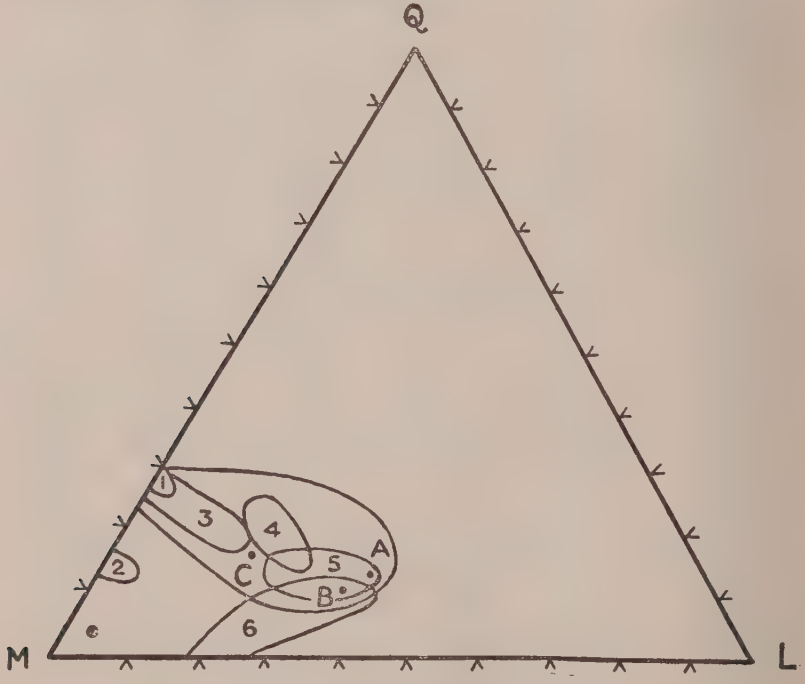

Fig. 1.

Niggli's Q L M diagram of amphiboles and melilites of eruptive rocks. 1. Grunerites and altered hornblendes. 2. Aenigmatites. 3. Alkali hornblendes. 4. Common hornblendes. 5. Barkevikite, Hastingsite, Basaltic hornblendes. 6. Melilite. A. R. 39. B. S. 46. C. S. 35.

Garnet: Garnet occurs in different sizes from almost pure big crystals to minute specks in the granoblastic garnetiferous amphibolites. It is isotropic and does not show anamolous birefringence. It is massive. Some grains have a sieve structure containing released vermicular Quartz. Garnet is found to develop at the expense of all the three main mafic minerals, augite, hypersthene and amphibole. The force of crystallisation of garnet is

strongest as shown by its straight crystallographic edges against other minerals, and has got its convexity towards the mafics showing that it develops at the expense of all the mafics.

$$\left.\begin{matrix}\text{Amphibole}\\ \text{Hypersthene}\\ \text{Augite}\end{matrix}\right\} + \text{plagioclase} \rightarrow \text{Garnet.}$$

In some cases, a certain amount of retrograde metamorphism is evident in garnets, on account of the following observations.

1. Some grains are surrounded by a rim of blue-green amphibole altering to chlorite. The blue-green amphibole is found to grow into garnet (Sketch 2).

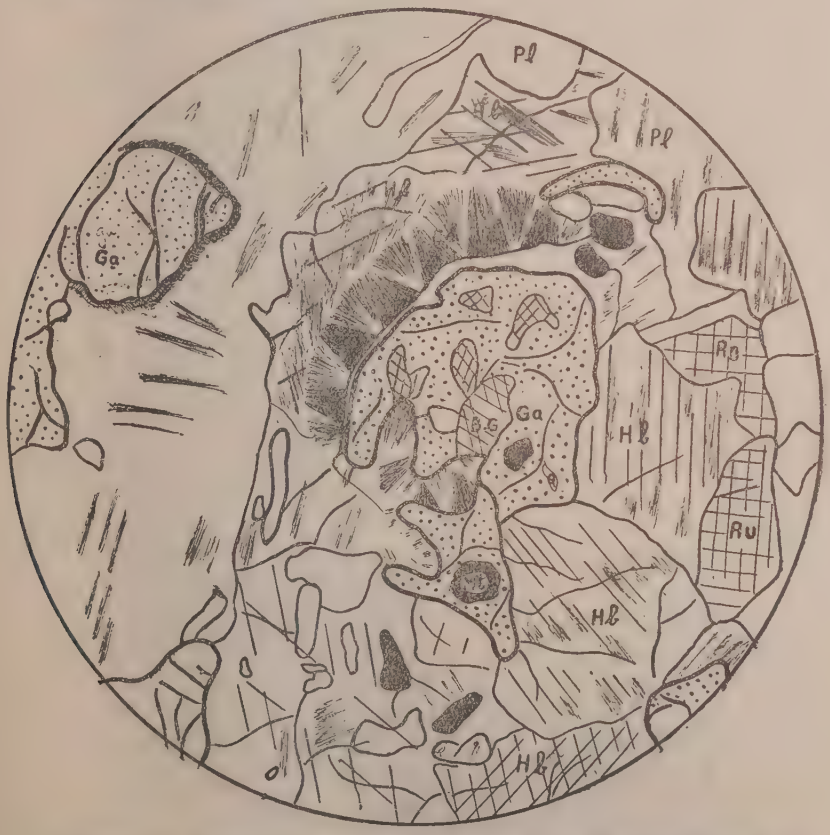

Sketch 2: Garnet grains are surrounded by a rim of chlorite passing on to hornblende. Blue green hornblende passes into garnet and develops freely. Ga—Garnet. Au—Augite. B.G.—Blue green hornblende. Hb—Hornblende. Ch—Chlorite. Pl—Plagioclase. Mt—Magnetite.

2. Some garnet grains contain veins of epidote, and
3. Some iron-ore grains adjacent to garnet are converted to limonite.

Garnet is poikilitic with augite and hypersthene. Some grains of garnet, from Nagaramalai, exhibit well developed partings parallel to the hexoctahedral faces and they have minute needle like inclusions, (whose characters could not be ascertained even under U M 4 objective), arranged parallel to the cubic faces and they appear as blebs on dodecahedral faces (sketch 3). The inclusions, however, have a positive elongation and show high birefringence. The nature of these inclusions have been discussed by Holland (1896). Some garnet grains have also tension cracks developed.

Sketch 3: Garnet has developed hexoctahedral partings and inclusions arranged parallel to the cubic faces.
Ga—Garnet. Am—Amphibole.

The specific gravity of the garnet is 4·03 and refractive index 1·798 for sodium light. The garnet from R. 43, has been separated and analysed. The analysis is given in Table V.

Table V

Chemical Anaysis of Garnet from R. 43

Oxides	Wt %	Wt % recalculated to 100	Mol. No.	Metal atoms	(O, OH, F)	Basis 12 (O, OH, F)		Valency, check	
SiO_2	36·29	36·50	608	608	1216	2·83	2·95	Si^{++++}	11·32
TiO_2	1·97	1·98	25	25	50	0·12		Ti^{++++}	0·48
Al_2O_3	21·87	22·00	216	432	648	2·01	2·01	Al^{+++}	6·03
Fe_2O_3	0·58	0·58	4	8	12	0·04		Fe^{+++}	0·12
FeO	24·21	24·34	338	338	338	1·57		Fe^{++}	3·14
MnO	Tr	—	—	—			3·08	Mg^{++}	1·74
MgO	7·41	7·45	186	186	186	0·87		Ca^{++}	1·20
CaO	7·12	7·15	128	128	128	0·60			
Na_2O	0·24	100·00			2578				24·03
K_2O	0·11								
H_2O+	0·25							O	24·00
H_2O-	0·18								
	100·23								
Sp. Gr.	4·03								

Formula :

$(Fe''', Fe'', Mg, Ca)_{3\cdot08}\ Al_{2\cdot01}\ (Si, Ti)_{2\cdot95}\ O_{12}$.

Analyst: S. Ramanathan.

Neglecting Na_2O,K_2O, H_2O^+ and H_2O^- and recalculating to a total of 100, the general formula of the mineral is

$$(Fe''', Fe'', Mg, Ca)_3\ Al_2\ (Si, Ti)_3\ O_{12}.$$

The Ti is regarded here as replacing Si after Kunitz (1935). Calculated in terms of standard molecules, it has the composition:

Almandite	..	51·9%
Pyrope	..	28·5%
Grossularite	..	18·8%
Andradite	..	0·8%

The standard molecules of this garnet are compared with a few others, cited by Heritsch (1927).

		1	2	3
Almandite	..	51·9	56·7	53·9
Pyrope	..	28·5	30·9	29·0
Grossularite	..	18·8	12·4	15·7
Andradite	..	0·8	—	—
Spessartite		—	—	4·4

1. Garnet, R. 43, Nagaramalai, Salem.
2. Garnet, Eclogit, Sanalpe, Hintze (Kunitz).
3. Garnet, Pegmatit, Val Dombastone, Doelter (Kunitz).

It is found that the analysed garnet closely resembles the one from eclogite. Heritsch has also prepared tables showing the paragenesis of garnets and rock types. The following paragenesis has data lying close to those of the analysed garnet.

III. Eclogitgranaten

Spessartin	..	0 — 3 %
Grossular	..	9 — 42%
Pyrop	..	19 — 37%
Almandin	..	33 — 57%
Andradit	..	0 — 21%

This similarity denotes an eclogitic origin for the analysed garnet.

Below is given in Table VI, the composition of garnets in different rock types after Wright (1938) and the position of the analysed garnet and also another garnet analysed from Shervaroys (described later), in his table. They are also compared with those analysed by Naidu (1955) and Howie (1955) from Pallavaram.

Table VI

Rock Type	Spessartite	Grossularite	Pyrope	Almandite	Andradite
Pegmatite ..	47·1	—	—	41·8	—
Granite ..	36·0	—	—	56·8	—
Garnets associated with contact action on siliceous rocks ..	30·7	—	—	56·4	—
Biotite schists ..	—	6·0	13·8	73·0	—
Garnet, leptynite, Pallavaram (Howie) ..	0·8	4·1	19·5	75·0	0·6
Leptite, Pallavaram (Naidu) ..	0·9	7·8	25·0	66·3	—
Amphibole schists ..	—	20·7	20·3	53·6	—
Garnet, Nagaramalai ..	—	18·8	28·5	51·9	0·8
Eclogites ..	—	18·5	37·4	39·1	—
Kimberlite and Peridotites ..	—	9·0	72·3	13·4	—
Garnet, Shervaroys ..	2·9	16·3	51·9	28·9	—
Various basic rocks ..	—	28·7	20·7	34·4	15·6
Charnockite, uganda ..	1·3	—	35·8	41·2	21·7
Calcareous contact rocks ..	—	51·5	—	—	40·8

In the above table, the garnet from Nagaramalai, can be placed between those of amphibolite schists and eclogites. This is in accordance with the data of Heritsch, (1927) given earlier. Naidu's (1955) garnet has the character of schists and Howie's (1955) has also the same character.

Petrochemistry

Among the rock types studied in this series, the following three were chemically analysed and their analyses are given in Table VII. Their modal composition is given below:

R. 43, Garnet, Pyroxene rock, Nagaramalai: Plagioclase 40·4% Hypersthene 16%, Augite 6·3%, Amphibole 16·9%, garnet 13·3% and ores 7·1%.

R. 32, Garnet free variation: Plagioclase 36·1%, Hypersthene 39·1%, Augite 9·5%, Amphibole 14·0% and ores 1·3%

R. 64, Pyroxenic variation: Amphibole 46·3%, Augite 37·7%, Hypersthene 14·6% and ores 1·4%.

Table VII

Constituents	I	II	III	IV	V	VI
SiO_2	44·04	45·16	43·68	47·00	48·24	52·11
TiO_2	0·74	0·25	0·42	0·69	Tr	0·77
Al_2O_3	21·67	18·91	17·71	15·59	13·03	18·08
Fe_2O_3	3·77	0·66	0·20	1·29	2·28	1·04
FeO	8·52	7·61	8·10	10·28	7·20	9·19
MnO	0·60	Nil	Tr	0·15	0·81	0·07
MgO	7·61	12·43	13·52	8·88	10·72	8·37
CaO	11·36	11·91	12·62	13·75	13·48	5·20
Na_2O	1·50	2·74	3·02	1·70	2·88	2·93
K_2O	0·13	0·54	0·17	0·07	0·23	1·63
P_2O_5	0·06	0·08	Tr	0·07	0·07	—
H_2O^+	0·17	0·42	0·28	0·40	0·64	0·38
H_2O^-	0·04	0·03	0·17	0·14		0·04
Sp. Gr.	3·25	3·13	3·00	—	—	—

I. R. 43, Garnet-pyroxene-hornblende rock, Nagaramalai, Salem. Analyst, S. Ramanathan.

II. R. 32. Garnet-free variation of the above rock. Analyst, S. Ramanathan.

III. R. 64. Pyroxenic variation, Kanjamalai, Analyst, S. Ramanathan.

IV. Basic garnetiferous norite, Niapea Hill, west Nile District, Uganda, Analyst, A. W. Groves.

V. N 477. Garnetiferous-hornblende-diopside-hypersthene rock, Dodkanya. Analyst, B. S. Raju (Reported by Rama Rao).

VI. Plagioclase-hypersthene-garnet-granulite, Kevijoki, Lapland, Analyst A. Huhma (Eskola, 1952).

The C. I. P. W. norm, Niggli values, Niggli Basis molecules, Q L M values and Katanormative minerals of the three analysed rocks are given in Table VIII.

Table VIII

C. I. P. W. Norm

	I	II	III
Or	0·56	2·78	0·56
Leu	—	—	0·44
Ab	12·58	6·29	—
Ne	—	9·09	13·63
An	52·82	37·81	34·47
Di	3·03	16·56	22·59
Hy	10·87	—	—
Ol	13·60	25·94	26·77
Mt	5·57	0·93	0·23
Il	1·37	0·61	0·76
Ap	0·34	0·34	—
	Niggli values		
al	26·43	21·21	19·29
fm	45·16	48·75	50·22
c	25·31	24·43	24·95
alk	3·10	5·61	5·54
Si	91·07	86·36	80·71
ti	1·11	0·458	0·554
k	0·04	0·10	0·04
mg	0·522	0·732	0·746
	Niggli Basis		
Cp	—	—	—
Kp	0·34	1·62	0·65
Ne	8·06	14·17	15·49

	I	II	III
Cal	31·56	21·91	20·01
Cs	1·34	6·17	8·18
Fs	4·03	0·64	0·16
Fo	15·95	25·07	27·27
Fa	10·57	8·52	9·09
Ru	0·50	0·21	0·27
Q	27·65	21·69	18·88
Q	27·65	21·69	18·88
L	39·96	37·70	36·15
M	32·39	40·61	44·97
	Katanorm		
Q	—	—	—
Or	0·56	2·70	1·09
Ab	13·44	10·67	6·11
An	52·60	36·51	33·35
Ne	—	—	11·83
Wo	1·79	8·23	10·91
En	10·32	—	—
Hy	—	—	—
Fo	8·21	25·07	27·27
Fa	8·55	8·20	9·01
Mt	4·03	0·64	0·16
Cp	—	—	—
Ru	0·50	0·21	0·27

The analyses are computed in terms of Barth's standard cell (1951) and the formula of the rocks are:

I. R. 43:

$$K_{0\cdot12}\ Na_{2\cdot82}\ Ca_{11\cdot98}\ Mg_{11\cdot16}\ Fe_{10\cdot06}\ Al_{23\cdot84}\ Si_{43\cdot11}\ Ti_{0\cdot53}\ [O_{157\cdot4}\ (OH)_{2\cdot6}]_{160}$$

II. R. 32.

$$K_{0\cdot57}\ Na_{5\cdot02}\ Ca_{12\cdot13}\ Mg_{17\cdot74}\ Fe_{7\cdot16}\ Al_{21\cdot12}\ Si_{42\cdot97}\ Ti_{0\cdot46}\ [O_{155}(OH)_5]_{160}.$$

III. R. 64:

$$K_{0\cdot24}\ Na_{5\cdot58}\ Ca_{13\cdot08}\ Mg_{19\cdot65}\ Fe_{7\cdot41}\ Al_{20\cdot23}\ Si_{42\cdot33}\ Ti_{0\cdot29}\ [O_{156}(OH)_4]_{160}.$$

The transfer of cations for the conversion of the different rocks, after Barth (op. cit.) has been worked out below in Table IX.

Table IX

Transfer of cations from R. 64 to R. 32 by metasomatism of salic liquid:

Addition of cations	Valences	Removal of cations	Valences
K 0·33	0·33	Na 0·56	0·56
Al 0·89	2·67	Ca 0·95	1·90
Si 0·64	2·56	Mg 1·91	3·82
Ti 0·17	0·68	Fe 0·25	0·50
H in (OH)	1		
2·03	7·24	3·67	6·78

and from R. 32 to R. 43 by the same process.

Addition of cations	Valences	Removal of cations	Valences
Fe 2·90	5·80	K 0·45	0·45
Al 2·72	8·16	Na 2·20	2·20
Si 0·14	0·56	Ca 0·15	0·30
Ti 0·07	0·28	Mg 6·58	13·16
		H in (OH)	2·4
5·83	14·80	9·38	18·51

It is seen from the above table that the valency could not be balanced to the extent demanded by the theory. It is also of interest to note that for the conversion of R. 64 to R. 32 and to R. 43

(more basic to less basic) there had been a general addition of Si, Ti and Al and removal of the alkalies with Ca and Mg.

III. *Basic Granulites*

The structure and texture of the basic granulites are often even grained and gabbroidal, some finely granular. The majority of them are granulitic. They occur as small lenticles and bands in the variegated gneisses and in the hillocks adjoining Kanjamalai.

Based on their mineralogical association, they can be divided into three main types.

1. Diopside—Hypersthene—Scapolite granulite occurring near Isangadu, R. 28.

2. Diopside—Hypersthene—Granulite, occurring as small lenticles in the variegated gneisses, R. 29, S. 57, S. 58.

and 3. Garnet—Diopside—Hornblende Granulite without hypersthene, occurring in the hillocks adjoining Kanjamalai. R. 80.

All these rocks are massive, medium to fine grained and almost dark in colour. The presence of felspar some times adds a little greyish tinge to their colour.

Under the microscope R. 28 is seen to be composed of plagioclase (about 1 mm), a little antiperthite (about 1 mm) diopside (about 1 mm), hypersthene (about 1 mm) and scapolite (about 1 mm). The texture is granulitic. The anorthite content of the plagioclase varies from An_{30} to An_{40}. The plagioclase grains are all clear. They are andesine and not labradorite. There are a few grains of antiperthite with irregular blebs of potash felspar. The antiperthitic inclusions are restricted to the cores of the grains and then, the plagioclase is often without twinning. When twinning is seen, the twinning lamellae are restricted to the edges, while the core is antiperthitic. Some non-perthitic grains are also free of twinning. This fact has been repeatedly emphasized, among many authors, by Quensel (1951), as characteristic of the rocks of the charnockite series. There are a few grains of untwinned microcline with $-2V=79°$, with well-developed cleavages. The felspars are all clear and not clouded.

The hypersthene and diopside grains are both greenish-tinged along one vibration-direction. Hypersthene is pleochroic from X = light pink, Y = colourless to Z = light green. Both are lamel-

lar; the hypersthene is lamellar, parallel to the optic axial plane, while in diopside, the lamellae are perpendicular to the optic axial plane. The discussion of the lamellar structure is reserved for a later section. Some of the hypersthene grains have got oriented inclusions parallel to (001), a fact noted from this area by Howie (1955).

The optical characters of the hypersthene are as follows:

$$-2V = 60°-64°; \quad \gamma-\alpha = \cdot016; \quad \gamma-\beta = \cdot004.$$

The optical characters of diopside are

$+2V = 58°-61°$ $\quad \gamma-\alpha = \cdot025$ $\quad \beta = 1\cdot705$
$Z\Lambda C = 38°-39°$ $\quad \gamma-\beta = \cdot020$

The scapolite grains are characterized by high birefringence and are invariably surrounded by a rim of carbon. They are also found always developed near the contact of the hypersthene-grains with plagioclase. Some grains are fresh and unaltered while others have been marginally altered to blue-green hornblende. Occasional grains have got only the dark border of carbon preserved while the rest of the grain is completely altered to an aggregate of calcite and blue-green hornblende. The mineral is uniaxial, negative.

$$\omega-\varepsilon = \cdot021-\cdot024$$

The birefringence value gives the composition of scapolite as Ma_{40} Me_{60}. A similar scapolite-bearing hypersthene-granulite has been noted by Quensel (1951).

The accessories include iron-ore and apatite. The apatite grains have got inclusions arranged parallel to the optic axis.

The modal composition of the rock is as follows:

Plagioclase	—	64·5%
Hypersthene	—	16·5%
Diopside	—	3·0%
Scapolite	—	10·1%
Quartz	—	2·0%
Magnetite and Biotite	—	2·1%
Apatite	—	1·8%

R. 29, under the microscope, is composed of plagioclase, diopside and hypersthene with enstatite, as the main constituents. Actinolite, apatite, biotite and iron-ore are the chief accessories with a few grains of released Quartz. The texture is again granulitic. The characters of the plagioclase are essentially the same as in R. 28.

The hypersthene is less distinctly pleochroic and are mostly, surrounded by a corona of an uniaxial, green to colourless, fibrous chlorite. The chlorite passes on to actinolite pleochroic from dark green to light green. The optical characters of hypersthene are

$-2V = 63°-65°$ $\gamma-\alpha = \cdot015-\cdot017.$ $\gamma-\beta = \cdot004$

Actinolite:

$-2V = 77°-83°$ $\gamma-\alpha = \cdot022.$ $Z\Lambda C = 15°$

There are also a few grains of colourless ortho-pyroxene. They have got an inclusion arranged parallel to (100).

$-2V = 80°.$ $\gamma-\alpha = \cdot012.$

Some grains of hypersthene also show the "so-called" inclined extinction, a subject of much discussion. The reason for such extinction has been clearly explained, among others, by Naidu (1943). A further discussion on this will not be made here.

A few hypersthene-grains in this and some intermediate charnockites also exhibit the amphibolic cleavage, found in literature (Groves, 1935). Amphibolic cleavages are said to be seen in hypersthenes of charnockites, as an evidence of conversion of amphibole to pyroxene (op. cit.). But these authors do not mention the angle between the two cleavages. A number of stereograms were drawn and when transformed with (010) at the centre, one of the two cleavages is found to be prismatic while the other is parallel to (100). As a result of drawing of more than thirty stereograms, it is found that the (100) parting is at least as common as the prismatic cleavage and the angle between (100) Λ (110) is about 45°, as measured on the stereogram, in the hypersthenes of basic granulites, and intermediate charnockites from Salem.

Diopside is green in colour and its optical characters are:

$+2V = 58°-61°$ $\gamma-\alpha = \cdot025$

$Z\Lambda C = 38°-40°$ $\gamma-\beta = \cdot020.$

In these basic granulites, there is a dyke of dark pyroxenite occurring, composed of blood-red hypersthene of the type seen in the amphibolites from Shervaroys, diopside and hornblende with some iron-ore. There is no plagioclase. The mafics have the same optical characters, as the mafics of the amphibolite from Shervaroys. The diopside and hypersthene have got very well-developed lamellae parallel to (100).

R. 80, the garnetiferous-diopside-granulite, though free from hypersthene, should be included in this group. The texture is gabbroidal and consists of plagioclase (about 3mm.) garnet (4 mm.), and green augite (about 1 to 2 mm.), with iron-ore and apatite.

The anorthite content of the plagioclase varies from An_{35} to An_{45}. Antiperthite is absent. Garnet is developed bordering the edges of diopside (sketch 4) and form well-defined Zones and they are also developed around grains of iron-ore (sketch 4).

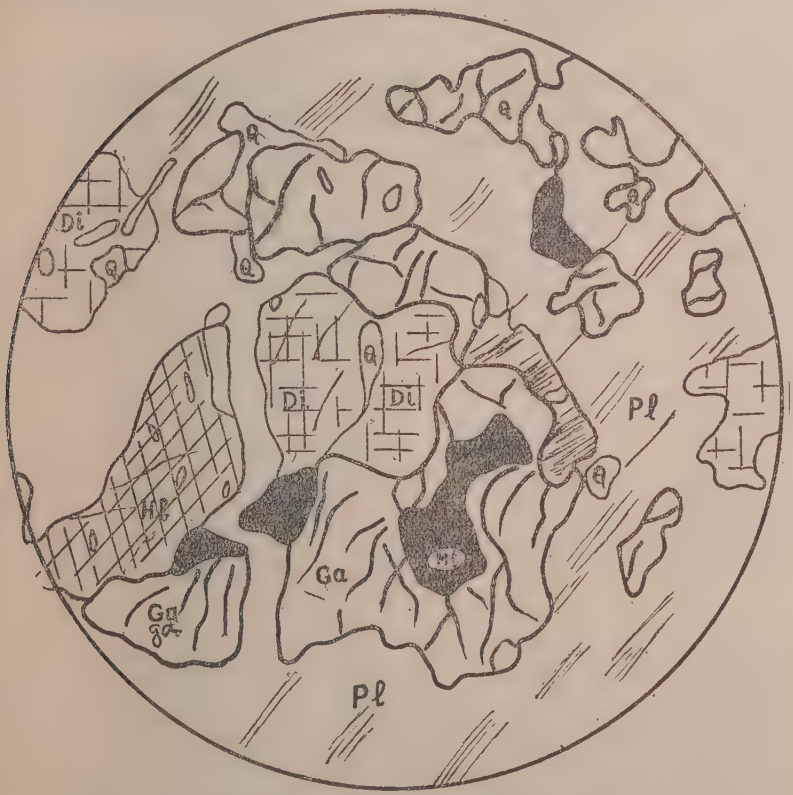

Sketch 4: Diopside grains are fringed by garnet around the edges. They are also developed around grains of iron-ore.
Ga—Garnet. Di—Diopside. Pl—Plagioclase. Hb—Hornblende. Q—Quartz. Mt—Magnetite.

Garnet grains have not established themselves with their force of crystallisation and they contain vermicular grains of quartz inside them. The augite has got the same characters as of the garnet pyroxene rock. The texture of the rock type with the initial stages

of development of garnet around ore-minerals and pyroxene, the formation of hornblende under similar instances around iron-ore and the presence of green augite relate this rock to the garnet Pyroxene rocks. Thus it serves to be a link between the basic granulites and the garnet Pyroxene rocks. The approximate modal composition of the rock is given below:

Plagioclase	—	53·6%
Garnet	—	17·8%
Diopside	—	21·1%
Ores	—	7·5%

The diopside-hypersthene-scapolite granulite, R. 28, has been chemically analysed and the analysis is given below with a few others for comparison, in Table X.

Table X

Oxides	I	II	III	IV
SiO_2	51·44	52·23	51·60	50·28
TiO_2	0·72	0·96	1·00	0·80
Al_2O_3	21·48	18·61	19·96	18·08
Fe_2O_3	2·31	5·04	7·06	2·10
FeO	5·45	4·09	3·60	9·28
MnO	0·15	0·11	0·16	0·36
MgO	4·76	4·58	3·04	7·02
CaO	9·17	7·74	10·44	9·34
Na_2O	3·25	4·25	1·80	2·38
K_2O	0·67	1·05	0·50	0·53
P_2O_5	0·10	0·94	0·50	0·30
H_2O^+	0·25	0·53	0·58	0·08
H_2O^-	0·05	0·22	—	0·03
Total	99·80	100·35	100·24	100·58
Sp. Gr.	2·88	—	—	—

I. Diopside-hypersthene-scapolite granulite, Salem. R. 28. Analyst, S. Ramanathan.
II. Diorite, near to norite, uganda, Analyst, H. L. Riley (Groves, 1935).
III. Intermediate charnockite, varberg district, Analyst, N. Sahlbom (Quensel, 1951).
IV. Norite, Ibrahimpatnam, Krishna district, Analyst, Srirama Rao.

It is seen from the table that the analysis agrees with the analyses of diorite and norite. The standard cell formula for this rock has been calculated and is as follows:

$$K_{0\cdot78}\ Na_{5\cdot94}\ Ca_{9\cdot19}\ Mg_{6\cdot67}\ Fe_{6\cdot00}\ Al_{23\cdot64}\ Si_{48\cdot04}\ Ti_{0\cdot51}\ [O_{157}(OH)_3]_{160}.$$

The C. I. P. W. Norm, Niggli values, Niggli basis and Katanormative values of the analysed rock are given in Table XI.

Table XI

C.I.P.W. Norm	Niggli Values	Niggli Basis	Katanorm
Q — 0·60	al — 31·98	Cp — 0·28	Q — 0·07
Or — 3·89	fm — 34·24	Kp — 2·33	Or — 3·89
Ab — 27·77	C — 24·69	Ne — 17·67	Ab — 29·45
An — 41·98	Alk — 9·09	Cal — 25·18	An — 41·97
Di — 2·32	Si — 129·9	Cs — 0·78	Wo — 1·04
Hy — 18·13	ti — 1·36	Fs — 2·33	En — 13·27
Il — 1·37	K — 0·117	Fo — 9·95	Hy — 7·20
Mt — 3·25	Mg — 0·527	Fa — 6·56	Mt. — 2·33
Ap — 0·34		Ru — 0·50	Cp — 0·28
		Q — 34·42	Ru — 0·50

IV. *Amphibolites*

The amphibolites occurring in Shervaroys, the amphibolite lenses and patches occurring in Jarugamalai, foot-hills of Shervaroys and Namam Hill are all included in this group. The amphibolites of Shervaroys are the most remarkable of these, and they occur as huge massive dykes, conforming with the strike and dip of the intermediate charnockites, more than 150 to 200 ft. in width and in length from the foot of the Shervaroys to about 3000 ft. elevation. In Jarugamalai, no amphibolites of similar dimension could be traced, but there are a number of small lenses, patches and xenoliths of amphibolite. At the foot hills of Shervaroys, the amphibolite occurs in the form of a main dyke about 50 ft. broad, running N.—S. throughout the length of △1441 and △1478 and it is also found to occur in the form of xenoliths and basic patches.

Some of these are occasionally faulted. At the top of Namam hill also, there is a dyke of amphibolite traversing the whole length of the hill, about 200 ft. broad, running due E—W, dipping towards north at 52°.

Based on the characters of the amphibole, these can be divided into three types:

(1) The amphibolites of Shervaroys (S. 46) and Jarugamalai (S. 50) are of the same type and they contain the greenish-brown hornblende.

(2) The amphibolite of Namam hill (S. 35) is characterized by the presence of a green amphibole.

(3) The amphibolite of △1441 and △1478 (S. 28) is characterized by the presence of an amphibole whose pleochroism is greenish-brown to bluish-green.

The amphibolites from Shervaroys and Jarugamalai are xenomorphic, granulitic in texture and dark green in colour. In thin section, the rock is granulitic in texture and is composed of greenish brown amphibole (about 4 mm. size), blood red hypersthene (about 2 mm.), and augite (about 2 mm.), together with iron-ore and a little plagioclase as accessories. The plagioclase is clear and varies in An. content from An_{35} to An_{40}. The hypersthene and augite are occasionally lamellar, parallel to (100) and when the lamellae are present, they are restricted only to the centre and do not traverse throughout the length of the mineral.

Augite:

$+2V = 56°—58°$ $\quad \gamma—\alpha = \cdot 025$
$Z\Lambda C = 41°—43°$ $\quad \gamma—\beta = \cdot 019$

Hypersthene:

$-2V = 70°—73°$ $\quad \gamma—\alpha = \cdot 014$ $\quad \beta—\alpha = \cdot 004$
X = blood red
Y = red
Z = light green

The amphibole is found to develop freely at the expense of hypersthene and plagioclase. It grows into grains of hypersthene and plagioclase.

$-2V = 79°—81°$ $\quad \gamma—\alpha = \cdot 022$
$Z\Lambda C = 15°$ $\quad \gamma—\beta = \cdot 009$ $\quad \beta = 1 \cdot 691—1 \cdot 693$

X = straw yellow
Y = dark brown
Z = greenish brown
X < Z < Y

The approximate modal composition of this rock is as follows:

Hypersthene } Augite }	..	21·4%
Amphibole	..	60·8%
Plagioclase	..	5·4%
Accessories	..	12·4%

The amphibole from this rock was separated and analysed. The analysis is given below and compared with a few others in Table XII.

Table XII

Oxides	I	II	III	IV
SiO_2	39·73	40·44	38·84	43·08
TiO_2	2·58	0·56	3·90	0·17
Al_2O_3	13·75	15·61	7·91	7·48
Fe_2O_3	4·06	2·63	3·89	3·01
FeO	7·64	12·40	9·42	15·37
MnO	0·05	Tr.	0·25	1·18
MgO	13·04	10·29	14·60	9·42
CaO	12·76	12·68	13·86	11·82
Na_2O	3·56	4·06	2·69	3·85
K_2O	1·25	0·42	0·97	0·53
H_2O+	0·14	0·53	3·67	4·09
H_2O-	1·29	0·16		
Sp. Gr.	3·33	3·31	3·33	3·418
ZΛC	15°	10—11°	10°	16°

I. Greenish brown amphibole, Amphibolite, S. 46, Shervaroys, Salem, Analyst, S. Ramanathan.
II. Brown amphibole, Karankaradu, Salem, Analyst, S. Ramanathan.
III. Barkevikit, Fuerteventura (Essek), Analyst, W. Kunitz.
IV. Barkevikit, Skuttersundskjar (Foyait), Analyst, W. Kunitz.

It is interesting to note that the analysed amphibole corresponds to barkevikites of Kunitz and is not very much different from the brown amphibole of the amphibolites of the garnet-pyroxene rock, Karankaradu. This affords an interesting link between these amphibolites, and the basic granulites, both of which are related to the garnet-pyroxene rocks.

The Basis molecules and Q L M values of the analysed mineral were calculated and are given in Table XIII with R. 39, for comparison.

Table XIII

Niggli Basis	Kp	Ne	Cal	Cs	Fs	Fa	Fo	Ru	Q
S. 46	4·62	18·81	10·55	13·52	4·29	8·74	26·89	1·81	10·77
R 39	1·32	21·81	13·71	11·90	2·64	14·21	21·25	0·44	12·72

	S. 46.	R. 39.
Q	10·77	12·72
L	33·98	36·84
M	55·25	50·44

The Q L M values of this mineral were also plotted in Niggli's diagram for amphiboles (Fig. 1) and it is found to occupy a place (B) inside the field for barkevikites, basaltic hornblendes and hastingsites.

Warren's formula for the mineral (Table XIV) is

$$(OH)_{1\cdot29}\ (Na, K, Ca)_{3\cdot32}\ (Mg, Fe''', Fe'', Al)_{5\cdot00}\ (Si, Ti, Al)_{8\cdot00}\ O_{22\cdot71}$$

Formula after Berman (1937) is

$$(WXY)_{8\cdot32}\ Z_8\ O_{22\cdot71}\ (O, OH, F)_{1\cdot29}$$

In the calculation of the atoms, Ti has been reckoned with Si, after Kunitz (1930). The formula after Berman indicates a slight excess of the bases and deficiency in (O, OH, F).

The amphibolite from △ 1441 and △ 1478 (S. 28) is dark in colour and granulitic. Under the microscope, it is found to be composed of bluish green to brown amphibole and plagioclase with a little iron-ore and apatite. These are the only mineralogical constituents of this rock.

Table XIV

Chemical Analysis of Greenish Brown Amphibole from S. 46

Oxides	Wt %	Mol. No.	Metal atoms	O, OH, F atoms	Basis 24 (O, OH, F)		Valency check		
SiO_2	39·73	662	662	1324	5·94	8·00	Si^{++++}		23·76
TiO_2	2·58	33	33	66	0·30		Ti^{++++}		1·20
Al_2O_3	13·75	135	270	405	2·42 (1·76 + 0·66)		Al^{+++}		7·26
Fe_2O_3	4·06	26	52	78	0·47		Fe^{+++}		1·41
FeO	7·64	106	106	106	0·95	5·00	Fe^{++}		1·90
MnO	0·05	1	1	1	—		—		—
MgO	13·04	326	326	326	2·92		Mg^{++}		5·84
CaO	12·76	228	228	228	2·05		Ca^{++}		4·10
Na_2O	3 56	57	114	57	1·02	3·32	Na^{+}		1·02
K_2O	1·25	14	28	14	0·25		K^{+}		0·25
H_2O^+	1·29	72	144	72	1·29	1·29			46·74
Total	99·71			2677				OH	1·29
								O	45·42
Sp. Gr.	3·33								46·71

Formula :

$(OH)_{1·29}$ (Na, K, Ca)$_{3·32}$ (Mg, Fe‴, Fe″, Al)$_{5·00}$ (Si, Ti, Al)$_8$ $O_{22·71}$

Analyst, S. Ramanathan.

The plagioclase is clear and has got an anorthite content ranging from An_{30} to An_{35} and is mostly untwinned. The amphibole grains are clear and unaltered and contain iron-ore and apatite as inclusions. A number of grains of amphibole are twinned on (100).

$+2V = 85°—87°$

$Z\Lambda C = 24°$ [average measused on eight grains by the method of Nemoto and Turner (Hess, 1949).]

$\gamma—\alpha = \cdot018$ $\gamma—\beta = \cdot013$

X = green

Y = bluish green

Z = greenish brown

The amphibolite from Namam Hill (S. 35) is dark green in colour with a crude gneissose texture in the hand specimen. Under the microscope, it is xenomorphic granular, and consists of green amphibole (about 2 mm.), hypersthene (·5 to 1 mm.) and augite (·5 to 1 mm.). There is no plagioclase. The minerals have got strain-shadows and exhibit abnormal birefringence. The hypersthene is pleochroic from pink to colourless and has $-2V = 73°—76°$. The augite is colourless. $+2V = 56°—58°$. $Z\Lambda C = 44°$.

The amphibole is found to develop at the expense of both hypersthene and augite. The optical characters are:

$-2V = 83°—85°$ $n_\beta = 1\cdot672—1\cdot674$

$Z\Lambda C = 19°—22°$ $n_\gamma' = 1\cdot679—1\cdot681$

$n_\alpha' = 1\cdot662—1\cdot664$

X = pale yellow

Y = bluish green

Z = yellowish green

$X < Y < Z$

The amphibole was separated and analysed and the analysis is given in Table XV.

Table XV

Analysis of Green Amphibole from S. 35

Oxides	Wt %	Mol. No.	Metal atoms	(O, OH, F) atoms	Basis 24 (O, OH, F)			Valency check		
SiO_2	44·31	738	738	1476	6·62		8·00	Si^{++++}		26·48
TiO_2	0·61	8	8	16	0·07			Ti^{++++}		0·28
Al_2O_3	8·29	81	162	243	1·45	1·31		Al^{+++}		4·35
						0·14		Fe^{+++}		2·37
Fe_2O_3	6·98	44	88	132	0·79		5·33	Fe^{++}		1·52
FeO	6·11	85	85	85	0·76			Mg^{++}		7·28
MnO	—	—	—	—	—			Ca^{++}		4·24
MgO	16·22	406	406	406	3·64			Na^{+}		0·72
CaO	13·20	236	236	236	2·12		2·91	K^{+}		0·07
Na_2O	2·54	40	80	40	0·72					47·31
K_2O	0·35	4	8	4	0·07					
H_2O^{+}	0·73	39	78	39	0·70		0·70		OH	0·70
									O	46·60
Total	99·34			2677						47·30
Sp. Gr.	3·08									

Formula:

$(OH)_{0·70}\ (Na, K, Ca)_{2·91}\ (Mg, Fe''', Fe'', Al)_{5·33}\ (Si, Ti, Al)_{8·00}\ O_{23·30}$

Analyst, S. Ramanathan.

The approximate modal composition of the rock is as follows:

Hypersthene + augite	..	29·9%
Green Amphibole	..	62·4%
Iron-ore	..	7·7%

The analysis is set below with a few others for comparison in Table XVI.

Table XVI

Oxides	I	II	III	IV
SiO_2	44·31	42·42	40·29	42·05
TiO_2	0·61	0·33	6·60	1·48
Al_2O_3	8·29	6·94	5·72	14·69
Fe_2O_3	6·98	1·71	0·63	3·21
FeO	6·11	10·82	12·65	6·30
MnO	—	—	0·10	0·04
MgO	16·22	16·73	13·51	14·91
CaO	13·20	11·74	12·82	12·83
Na_2O	2·54	1·59	4·18	2·01
K_2O	0·35	0·74	1·22	0·65
H_2O^+	0·73	6·98	2·40	1·53
H_2O^-	0·33		0·01	0·09
Sp. Gr.	3·08	3·284	3·20	3·16

I. Green Amphibole. Amphibolite dyke. Namam hill, Salem. Analyst, S. Ramanathan.
II. Gem. Hornblende. Arendal (syenit) Analyst, W. Kunitz.
III. Green Hornblende (uralite) from granulite. Kailasgarh, Vellore. Analyst, H. Schwander (P. R. J. Naidu, 1955).
IV. 3709. Hornblende. Ultrabasic rock, Pammal hill, Madras. Analyst, R. A. Howie.

It is seen from the table that the analysis generally resembles the other common green hornblendes reported by Kunitz (1930), Naidu (1955) and Howie (1955). The Q L M values of the mineral, when plotted in Niggli's diagram for amphiboles (Fig. 1 C), falls inside the field for common hornblendes.

The amphibolites of this type containing mainly hypersthene and amphibole with subordinate clino-pyroxene have been reported as the ultrabasic type of charnockite from different places. According to Washington (1916), "The name bahiaite from an occurrence in Brazil, was recently suggested for the phanerites composed essentially of hypersthene and hornblende,...". Washington (1916) had extended the term to the ultrabasic pyroxenite from Pammal hill, Madras. This term may as well be applied to this group of amphibolites which have mainly amphibole and hypersthene with subordinate clinopyroxene and a little or no plagioclase. Hence these rock types are also termed "Bahiaites".

(To be continued)

Printed and Published by G. Srinivasachari B.A., at G. S. Press,
21, Narasingapuram Street, Mount Road, Madras.

PUBLICATIONS

OF

THE INTER-UNIVERSITY BOARD, INDIA

		Price Rs.	A.	P.	
1.	**Handbook of Indian Universities** ..	3	0	0	*or* 5*s*
2.	**Facilities for Oriental Studies and Research at Indian Universities** ..	0	8	0	
3.	**Facilities for Scientific Research at Indian Universities** ..	0	12	0	
4.	**Bulletin of the Inter-University Board, India, Nos. 1 to 13** ..	1	0	0	*each*
5.	**Biological Outlook on Life and its Problems.** By J. ARTHUR THOMSON, M.A., LL.D., Regius Professor of Natural History, University of Aberdeen ..	0	2	0	
6.	**Second, Third and Fourth Conference of Indian Universities** ..	1	0	0	*each*
7.	**Training of Teachers in Indian Universities** ..	0	8	0	
8.	**Bibliography of Doctorate Theses in Science and Arts (Accepted by Indian Universities from January 1930 and from 1934)** ..	0	8	0	*each*
9.	**Annual Report of the Inter-University Board for 1940-41** ..	1	0	0	

[POSTAGE AND V. P. CHARGES EXTRA]

Available from :

BANGALORE PRESS,
"LAKE VIEW", MYSORE ROAD,
BANGALORE CITY.